

# **Ecological variability in coastal oceans: simulating biological-physical interactions with Lagrangian Individual-based models**

An der Fakultät für Mathematik und Naturwissenschaften  
der Carl von Ossietzky Universität Oldenburg  
zur Erlangung des Grades und Titels eines

**Doktors der Naturwissenschaften (Dr. rer. nat.)**

angenommene Dissertation von

**Dipl.-Umweltwissenschaftler Gunnar Brandt**

geboren am 21.05.1978

in Minden (Westfl.)



Erstgutachter: Prof. Dr. Kai W. Wirtz

Zweitgutachter: Prof. Dr. Bernd Blasius

Tag der Disputation: 25. September 2009



To my girls, Steffi and Karla Joanna

*With Arms Wide Open ...*



---

## Abstract

Coastal oceans constitute the link between terrestrial and oceanic ecosystems and play an important role in marine ecology. They exhibit a very high primary productivity that is fueled by nutrient inputs from rivers or from upwelling and consequently also sustain an elevated productivity in higher trophic levels. High variability, particularly in ecological variables, is a common feature in such systems. It is mainly caused by highly variable physical conditions and significantly impedes the understanding, let alone the predictability, of ecological processes in coastal oceans. The central aim of this thesis, which consists of three self-contained chapters, is to assess the effects of biological-physical interactions on two fundamental processes in coastal oceans. The first is the recurring phenomenon of phytoplankton spring blooms and the second is the dispersal of planktonic larvae of benthic marine invertebrates. All studies have in common that Lagrangian particle tracking models, which account for the transport of individuals through the water body, are combined with Individual-based Models, which describe the state or behaviour of the simulated organisms.

In chapter 2 an example for distinct interannual differences in the spatio-temporal chlorophyll *a* (CHL-*a*) distribution is presented. This variability becomes apparent in the high-frequency data that was measured by an autonomous measuring device (FerryBox) operating on an alongshore route in the coastal North Sea. While in one year CHL-*a* was spatially homogeneous (2004), a bloom only developed in one part of the transect in the following spring period (2005). In this study, we use a one-dimensional Lagrangian particle tracking model, which operates along the mean current direction, combined with a NPZ-model (Nutrients, Phytoplankton, Zooplankton) to identify the mechanisms controlling the interannual bloom variability. The model results clearly indicate that in 2004, the local light climate triggered phytoplankton growth, whereas in the following year, advective transport determined the spatial structure of the spring bloom. A pronounced eastward inflow event in 2005 imported a high CHL-*a* patch into the western half of the study area from the adjacent Southern Bight. It did, however, not last long enough to also spread the bloom into the eastern part, where high turbidity prevented local phytoplankton growth. The model clearly identified two interacting mechanisms, light climate and hydrodynamics that control the alongshore dynamics. Especially the occurrence of a pro-

---

nounced spring bloom despite unfavourable light conditions in 2005 underlines the need to carefully consider hydrodynamics to understand ecosystem functioning in coastal environments.

In chapter 3 the invasion of a benthic invertebrate into a previously uncolonised habitat over several years is simulated. Therefore, we present field data from a monitoring programme revealing the rapid invasion of the oyster *Crassostrea gigas* into the East Frisian Wadden Sea, North Sea, between 2003 and 2005. The applied model combines a simple, spatially-explicit population dynamics model for the adult stage with a particle tracking model for the larval stage of the life cycle. Simulation results are able to reproduce the large-scale pattern of the field data and indicate a domination of larval supply on the population dynamics in the early stage of the invasion. Though monitoring and simulations suggest a single larval source outside the study area in the west, the population dynamics in the eastern part is only explainable with an additional source within the study area attributed to an unintentional input of juveniles by mussel fishery. High sensitivities to uncertain parameters result in distinct deviations between monitoring and simulations at particular sites. Especially the impact of site-specific variations of the post-settlement mortality underlines the potential impact of variability in local recruitment conditions and indicates the need for spatially resolved information for exact predictions. Chapter 4 evaluates the effects of three different behavioural strategies, namely passive drifting, diurnal vertical migration and tidal vertical migration, on the dispersal of larvae in a dynamic coastal environment by means of a Lagrangian particle tracking model. Passive drifting results in a dispersal from the intertidal to unfavourable offshore areas for most of the larvae. Diel vertical migration changes this pattern only marginally, whereas tidal vertical migration significantly enhances nearshore retention or the return from offshore waters to the coast. Triggered by salinity changes, larvae follow the decreasing salinity gradient towards the coast and accumulate in favourable intertidal habitats or estuaries. These results indicate that even slow swimming larvae may actively influence their horizontal dispersal in coastal seas and, by this means, minimise losses due to the failure of finding a suitable settlement site. The sensitivity of larval distributions to vertical behaviour questions the common *a priori* assumption that larvae are passive tracers and underlines the need for further observational evidence regarding larval behaviour to better constrain estimates of larval dispersal.

---

## Zusammenfassung

Küstenmeere sind das Bindeglied zwischen terrestrischen und marinen Ökosystemen und nehmen eine wichtige Funktion in der marinen Ökologie ein. Sie weisen eine sehr hohe Primärproduktivität aus, die durch Nährstoffeinträge aus Flüssen oder aus Upwelling-Ereignissen angetrieben wird und auch eine erhöhte Produktivität in höheren trophischen Ebenen ermöglicht. Eine hohe Variabilität, vor allem ökologischer Variablen, ist ein häufiges Merkmal solcher Systeme. Sie wird vor allem durch stark fluktuierende physikalische Bedingungen verursacht und erschwert das Verständnis und die Berechenbarkeit ökologischer Prozesse in Küstenmeeren.

Das zentrale Ziel dieser Doktorarbeit, die aus drei eigenständigen Kapiteln besteht, ist es, die Auswirkungen biologisch-physikalischer Interaktionen auf zwei fundamentale Prozesse in Küstenmeeren zu beurteilen. Der erste Prozess ist das wiederkehrende Phänomen von Frühjahrsblüten des Phytoplanktons und der zweite ist die Verbreitung planktischer Larven von marinen benthischen Invertebraten. Die einzelnen Studien haben gemein, dass jeweils ein Lagrangesches Modell, das für den Transport von Individuen im Wasserkörper sorgt, mit einem Individuenbasierten Modell, das den Zustand oder das Verhalten des simulierten Organismus beschreibt, kombiniert wird.

In Kapitel 2 wird ein Beispiel für deutliche interannuelle Unterschiede in der raumzeitlichen Verteilung von Chlorophyll *a* (CHL-*a*) vorgestellt. Diese Variabilität wird auch in einem hochfrequenten Datensatz deutlich, der durch ein autonomes Messsystem (FerryBox) entlang einer küstenparallelen Route in der Nordsee gemessen wurde. Während in einem Jahr CHL-*a* homogen verteilt war (2004), entwickelte sich im folgenden Frühling eine Blüte nur entlang eines Teiles des Transektes (2005). In dieser Studie verwenden wir ein eindimensionales Lagrangesches Driftmodell, das entlang der Hauptströmungsrichtung operiert und mit einem NPZ-Modell (Nutrienten, Phytoplankton, Zooplankton) kombiniert wird um die Mechanismen zu identifizieren, die die interannuelle Variabilität der Blüte kontrollieren. Die Modellergebnisse zeigen deutlich, dass in 2004 das lokale Lichtklima das Phytoplanktonwachstum ausgelöst hat, wohingegen der advective Transport die räumliche Struktur der Frühjahrsblüte im folgenden Jahr bestimmt hat. Ein Ereignis ausgeprägten, ostwärtigen Einstroms hat in 2005 einen Wasserkörper mit hohen CHL-*a* Konzentrationen aus der angrenzenden

---

Südlichen Bucht in die westliche Hälfte des Untersuchungsgebietes importiert. Dieses Ereignis hat jedoch nicht lange genug andauert, um die Blüte auch in den östlichen Teil des Untersuchungsgebietes auszudehnen, wo starke Trübung lokales Phytoplanktonwachstum verhindert hat. Das Modell hat mit dem Lichtklima und der Hydrodynamik zwei wichtige Mechanismen identifiziert, die die Phytoplanktondynamik entlang der Küste maßgeblich beeinflussen. Besonders das Auftreten einer ausgeprägten Frühjahrsblüte trotz ungünstiger Lichtbedingungen in 2005 unterstreicht die Notwendigkeit die hydrodynamischen Verhältnisse zu berücksichtigen um ein Verständnis von Küstenökosysteme zu erlangen.

In Kapitel 3 wird die Invasion eines benthischen Invertebraten in einen vorher unbesiedelten Lebensraum simuliert. Daten eines Monitoringprogrammes dokumentieren die schnelle Invasion der Auster *Crassostrea gigas* in das Ostfriesische Wattenmeer, Nordsee, zwischen 2003 und 2005. Das verwendete Modell ist eine Kombination aus einem einfachen, räumlich-expliziten Model für die adulte Lebensphase der Auster und einem Partikeldriftmodell für das Larvenstadium. Die Simulationsergebnisse reproduzieren das großräumige Muster der Messdaten und deuten, zumindest im frühen Stadium der Invasion, auf eine entscheidende Rolle der Larvenversorgung für die Populationsdynamik hin. Obwohl Monitoringdaten und Simulationsergebnisse eine einzelne Larvenquelle außerhalb des Untersuchungsgebietes im Westen nahe legen, lässt sich die Populationsdynamik im östlichen Teil nur durch eine zusätzliche Larvenquelle innerhalb des Untersuchungsgebietes erklären. Diese könnte einem unabsichtlichen Eintrag von Juvenilen durch Aktivitäten der Muschelfischerei zugeordnet werden. Allerdings führen hohe Sensitivitäten gegenüber unsicheren Parametern an manchen Standorten zu zum Teil deutlichen Abweichungen zwischen Ergebnissen des Monitoringprogramms und den Simulationsergebnissen. Besonders der Einfluss von ortsspezifischen Abweichungen der Mortalität nach der Ansiedlung verdeutlicht den potentiellen Effekt der Variabilität lokaler Rekrutierungsbedingungen und unterstreicht den Bedarf räumlich aufgelöster Informationen für exakte Vorhersagen.

Kapitel 4 untersucht die Auswirkungen von drei verschiedenen Verhaltensstrategien planktischer Larven in dynamischen Küstengewässern (passives Driften, vertikale Migration im Tagesrhythmus und tidale vertikale Migration) auf ihre Verdriftung mit einem Lagrangeschen Driftmodell. Passives Driften führt für die meisten Larven zu einem Verdriften aus dem Intertidal in ungünstige, küstenferne Gebiete. Vertikale Migration im Tagesrhythmus verändert dieses Muster nur marginal, wohingegen tidale vertikale Migration signifikant die Retention von Larven in Küstennähe oder die Rückkehr von Larven zur Küste erhöht. Ausgelöst durch Salinitätsunterschiede folgen die Larven dem zur Küste abnehmenden Salinitätsgradienten und sammeln sich im für eine Ansiedlung geeigneten Intertidal oder in Ästuaren. Die Ergebnisse zeigen, dass sogar langsam schwimmende Larven aktiv ihre horizontale Verteilung in Küstenmeeren beeinflussen und somit Verluste verringern können, die durch das Scheitern des Auffindens eines passenden Ansiedlungsortes entstehen. Die Sensitivität räumlicher Larvenverteilungen gegenüber verschiedenen vertikalen Bewegungsstrategien stellt die häufige Annahme in

---

Frage, dass Larven passive Tracer sind. Es unterstreicht außerdem die Notwendigkeit weitere Hinweise von *in situ* Messungen bezüglich des Migrationsverhaltens von Larven zu erhalten um bessere Abschätzungen von räumlichen Larvenverteilungen erstellen zu können.



---

# Contents

<b>1</b>	<b>General Introduction</b>	<b>1</b>
1.1	Biological-physical interactions in coastal oceans . . . . .	1
1.2	Lagrangian particle tracking models and Individual-based models in oceanography . . . . .	4
1.3	Thesis outline . . . . .	5
<b>2</b>	<b>Interannual variability of alongshore spring bloom dynamics in a coastal sea caused by the differential influence of hydrodynamics and light climate</b>	<b>11</b>
2.1	Introduction . . . . .	11
2.2	Study area . . . . .	13
2.3	Methods . . . . .	14
2.3.1	Measured data . . . . .	14
2.3.2	Model architecture . . . . .	14
2.3.3	Ecosystem Model . . . . .	15
2.4	Parametrisation, initial conditions and forcing . . . . .	16
2.5	Results . . . . .	17
2.5.1	Measured spring bloom dynamics . . . . .	17
2.5.2	Sensitivity analysis . . . . .	18
2.5.3	Bloom control by light climate in 2004 . . . . .	19
2.5.4	Bloom advection in 2005 . . . . .	19
2.6	Discussion . . . . .	22
2.6.1	Light climate . . . . .	23
2.6.2	Hydrodynamics . . . . .	23
2.6.3	Nutrients . . . . .	24
2.6.4	Grazing . . . . .	25
2.6.5	Algal community structure and stoichiometry . . . . .	26

2.6.6	1D Lagrangian modelling . . . . .	27
2.7	Conclusion . . . . .	27
2.8	Appendix . . . . .	29
2.8.1	Data integration . . . . .	29
2.8.2	Model architecture . . . . .	29
2.8.3	Ecosystem model . . . . .	30
2.8.4	Initial conditions and forcing . . . . .	31
<b>3</b>	<b>Rapid invasion of <i>Crassostrea gigas</i> into the German Wadden Sea dominated by larval supply</b>	<b>39</b>
3.1	Introduction . . . . .	39
3.2	Methods . . . . .	42
3.2.1	Monitoring data . . . . .	42
3.2.2	Population dynamics model . . . . .	43
3.2.3	Simulations and Model set-ups . . . . .	47
3.2.4	Drift characteristics . . . . .	49
3.3	Results . . . . .	49
3.3.1	Rapid invasion of <i>Crassostrea gigas</i> . . . . .	49
3.3.2	Reference run with supply-domination . . . . .	51
3.3.3	Site-specific recruitment and an additional larval source . . . . .	52
3.3.4	Drift characteristics . . . . .	54
3.3.5	Constraining ecological parameters . . . . .	55
3.4	Discussion . . . . .	57
3.4.1	Monitoring data . . . . .	57
3.4.2	Simulations . . . . .	58
3.4.3	Drift distances . . . . .	59
3.4.4	Constraining ecological parameters . . . . .	59
3.4.5	Potential and limitations of the model . . . . .	61
3.5	Conclusion . . . . .	62
<b>4</b>	<b>Tidal vertical migration enhances nearshore retention in weak-swimming meroplanktonic larvae</b>	<b>69</b>
4.1	Introduction . . . . .	69
4.2	Methods . . . . .	70
4.2.1	Study area and model organism . . . . .	70
4.2.2	Model . . . . .	71
4.3	Results . . . . .	73

## Contents

---

4.3.1	Passive larvae . . . . .	73
4.3.2	Diurnal vertical migration . . . . .	74
4.3.3	Tidal vertical migration . . . . .	75
4.4	Discussion . . . . .	76
4.5	Conclusion . . . . .	79
4.6	Appendix . . . . .	81
<b>5</b>	<b>Synthesis</b>	<b>89</b>
	<b>Acknowledgements</b>	<b>93</b>
	<b>Curriculum Vitae</b>	<b>95</b>



Coastal oceans present the transition zone between continents and oceans, from the continental shelf to the high-water mark. Although they only comprise a small part of the world's oceans, shallow coastal zones play an important role in marine ecology. Primary production is very high in nearshore environments compared to deep ocean basins [Muller-Karger et al. 2005], because either river discharge or upwelling supplies the ecosystem with vital nutrients. Organisms in higher trophic levels benefit from this production, an effect known as the trophic cascade. As a consequence, the biomass of most functional groups including zooplankton, benthic invertebrates, fish, and birds, is higher in coastal oceans than in other marine areas. A characteristic feature of such ecosystems is, however, a high variability on all temporal and spatial scales. Typical examples for highly variable processes in coastal ecology are phytoplankton blooms [Cloern 1996], the recruitment of fish and benthic invertebrates [Werner et al. 1997], or the mass occurrence of jellyfish [Boero et al. 2008].

Coastal ecosystems have been intensively studied by researchers of all oceanographic disciplines, because of their relevance, but also because of the proximity of many marine institutes to coastal oceans. The potential impact of climate change on these sensible systems and the emerging consequences for humans living on the coast have lately attracted additional attention. Nevertheless, the complexity of coastal systems is still not fully understood and their unpredictability continues to challenge researchers of many disciplines. In recent years, the pivotal influence of physics on biological variability have become increasingly evident for many phenomena and several open questions in marine ecology have been addressed by combining both disciplines. Numerical modelling proved to be very useful to generate understanding of biological-physical interactions and to handle complex systems.

### **1.1 Biological-physical interactions in coastal oceans**

All organisms live in environments that are largely determined by their physical and chemical properties. Particularly the properties of seawater and its motion are affecting organisms in marine environments over a range of scales from less than a micrometer to several thousands of kilometers. Correspondingly, ecologically relevant time scales range from less than a second to decades.

The nutrient uptake of small algal cells, for example, greatly relies on molecular diffusion to over-

come the thin viscous layer surrounding their body [Lazier and Mann 1989]. Tides exercise a periodic forcing that has dramatic consequences for many species living in coastal ecosystems. Within one tidal cycle, i.e. within several hours, benthic organisms in the intertidal experience a change from aquatic to terrestrial conditions, whereas planktonic organisms may be dispersed several kilometers to a different ecosystem. The annual period of the insolation cycle is responsible for the occurrence of articulate spring blooms in temperate and boreal parts of the oceans [Townsend et al. 1992]. Much of the observed variability in marine ecosystems that occurs on scales of entire ocean basins and over periods exceeding a year is attributed to changes in the climatic forcing explaining the increasing number of publications on ecological consequences of climate change [Walther et al. 2002]. The climate phenomena El Niño Southern Oscillation and the North Atlantic Oscillation are probably the best known and studied examples for such large-scale effects [Stenseth et al. 2002, Barber and Chavez 1983]. Falkowski and Oliver [2007] argue that even cell sizes and taxa-level distributions are ultimately determined by the climate through cascading effects of the global distribution of solar energy. There are so many examples illustrating the intimate link between biology and physics that essentially every compilation of them remains incomplete.

In this thesis, I focus on two selected phenomena, both are ubiquitous in temperate coastal oceans, relevant for the functioning of coastal ecosystems, and still not fully understood. The one is the spatial and temporal dynamics of phytoplankton spring blooms and the other is the dispersal and recruitment of benthic marine invertebrates.

Phytoplankton spring blooms develop as a consequence of increasing incident irradiance. Improving light conditions in spring and the potential development of a density stratification induced by rising surface water temperatures enable rapid phytoplankton growth that is fueled by replenished nutrients [Sverdrup 1953]. In coastal environments, however, the interference of further factors requires an extension of this simple concept [Lucas et al. 1998]. Light availability is influenced by the concentration of suspended particulate matter, which exhibits a complex dynamics in coastal oceans [Tian et al. 2009]. It is resuspended from sediments by strong wind-, wave-, or tide-induced currents or supplied by river discharge [van der Molen 2002]. At shallow depths, the water column remains well mixed throughout the year so that the concept of varying mixed layer depth is not applicable. Primary production is therefore directly affected by the bathymetrie. Especially in heterogeneous coastal environments horizontal advection further complicates the understanding of the system [Lucas et al. 1999], since currents may separate water masses with a specific phytoplankton assemblage from the conditions under which this community developed. A consequence of the considerable variability of physical conditions during the spring bloom period is the alternating dominance of several phytoplankton species [Peperzak et al. 1998, Egge and Aksnes 2002].

Most marine benthic invertebrates are immobile or move only over short distances. Many species have, however, a planktonic larval stage that facilitates the dispersal over far greater distances, typi-

cally in the range of kilometers. While all disadvantages associated to a settlement close to the parents are eliminated by having a mobile planktonic life-stage, the problem of finding an adequate habitat arises [Pechenik 1999]. Since larvae are not traceable with direct observational methods, the estimation of dispersal distances and destinations of larvae is uncertain. High variability of reported dispersal distances may be a direct consequence of unsteady currents in many coastal oceans, but often also an outcome of the different research foci. Levin [2006] argues that probably both mechanisms, local retention and dispersal over large distances, occur regularly, but each of them serves another purpose. While the retention of the majority of larvae ensures the persistence of a local stock, the dispersal of a few individuals to remote sites is important to sustain genetic and biotic diversity or to facilitate the invasion of a new species. The importance of the influx of new members into existing communities for their recruitment has coined the phrase supply-side ecology [Underwood and Fairweather 1989, Lewin 1986]. Particularly the invasion of new species into a formerly uncolonised habitat offers the chance to assess dispersal distances and the relative relevance of larval supply and recruitment processes for the population dynamics of a species [McQuaid and Phillips 2000]. With the concept of supply-side ecology, the paramount role of hydrodynamics for the population dynamics, which has been known since decades [e.g. Redfield 1939], gained a lot of attention [Berge et al. 2005, McQuaid and Phillips 2000, Young et al. 1996]. Usually, larvae are assumed to behave like passive particles, but often there is a discrepancy between predicted and observed dispersal distances, which is usually attributed to active larval behaviour [Cowen and Sponaugle 2009, Metaxas 2001]. Since most larvae of benthic invertebrates are weak swimmers compared to the speed of horizontal ocean currents [Mileikovsky 1973], the effect of swimming is limited to the vertical position in the water column. Despite strong evidence for active vertical migration [Knights et al. 2006, Shanks and Brink 2005, Dobretsov and Miron 2001, Verwey 1966], the consequences of such behaviour in complex hydrodynamic environments remains unclear.

One of the reasons for this uncertainty that persists despite decades of intensive research is the broad range of scales involved in this problem. Observational tools span only a limited range of scales similar to the processes they measure. For example, high-resolution sampling of planktonic larvae may yield insight to the vertical distribution of larvae and their behaviour, but it does not reveal the consequences of such behaviour on a scale of kilometers and weeks. One can think of similar examples regarding the observation of phytoplankton blooms. A plankton haul yields detailed information regarding the species composition of the community at the sampling site and at the sampling time, but it does not provide an overview of the spatial or temporal extent and the variability of a phytoplankton bloom. For that purpose, the synoptic view of a satellite is clearly more appropriate. It is, however, essential to obtain knowledge on a broad range of relevant scales for the phenomenon of interest, because processes on smaller scales may have significant impacts on larger scales. Observable patterns often emerge as a result of mechanisms on underlying smaller scales [Levin 1992]. The dilemma for

ecological research is that the limited scope of observational tools is hampering the development of a generalised understanding of ecosystems. Numerical modelling may offer a way out of this dilemma, because it facilitates a synthesis of available knowledge spanning over a wide range of scales. Today many biological-physical processes can be simulated properly, because the description of physics and the resolution of physical models have both reached sufficient levels.

## 1.2 Lagrangian particle tracking models and Individual-based models in oceanography

Lagrangian particle tracking models (LPTMs) describe trajectories of individual objects through space and time using current and diffusivity data from hydrodynamic models. The results of a LPTM are position data at arbitrary times, which are mostly set by the time-step of the hydrodynamic model supplying the current data. They, hence, differ qualitatively from the results of the more common Eulerian models that yield the temporal evolution of a quantity at fixed positions.

The propagation of a particle in its surrounding medium is determined by two processes, advection and diffusion. Both are represented in the Lagrangian equation describing the displacement  $dx_i$  of a particle located in  $x$  in the  $i$ -th dimension  $i = (x, y, z)$

$$dx_i = u_i(x, t) \cdot dt + \frac{\partial K_i(x, t)}{\partial i} \cdot dt + Z \cdot \sqrt{2 \cdot K_i(x, t)} \cdot dt \quad (1.1)$$

with the current velocity  $u$ , the temporal increment  $dt$ , the diffusivity  $K_i$ , and the  $\mathcal{N}(0, 1)$  distributed Gaussian random number  $Z$ . The diffusion is, hence, simulated as a stochastic process, a random walk, with the magnitude of the random displacement corresponding to the strength of diffusivity (see Gardiner [1983] for a comprehensive derivation). The non-random term  $\frac{\partial K_i(x, t)}{\partial i} \cdot dt$  is required to prevent erroneous aggregations or evacuations of particles in environments with spatially non-uniform diffusivities [Visser 1997, Hunter et al. 1993].

LPTMs are commonly applied to simulate the dispersal of tracers originating from a limited number of sources. A simulation of ubiquitous tracers with this approach is computationally prohibitive and does furthermore not provide the synoptic result of Eulerian models that are clearly more appropriate for this task.

A typical example of an application is the dispersal of neutrally buoyant and physically conservative tracers [Law et al. 2001, Dahlgaard et al. 1995]. There is, however, also a growing number of ecological processes, particularly the dispersal and development of invertebrate and fish larvae, that have been explained by means of a combination of LPTMs with Individual-based models (IBMs) [Werner et al. 2001]. IBMs intuitively describe populations as the conglomerate of many individuals. The characteristics of a population or an entire ecological system emerge from the properties of all associated individuals and the system's variability is an inherent part of the model result. While Eulerian

models deliver the temporal evolution of the mean value of a state variable, the result of an IBM yields a variety of realisations of a simulated process with slightly different boundary conditions or parameterisations, which are often derived from a probability distribution. The mean value is, thus, only one determinable statistical property of the result of IBMs. IBMs are therefore especially suited to account for rare events, when the impact of a few individuals with non-average properties is significant for an ecological system [Werner et al. 2001]. The first individuals of an invasive species that arrive in an uncolonised habitat, for example, are unlikely average with regard to the dispersal distance, but may change the receiving ecosystem irreversibly.

Models of the larval phase of fish and invertebrates assess the connectivity between locations of spawning and recruitment, i.e. sources and sinks of larvae [Cowen and Sponaugle 2009, Cowen et al. 2000]. Besides passive drift [Barnay et al. 2003], growth and mortality are also commonly considered [Ellien et al. 2004, Garvine et al. 1997]. Additionally, some models simulate vertical swimming of larvae, since it may provoke a change in habitat connectivity in many ecosystems [Guizien et al. 2006, Hare et al. 1999, Verdier-Bonnet et al. 1997]. Albeit less common, also entire planktonic ecosystems can be simulated with Lagrangian IBMs [Woods 2005]. While in larvae models, the origin and the destination of propagules are the most valuable insight, the different life-histories of individuals are of greatest interest in models of holoplanktonic communities. IBMs allow to produce variability, which is an inherent feature of ecological data, as a consequence of differences in the physical environment the individuals of a community experienced.

The combination of LPTMs with IBMs of planktonic organisms therefore offers a powerful tool to address the interactions between physics and biology in coastal oceans. Or as Crowder et al. [1992] consisely puts it:

*It is individuals that survive to recruit; the unique characteristics of individuals, and not population averages, determine which individuals survive. Individual-based models are not only interesting, but are perhaps the only logical way to model these processes.*

### **1.3 Thesis outline**

The aim of this study is to determine the effects of biological-physical interactions, with special emphasis on the influence of hydrodynamics on the temporal and spatial dynamics of ecological processes in the coastal sea. Therefore, I present models of two prominent processes in the coastal sea, the phytoplankton spring bloom and the larval dispersal of marine benthic invertebrates. In all studies, measured data is extensively used to constrain boundary conditions and to validate model results.

In chapter 2 the alongshore spring bloom dynamics in the German Bight is simulated by a simple three compartment ecosystem model that is combined with a one-dimensional LPTM. The ecosystem

model describes the evolution of a nutrient, phytoplankton and zooplankton. The description of the pivotal process in this ecosystem, the primary production, accounts for temperature, light, and nutrient limitation. High resolution data of chlorophyll *a*, temperature, turbidity, which were measured along the alongshore track of a regularly operating ferry, show considerable variability in all measured variables, including qualitative differences in the spring bloom development in two consecutive years, and provide realistic constraints for the model. The central question in this study is: What are the mechanisms that led to the observed interannual differences in chlorophyll *a*?

Chapter 3 focuses on the invasion of the non-native oyster *Crassostrea gigas* into the intertidal Wadden Sea in the North Sea. A two-dimensional LPTM, which simulates the larval dispersal, is combined with a population dynamics model, which accounts for the population structure of adults in the intertidal and their reproductive output. The model simulates the spatial and temporal dynamics of the invasion in eight consecutive years covering the entire period from the occurrence of first individuals to the prevalence of the species in the study area. At several mussel beds, which provide the major habitat for the invading oysters in the Wadden Sea, the development of the oyster population was measured in a monitoring programme allowing for a comprehensive model calibration. The main questions in this study are: How do hydrodynamics influence the speed of an invasion and which of the two processes, larval supply or early mortality, does have a bigger impact on the growth of the adult population?

In chapter 4 the consequences of different larval swimming strategies in the tidally dominated German Bight are assessed by means of a three-dimensional LPTM. Besides passive drifting, diel vertical migration and tidal vertical migration of larvae are simulated with varying swimming speeds. While in the former case larval swimming is triggered by the daily light cycle, in the latter case larvae swim upwards during flood and downwards during ebb, thus, interacting with the vertically sheared horizontal currents in the study area. Simulated larvae are released at the positions of intertidal mussel beds in the study area and disperse until they become competent. A spatial distribution of competent larvae is compiled to compare the effects of the tested behavioural strategies. The main question in this study is: How do different behavioural strategies affect the spatial distribution of competent larvae in a tidally dominated coastal sea?

## Bibliography

- R. T. Barber and F. P. Chavez. Biological consequences of El Niño. *Science*, 222(4629):1203–1210, 1983.
- A. S. Barnay, C. Ellien, F. Gentil, and E. Thiébaud. A model study on variations in larval supply: are populations of the polychaete *Owenia fusiformis* in the English Channel open or closed? *Helgol Mar Res*, 56(4):229–237, 2003.
- J. Berge, G. Johnsen, F. Nilsen, B. Gulliksen, and D. Slagstad. Ocean temperature oscillations enable reappearance of blue mussels *Mytilus edulis* in Svalbard after a 1000 year absence. *Mar Ecol Prog Ser*, 303:167–175, 2005.
- F. Boero, J. Bouillon, C. Gravili, M. P. Miglietta, T. Parsons, and S. Piraino. Gelatinous plankton: irregularities rule the world (sometimes). *Mar Ecol Prog Ser*, 356:299–310, 2008.
- J. E. Cloern. Phytoplankton bloom dynamics in coastal ecosystems: a review with some general lessons from sustained investigation of San Francisco Bay, California. *Rev Geophys*, 34(2):127–168, 1996.
- R. K. Cowen and S. Sponaugle. Larval dispersal and marine population connectivity. *Annu Rev Mar Sci*, 1:443–466, 2009.
- R. K. Cowen, K. M. M. Lwiza, S. Sponaugle, C. B. Paris, and D. B. Olson. Connectivity of marine populations: open or closed. *Science*, 287:857–859, 2000.
- L. B. Crowder, J. A. Rice, T. J. Miller, and E. A. Marschall. Empirical and theoretical approaches to size-based interactions and recruitment variability in fishes. In D. L. DeAngelis and L. J. Gross, editors, *Individual-based Models and Approaches in Ecology: Populations, Communities and Ecosystems*, pages 237–255. Chapman and Hall, 1992.
- H. Dahlgaard, J. Herrmann, and J. C. Salomon. A tracer study of the transport of coastal water from the English Channel through the German Bight to the Kattegat. *J Mar Syst*, 6:415–425, 1995.
- S. V. Dobretsov and G. Miron. Larval and post-larval vertical distribution of the mussel *Mytilus edulis* in the White Sea. *Mar Ecol Prog Ser*, 218:179–187, 2001.
- J. K. Egge and D. L. Aksnes. Silicate as regulating nutrient in phytoplankton competition. *Mar Ecol Prog Ser*, 83(2):281–289, 2002.
- C. Ellien, E. Thiébaud, F. Dumas, J. C. Salomon, and P. Nival. A modelling study of the respective role of hydrodynamic processes and larval mortality and larval dispersal and recruitment of benthic

- invertebrates: example of *Pectinaria koreni* (Annelida: Polychaeta) in the Bay of Seine (English Channel). *J Plankton Res*, 26(2):117–132, 2004.
- P. G. Falkowski and M. J. Oliver. Mix and match: how climate selects phytoplankton. *Nature*, 5(10): 813–819, 2007.
- C. W. Gardiner. *Handbook of Stochastic Methods for Physics, Chemistry and the Natural Sciences*. Springer, 1983.
- R. W. Garvine, C. E. Epifanio, C. C. Epifanio, and K.-C. Wong. Transport and recruitment of blue crab larvae: a model with advection and mortality. *Estuar, Coast and Shelf Sci*, 45:99–111, 1997.
- K. Guizien, T. Brochier, J.-C. Duchêne, B.-S. Koh, and P. Marsaleix. Dispersal of *Owenia fusiformis* larvae by wind-driven currents: turbulence, swimming behaviour and mortality in a three-dimensional stochastic model. *Mar Ecol Prog Ser*, 311:47–66, 2006.
- J. A. Hare, J. A. Quinlan, F. E. Werner, B. O. Blanton, J. J. Govoni, R. B. Forward, L. R. Settle, and D. E. Hoss. Larval transport during winter in the SABRE study area: results of a coupled vertical larval behaviour-three-dimensional circulation model. *Fish Oceanogr*, 8(2):57–76, 1999.
- J. R. Hunter, P. D. Craig, and H. E. Phillips. On the use of random walk models with spatially variable diffusivity. *J Comp Phy*, 106:366–376, 1993.
- A. M. Knights, T. P. Crowe, and G. Burnell. Mechanisms of larval transport: vertical distribution of bivalve larvae varies with tidal conditions. *Mar Ecol Prog Ser*, 326:167–174, 2006.
- C. S. Law, A. P. Martin, M. I. Liddicoat, A. J. Watson, K. J. Richards, and E. M. S. Woodward. A Lagrangian SF6 tracer study of an anticyclonic eddy in the North Atlantic: patch evolution, vertical mixing and nutrient supply to the mixed layer. *Deep-Sea Res II*, 48(4-5):705–724, 2001.
- J. R. N. Lazier and K. H. Mann. Turbulence and the diffusive layers around small organisms. *Deep-Sea Res*, 36(11):1721–1733, 1989.
- L. A. Levin. Recent progress in understanding larval dispersal: new directions and digressions. *Integr Comp Biol*, 46(3):282–297, 2006.
- S.A. Levin. The problem of pattern and scale in ecology: the Robert H. MacArthur award lecture. *Ecology*, 73(6):1943–1967, 1992.
- R. Lewin. Supply-side ecology. *Science*, 234:25–27, 1986.
- L. V. Lucas, J. E. Cloern, J. R. Koseff, S. G. Monismith, and J. K. Thompson. Does the Sverdrup critical depth model explain bloom dynamics in estuaries? *J Mar Res*, 56(2):375–415, 1998.

- L. V. Lucas, J. R. Koseff, S. G. Monismith, J. E. Cloern, and J. K. Thompson. Processes governing phytoplankton blooms in estuaries 2: the role of horizontal transport. *Mar Ecol Prog Ser*, 187: 17–30, 1999.
- C. D. McQuaid and T. E. Phillips. Limited wind-driven dispersal of intertidal mussels larvae: *in situ* evidence from the plankton and the spread of the invasive species *Mytilus galloprovincialis* in South Afrika. *Mar Ecol Prog Ser*, 201:211–220, 2000.
- A. Metaxas. Behaviour in flow: perspectives on the distribution and dispersion of meroplanktonic larvae in the water column. *Can J Fish Aquat Sci*, 58(1):86–98, 2001.
- S. A. Mileikovsky. Speed of active movement of pelagic larvae of marine bottom invertebrates and their ability of regulate their vertical positions. *Mar Biol*, 23:11–17, 1973.
- J. van der Molen. The influence of tides, wind and waves on the net sand transport in the North Sea. *Cont Shelf Res*, 22(18-19):2739–2762, 2002.
- F. E. Muller-Karger, R. Varela, R. Thunell, R. Luerssen, C. Hu, and J. J. Walsh. The importance of continental margins in the global carbon cycle. *Geophys Res Lett*, 32:L01602, 2005.
- J. E. Pechenik. On the advantages and disadvantages of larval stages in benthic marine invertebrate life cycles. *Mar Ecol Prog Ser*, 177:269–297, 1999.
- L. Peperzak, F. Colijn, W. W. C. Gieskes, and J. C. H. Peeters. Development of the diatom-*Phaeocystis* spring bloom in the Dutch coastal zone of the North Sea: the silicon depletion versus the daily irradiance threshold hypothesis. *J Plankton Res*, 20(3):517–537, 1998.
- A. C. Redfield. The history of a population of *Limacina retroversa* during its drift across the Gulf of Maine. *Biol Bull*, 76(1):26, 1939.
- A. L. Shanks and L. Brink. Upwelling, downwelling, and cross-shelf transport of bivalve larvae: test of a hypothesis. *Mar Ecol Prog Ser*, 302:1–12, 2005.
- N. C. Stenseth, A. Mysterud, G. Ottersen, J. W. Hurrell, K. S. Chan, and M. Lima. Ecological effects of climate fluctuations. *Science*, 297(5585):1292–1296, 2002.
- H. U. Sverdrup. On conditions for the vernal blooming of phytoplankton. *J Conseil*, 18(3):287, 1953.
- T. Tian, A. Merico, J. Su, J. Staneva, K. Wiltshire, and K. W. Wirtz. Importance of resuspended sediment dynamics for the phytoplankton spring bloom in a coastal marine ecosystem. *J Sea Res*, 2009. doi: 10.1016/j.seares.2009.04.001.

- D. W. Townsend, M. D. Keller, M. E. Sieracki, and S. G. Ackleson. Spring phytoplankton blooms in the absence of vertical water column stratification. *Nature*, 360(6399):59–62, 1992.
- A. J. Underwood and P. G. Fairweather. Supply-side ecology and benthic marine assemblages. *Trends Ecol Evol*, 4(1):16–20, 1989.
- C. Verdier-Bonnet, F. Carlotti, C. Rey, and M. Bhaud. A model of larval dispersion coupling wind-driven currents and vertical larval behaviour: application to the recruitment of the annelid *Owenia fusiformis* in Banyuls Bay, France. *Mar Ecol Prog Ser*, 160:217–231, 1997.
- J. Verwey. The role of some external factors in the vertical migration of marine animals. *Neth J Sea Res*, 3(2):245–266, 1966.
- A.W. Visser. Using random walk models to simulate the vertical distribution of particles in a turbulent water column. *Mar Ecol Prog Ser*, 158:275–281, 1997.
- G. R. Walther, E. Post, P. Convey, A. Menzel, C. Parmesan, T. J. C. Beebee, J. M. Fromentin, O. Hoegh-Guldberg, and F. Bairlein. Ecological responses to recent climate change. *Nature*, 416(6879):389–395, 2002.
- F. E. Werner, J. A. Quinlan, B. O. Blanton, and R. A. Luetlich. The role of hydrodynamics in explaining variability in fish populations. *J Sea Res*, 37(3-4):195–212, 1997.
- F. E. Werner, J. A. Quinlan, R. G. Lough, and D. R. Lynch. Spatially explicit individual based modeling of marine populations: a review of the advances in the 1990s. *Sarsia*, 86:411–421, 2001.
- J. D. Woods. The Lagrangian Ensemble metamodel for simulating plankton ecosystems. *Prog Oceanogr*, 67(1-2):84–159, 2005.
- E. F. Young, G. R. Bigg, and A. Grant. A statistical study of environmental influences on bivalve recruitment in The Wash, England. *Mar Ecol Prog Ser*, 143:121–129, 1996.

## Chapter 2

# Interannual variability of alongshore spring bloom dynamics in a coastal sea caused by the differential influence of hydrodynamics and light climate

## 2.1 Introduction

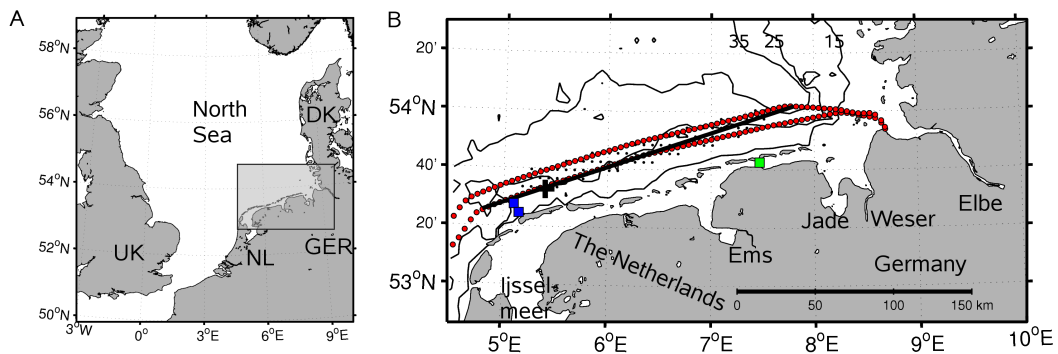


Figure 2.1: **A** North Sea region including the study area. **B** Study area with the FerryBox route (red dots), the model transect (black line) and the release positions of the particles (black cross) at  $5.4^{\circ} E$ . Black dots indicate General Estuarine Transport Model (GETM) grid points used in the current analysis (see Fig. 2.3). Coastal measurement pile (green square), nutrient measurement stations (blue squares) and depth contours (15, 25 and 35 m).

The phytoplankton spring bloom drives food web dynamics and matter cycling in most temperate aquatic ecosystems [Sommer 1998]. Despite its recurrence, the timing, the spatial extent, and the duration of the first seasonal peak in algal concentration show considerable interannual variation. While in deep waters the onset of a bloom typically follows stratification in spring, in shallow coastal seas interannual variability and spatial heterogeneity are particularly strong [Thomas et al. 2003, Cloern 1996]. Only the magnitude of the bloom seems to be predictable as a function of winter nutrient concentration [Loebl et al. 2009, Muylaert et al. 2006, Cloern 1996]. Before and during the bloom event, however, the balance between algal production and loss in near-shore waters is sensitive to a multitude of different factors such as temperature, water transparency, abundance of herbivores, stratification, or incident irradiance. Thus, observed irregularities mainly reflect the sensitivity of spring bloom de-

velopment to fluctuating physical and, to a lesser extent, biological conditions of which turbidity and benthic grazing are typically considered to be most important [Cloern 1996]. Turbulence, generated by wind- or tide-induced currents, affects both factors: It decreases light availability for phytoplankton by enhancing turbidity, which is suggested to be pivotal for phytoplankton bloom control [Townsend et al. 1994], and strengthens vertical mixing. The latter also increases mortality because of grazing by benthic filter-feeders Cloern [1996], Prins et al. [1996]. Mixing is, however, not always retarding blooms [Iriarte and Purdie 2004] underlining the importance of other site-specific mechanisms such as freshwater induced stratification, resuspension of benthic diatoms, or species composition. The range of potential mechanisms considerably complicates the establishments of general rules for biological responses to various physical forcings.

Strong horizontal advection, which in coastal seas is usually connected to winds and tides, links temporal variability to spatial gradients. Advection also translates local growth or loss to commonly observed patchiness in phytoplankton distributions [Martin 2003]. Lucas et al. [2009; 1999] have shown how lateral transport from a productive area can result in chlorophyll *a* (CHL-*a*) accumulation in an adjacent deep and unproductive channel proposing that spatial structures are either of local origin or a consequence of variable transport. Apart from the studies of Lucas et al. [1999] in a shallow estuary, little is known about the interaction of advection with spatio-temporal variability in phytoplankton growth at intermediate to larger scales.

In the North Sea, Levin [1992] documented patchiness in CHL-*a* along a 5 to 10 *km* latitudinal transect. In the last two decades, satellite imagery has added a wealth of data on phytoplankton blooms around the globe and proven to be a useful tool to enhance the understanding of ecosystem function. In temperate coastal seas and especially in the North Sea, however, high cloudiness strongly restricts the availability of data and often prevents the use of satellite imagery to detect fast biological dynamics on a scale of only a few days.

High-frequency and time-continuous measurements by autonomous systems installed on ferries are filling this gap since recently. These FerryBoxes enable physical, chemical and biological observations along the one-dimensional tracks of a growing number of ships of opportunity, mostly sailing in European waters [Ainsworth 2008]. Data from a FerryBox operating on the route between Cuxhaven, Germany and Harwich, UK, reveal intense mesoscale patterns in CHL-*a* [Petersen et al. 2008]. Bloom development in the English Channel as well as along the continental coast significantly differed in timing, location, and magnitude from 2004 to 2005.

Mesoscale patchiness (1 to 100 *km*) is a property of phytoplankton distributions, which still challenges state-of-the-art ecosystem models. Coupled physical–biogeochemical models for the North Sea reproduce typical cross-shore gradients in CHL-*a* in the Southern Bight [Lacroix et al. 2007] or the German Bight [Tian et al. 2009], but fail to reproduce prominent characteristics observed in time-series or FerryBox data. Despite high-frequency physical forcing and narrow grid spacing, these

models are not able to generate significant alongshore variability and sharp temporal gradients. One reason for this limited capability is that in coupled ecosystem models lateral gradients in CHL-*a* are to a high degree determined by local factors. In the study of [Tian et al. 2009], for example, even the integration of (model-derived) turbidity fields did not lead to much increased spatio-temporal variability. This demonstrates that Eulerian ecosystem models, despite resolving mesoscale features of the circulation and spatially heterogeneous physical forcing, still tend to underestimate the variability of biological state variables in coastal seas.

We therefore apply a Lagrangian approach for simulating and understanding mesoscale dynamics in coastal spring blooms. For theoretical or educational purposes, Woods et al. [2005] introduced ensembles of "ecosystem tracers" advected by physical circulation. Developing further this concept, we use ensembles of Lagrangian ecosystems to study the origin of strong alongshore (i.e. isobath) gradients in net phytoplankton growth.

## 2.2 Study area

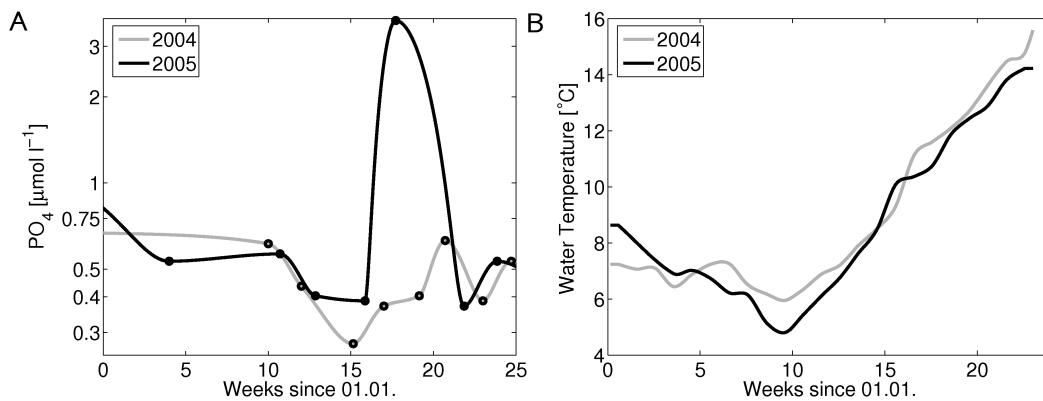


Figure 2.2: **A** Phosphate in filtered surface water as the mean of measurements at two stations off the Dutch coast ( $5.10^{\circ} E$ ,  $53.46^{\circ} N$  and  $5.15^{\circ} E$ ,  $53.41^{\circ} E$ , fig. 2.1) in 2004 (grey line) and 2005 (black line) (source: DONAR database operated by the Dutch Ministry of Transport, Public Works and Water Management). **B** Weekly mean sea surface temperature, averaged between  $5$  and  $8^{\circ} E$  measured by the FerryBox in 2004 (grey line) and 2005 (black line).

The study area is a section off the German and Dutch North Sea coast ranging from the IJsselmeer in the West to the Elbe estuary in the East. It is limited by the Wadden Sea in the South and German Bight offshore waters in the North. Prevailing westerly winds [Siegismund and Schrum 2001] and the counter-clockwise tidal wave result in an eastward mean current that closely follows the coastline [Staneva et al. 2009]. Winds and tides also keep this shallow coastal sea with water depths below  $40 m$  well mixed throughout most of the year. Several rivers (Fig. 2.1: Elbe, Weser, Ems, and Rhine

through the IJsselmeer) discharge into the German Bight supplying it with high nutrient loads [Beddig et al. 1997, Radach 1992]. Especially in the estuaries in the East, waters are highly turbid due to riverine suspended particulate matter. Waves and currents additionally enhance the resuspension of sediment from the soft bottom [Staneva et al. 2009] causing a steep turbidity gradient from the shore to the open sea. Water temperatures range from close to zero in winter to values exceeding  $20^{\circ}\text{C}$  during calm periods in warm summers [Wiltshire and Manly 2004].

Phytoplankton in this region exhibits an articulate annual cycle with low winter production due to light limitation and low temperatures followed by a distinct spring bloom that is later terminated by nutrient limitation and grazing [Iriarte and Purdie 2004]. Often, a second phytoplankton bloom develops in late summer before light conditions prevent significant primary production. Thereafter, nutrients recover to maximum winter values [Loebl et al. 2009, Wiltshire et al. 2008].

## 2.3 Methods

### 2.3.1 Measured data

Most data presented in this study were measured by a FerryBox [Petersen et al. 2008; 2003] that was installed on a ferry sailing from Cuxhaven, Germany to Harwich, UK several times a week (Fig. 2.1). In this study, the FerryBox variables temperature, turbidity and CHL-*a* are used. Irradiance data was obtained from a measurement pile in the Wadden Sea, which is located on the eastern edge of the study area (Fig. 2.1, [www.coastlab.org](http://www.coastlab.org)). Nutrient data from the FerryBox are not considered because of the unsatisfactory data coverage in the study period and their uncertain quality. Instead, phosphate data from two stations in Dutch waters ( $5.10^{\circ}\text{E}$ ,  $53.46^{\circ}\text{N}$  and  $5.15^{\circ}\text{E}$ ,  $53.41^{\circ}\text{E}$ ) are used. See Appendix for more details.

### 2.3.2 Model architecture

An individual-based model describes the physical and ecological dynamics of the phytoplankton in the study area. While transport due to advective processes is simulated by a Lagrangian particle tracking model, the dynamics of nutrients  $N$ , phytoplankton  $P$  and zooplankton  $Z$  is accounted for by an ecosystem model, which runs in each particle.

Hydrodynamics in the German Bight are driven by prevailing westerly winds and semi-diurnal tides resulting in a dominant alongshore, i.e. north-easterly or south-westerly, current. This feature is relatively stable throughout the year and becomes also evident from the analysis of currents generated by the General Estuarine Transport Model (GETM, Staneva et al. [2009], Stips et al. [2004]), which is especially suited to simulate the hydrodynamics in tidally-dominated shallow seas (Fig. 2.3). Significant correlations between the horizontal current components motivated a projection of the two-

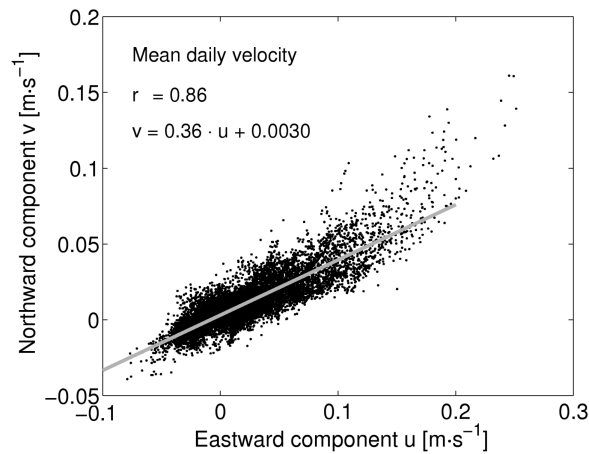


Figure 2.3: Mean daily current components near the ferry route calculated by the General Estuarine Transport Model (GETM) for the first 20 weeks in 2004. Considered GETM grid points are indicated as black dots in Fig. 2.1

dimensional flow field onto the mean axis of transport. In doing so, the model domain is reduced to a one-dimensional transect, while the general hydrodynamic properties are preserved. Furthermore, vertical homogeneity is assumed, since the study area is shallow with depths between 25 and 35 m and the water column is well-mixed during the period of interest in spring. This is supported by Joint and Pomroy [1993], who found no chlorophyll gradients within the euphotic zone at most sites in the North Sea.

Particles are transported by a particle tracking model, which uses the zonal component  $u$  of the mean daily current velocity generated by GETM while the meridional component  $v$  is defined as a linear function of  $u$  (see Appendix). A Lagrangian particle, thus, moves along the one-dimensional transect shown in Fig. 2.1. The entire simulation then consists of an ensemble of particles with different initial conditions (for  $N$ ,  $P$  and  $Z$ ) and particle trajectories, which are subject to different physical forcings (temperature, turbidity and photosynthetically active radiation (PAR)).

### 2.3.3 Ecosystem Model

Each particle carries a conceptualised ecosystem consisting of three compartments for one nutrient  $N$ , phytoplankton  $P$  and zooplankton  $Z$ . All variables are in phosphorus units. Primary production  $P_P$  is regulated by light following the approach of Ebenhöf et al. [1997]. Furthermore, temperature and the availability of nutrients affect the production of phytoplankton biomass.

$$P_P = \mu_P \cdot TPT \cdot NPT \cdot LPT \cdot P \quad (2.1)$$

where  $\mu_P$  denotes the maximum growth rate of phytoplankton and TPT, NPT, and LPT are the production terms of temperature, nutrients and light, respectively.  $P_P$  links the consumption of nutrients to the growth of phytoplankton, which is additionally subject to zooplankton grazing  $P_Z$ . Thus, the model system describing the dynamics of all three compartments is given by

$$\frac{\partial N}{\partial t} = -P_P \quad (2.2)$$

$$\frac{\partial P}{\partial t} = P_P - P_Z \quad (2.3)$$

$$\frac{\partial Z}{\partial t} = \beta \cdot P_Z, \quad (2.4)$$

with the zooplankton assimilation efficiency  $\beta$ . A more detailed model description is given in the Appendix. Because of the omission of detritus and, consequently, the remineralisation, the model systematically underestimates nutrient concentrations. To our understanding, this simplification is not critical in winter and spring, since the nutrient concentration remains above limiting levels during most of the simulation period.

## 2.4 Parametrisation, initial conditions and forcing

Table 2.1: Model parameters and their values (see also Appendix).

Symbol	Definition	Value	Unit	Ref.
$a$	Light extinction parameter	0.15	$[m^{-1} \cdot FTU^{-1}]$	Devlin et al. [2008]
$b$	Extinction offset	0.05	$[m^{-1}]$	Devlin et al. [2008]
$\beta$	Zooplankton assimilation efficiency	0.5	[ ]	
$I_{opt}$	Scaling parameter of the $p/I$ -curve	225	$[W \cdot m^{-2}]$	Ebenhöh et al. [1997]
C:P	Carbon to phosphorus ratio	106	$[mol C \cdot (mol P)^{-1}]$	Redfield ratio
CHL:C	CHL- $a$ to carbon ratio	0.3	$[g CHL-a \cdot (mol C)^{-1}]$	Faure et al. [2006] Llewellyn et al. [2005] Geider [1987]
$k_N$	Half-saturation of nutrients limitation	0.5	$[\mu mol P \cdot l^{-1}]$	
$k_P$	Half-saturation of grazing	0.75	$[\mu mol P \cdot l^{-1}]$	
$\mu_P$	Phytoplankton maximum growth rate	0.69	$[d^{-1}]$	Cloern [1995], Furnas [1990]
$\mu_Z$	Zooplankton maximum growth rate	0.56	$[d^{-1}]$	Stelfox-Widdicombe et al. [2004]
$Q_{10,P}$	Temperature sensitivity zooplankton	3.0	[ ]	Raven and Geider [1988]
$Q_{10,Z}$	Temperature sensitivity phytoplankton	2.0	[ ]	Hansen et al. [1997]
$r_{PAR}$	Ratio between incident irradiance and PAR	0.5		Ebenhöh et al. [1997]
$r_Z$	Initial zooplankton fraction	0.04	[ ]	
$\tau_Z$	Time lag for zooplankton initialisation	14	$[d]$	
$T_0$	Reference temperature	10	$[^{\circ}C]$	
$Z_{min}$	Minimum zooplankton biomass	0.0075	$[\mu mol P \cdot l^{-1}]$	

Every six hours a particle is released at  $5.4^{\circ} E$  during the first 20 weeks in 2004 and 23 weeks in 2005. Initial values for nutrient and phytoplankton concentrations are derived from measurements (Fig. 2.2). Phytoplankton biomass is converted from CHL- $a$  data by means of two constant ratios.

A Redfield C:P ratio and a Chl:C ratio of  $0.3 \text{ g CHL-}a \cdot (\text{mol C})^{-1}$  are assumed. The latter is in agreement with several measurements in the southern North Sea [Llewellyn et al. 2005, Geider 1987]. These authors, however, also clearly report a high variability in Chl:C and its dependence on several factors of which temperature, nutrient and light availability have been regarded to be most important [Taylor et al. 1997, Cloern 1995]. Similar effects are known for C:P [Elser et al. 2000, Klausmeier et al. 2004]. Fixing the the Chl:P ratio, thus, implies a strong simplification, which introduces a significant uncertainty into the model. Zooplankton data are unavailable in the required spatial and temporal resolution. Instead, initial zooplankton biomass at the initial position  $x_0$  is estimated as a fraction of the phytoplankton biomass at a previous time. During the first half of the year, the assumption of zooplankton lagging behind phytoplankton is well documented at the nearby time-series station of Helgoland roads [Greve et al. 2004]. Later in the year, however, the zooplankton initialisation clearly loses its validity. After initialisation, the evolution of the three ecosystem variables is determined by the water depth  $\zeta$ , the water temperature  $T$ , and the light climate.  $T$  and  $\zeta$  are derived from FerryBox measurements and the GETM bathymetrie, respectively. The light climate is calculated using hourly surface PAR  $I_0$ , which is derived from incident irradiance data from a measurement pile, and measured turbidity (Fig. 2.5, cf. Appendix).

Most parameter values have been manually calibrated within known ranges and according to literature values (Tab. 2.1). Four sensitive parameters ( $I_{opt}$ ,  $k_N$ ,  $k_P$  and  $Z_{min}$ ) that were identified manually, however, are calibrated with the objective of (1) maximising the lateral CHL-*a* gradient along the transect in 2005, and (2) minimising the gradient in 2004(cf. Fig2.4). Therefore, the simulated ratio of mean CHL-*a* in two neighbouring regions during the spring bloom is calculated and compared to the rati derived from measurements.

## 2.5 Results

### 2.5.1 Measured spring bloom dynamics

A continuous spring bloom is observed by the FerryBox throughout the study area in 2004 (Fig. 2.5). Starting in the western part in week 12, a patch with CHL-*a* concentrations above  $30 \mu\text{g l}^{-1}$  developed eastward within six weeks. Measured turbidity data, however, exhibits an inverse pattern (Fig. 2.5). While winter values fluctuated considerably between 2 and 10 *FTU*, the variability decreased throughout spring and values below 3 *FTU* indicate good light availability. The spatial and temporal extend of the minimum in turbidity closely resembles the pattern of maximum CHL-*a* . Parallel to turbidity, incident irradiances (not shown) supported the onset and decay of the bloom with already high values in week 12 and 13 and several days with relatively low values in week 19. Low temperatures did not prevent the growth of phytoplankton, as the onset of the spring bloom around week 12 in 2004 coincided with the coldest period in this year (Fig. 2.2). Thereafter, temperature was steadily

rising as was CHL-*a* .

Though phosphate data are relatively sparse compared to Ferrybox measurements, it nonetheless outline the high temporal dynamics of phosphate during the spring (Fig. 2.2). After a steep decrease from winter values phosphate concentrations already marked a turning point around week 15, which was followed by a significant recovery until week 20. Phosphate concentration started to decrease from winter values of  $0.7 \mu\text{mol l}^{-1}$  between week 10 and 12, marked a low in week 15, and recovered until the end of the period considered in this study (week 20).

In 2005, an articulate bloom with CHL-*a* above  $20 \mu\text{g l}^{-1}$  only occurred in the western part of the study area (Fig. 2.5). Measured CHL-*a* rarely exceeded  $5 \mu\text{g l}^{-1}$  further east between  $6.4^\circ E$  and  $7.5^\circ E$ . Unlike in 2004, patterns of high chlorophyll concentrations were associated with high turbidity in 2005 and the minimum of turbidity already occurred before the onset of the spring bloom between week 12 and 15. After phosphate concentrations decreased slightly during the initial phase of the bloom, exceptionally high values exceeding  $3 \mu\text{mol l}^{-1}$  were measured during the maximum of the bloom in week 18 (Fig. 2.2).

### 2.5.2 Sensitivity analysis

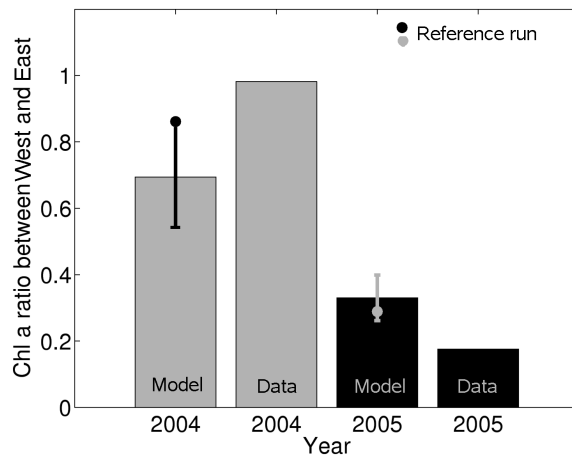


Figure 2.4: Sensitivity of model results to the systematic variation of four parameters ( $I_{opt}[125 \dots 225 W \cdot m^{-2}]$ ,  $k_N[0.3 \dots 0.7 \mu\text{mol P} \cdot l^{-1}]$ ,  $k_P[0.25 \dots 0.9 \mu\text{mol P} \cdot l^{-1}]$  and  $Z_{min}[0.0075 \dots 0.015 \mu\text{mol P} \cdot l^{-1}]$ ) regarding the zonal gradient in CHL-*a* . The gradient is expressed as the ratio of mean CHL-*a* concentrations in two adjacent areas as shown in Fig. 2.5. Values below one indicate higher CHL-*a* in the West than in the East. Errorbars show the standard deviation of a total of 162 model runs, solid circles denote the ratios of the reference run. Data bars display the same ratio derived from FerryBox measurements.

A systematic variation of the four parameters  $I_{opt}$ ,  $k_N$ ,  $k_P$  and  $Z_{min}$  reveals considerable robustness of the obtained CHL-*a* patterns with respect to uncertain parameters. While absolute values

of CHL-*a* are strongly depending on the parametrisation, the ratio of CHL-*a* concentrations in two zonally adjacent areas turned out to be rather consistent (see Fig. 2.5 for the definition of the areas) indicating that a different mechanism was dominant in each of the years.

In 2004, there is no spatial gradient in the measured data and the simulations reveal a mean ratio close to 0.7, i.e. slightly higher CHL-*a* values in the West than in the East (Fig. 2.4). In the following year, the measured ratio indicates distinctively higher CHL-*a* concentrations in the West than in the East and the simulations resemble that relation with a mean value below 0.4. Even the systematic sensitivity study did not produce much higher values. The selected reference parametrisation given in Table 2.1 is not optimal for reproducing the CHL-*a* data in each of the years, but presents a compromise to simulate qualitatively different phytoplankton dynamics in two consecutive years with a constant set of parameters. Following model results have been produced with this reference parameter set.

### 2.5.3 Bloom control by light climate in 2004

The model produces an articulate spring bloom extending over the entire longitudinal range of the study area in 2004 (Fig. 2.5). In the West, where the phytoplankton bloom develops earliest around week 11, CHL-*a* already declines again at the end of the simulation, while the phytoplankton population is still growing in the eastern part of the German Bight. While the timing of the spring bloom is closely matched, its amplitude of around  $30 \mu\text{g l}^{-1}$  east of  $6.4^\circ E$  is slightly underestimated. As in the data, the phase of strong phytoplankton growth initiates shortly after a sharp drop in turbidity from above  $3 \text{ FTU}$  to  $1.5 \text{ FTU}$  (Fig. 2.6). The drop in the light production term (LPT) at the end of the bloom period is, however, not linked to turbidity but to low incident irradiances.

Primary production in the model is mostly determined by the availability of light and nutrients. While the distribution of the LPT closely resembles the chlorophyll distribution, the nutrient production term (NPT) indicates only negligible nutrient limitation throughout most of the simulation period (Fig. 2.5). The NPT only reaches growth-limiting values close to zero west of  $6.4^\circ E$  after week 17. Farther east, nutrients are not yet limiting phytoplankton growth by the end of the simulation period. Zooplankton (not shown) only has a minor impact on the phytoplankton during most of the simulation. Grazing causes, however, the collapse of the phytoplankton bloom after the exhaustion of nutrients in the western part. Since net growth rates under nutrient-depleted conditions are low, phytoplankton then becomes increasingly vulnerable to grazing pressure.

### 2.5.4 Bloom advection in 2005

No continuous plankton bloom develops during the first 23 weeks of 2005. Simulated CHL-*a* exceeds  $30 \mu\text{g l}^{-1}$  only in the vicinity of the initial particle position at  $5.4^\circ E$  in late spring. Nonetheless, the patch of elevated CHL-*a* values, extending from the western border of the study area to approximately

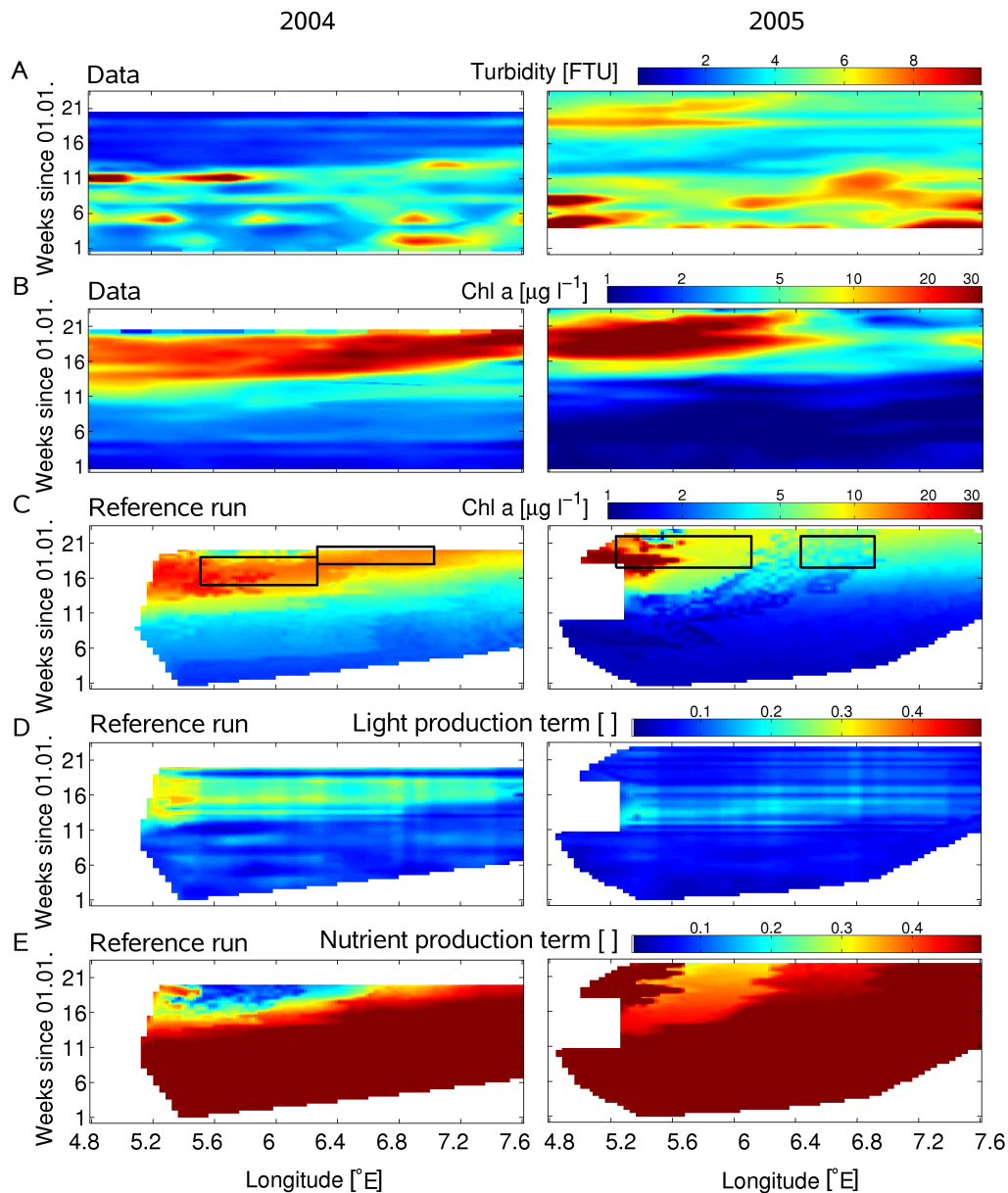


Figure 2.5: **A** Turbidity measured by the FerryBox between Cuxhaven, Germany and Harwich, UK in 2004 and 2005 (Fig. 2.1); See Appendix for more details on the data treatment. **B** CHL-*a* measured by the FerryBox (cf. A). **C** Simulated CHL-*a* concentration; squares indicate areas that are used to calculate the CHL-*a* gradient for the sensitivity study (see section 2.3 for more details); the data gap at the western edge in 2005 is due to missing particle coverage. **D** Simulated light production term (Eq. (2.1), (2.8)). **E** Simulated nutrient production term (Eq. (2.1), (2.8)).

6.4° E, is also reproduced by the model, albeit less pronounced than in the measurements.

While the model clearly underestimates enhanced growth rates between week 15 and 18, the temporal dynamics of phytoplankton in the first weeks of the spring bloom is well captured (Fig. 2.6). In the

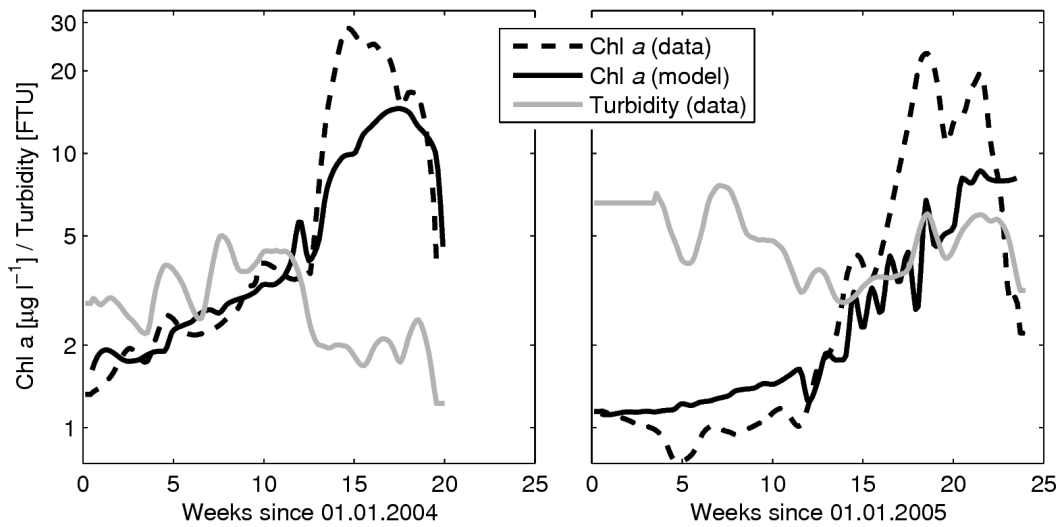


Figure 2.6: Measured (black dashed) and simulated (black solid) CHL-*a* and measured turbidity (grey) at  $6.2^{\circ} E$ .

last weeks of simulation, phytoplankton biomass is still growing when measurements already indicate the collapse of the bloom (week 22 – 23).

Although light conditions begin to improve between week 12 and 16, they never reach the favourable levels observed in 2004 (Fig. 2.5). Indeed, the LPT even falls back to winter values in the West. In this year, turbidity is clearly determining the light availability while the variability in the incident irradiance is not noticeable in the LPT. In contrast to light conditions, nutrient availability does not limit the growth of phytoplankton in spring. As in 2004, a notable impact of zooplankton (not shown) only occurs in areas of high phytoplankton biomass. Grazing is, thus, strongest near the particle release position in the late phase of the spring bloom.

By resolving the path of single trajectories it is possible to assess the role of hydrodynamics in the spatial division of the study area into a western and an eastern part (Fig. 2.7). All particles that are located east of  $6.3^{\circ} E$  after week 15 are initialised with rather low CHL-*a* values during the first weeks of 2005 and stay off the Frisian coast during the entire simulation period. Algal biomass of the majority of these particles does never exceed  $7 \mu g \text{ CHL-}a \text{ l}^{-1}$  because low light availability prevents higher productivity (Fig. 2.5). In contrast, water masses that form the high CHL-*a* patch west of  $6.3^{\circ} E$  entered the study area during a period of strong eastward drift within only a few days (small circle in Fig. 2.7). Along with this eastward inflow in week 14, the measured CHL-*a* at the initial position rises severalfold. The trajectories originating during this event later constitute the eastern envelope of the high CHL-*a* patch. Furthermore, they even resemble the characteristic two-tailed shape of the CHL-*a* maximum between  $6$  and  $6.5^{\circ} E$  (big grey circle in Fig. 2.7), which appears in the data between week 18 and 21 (Fig. 2.5).

To summarise, growth conditions in the study area are rather homogeneous throughout the study

area in 2005. The division between high CHL-*a* in the West and significantly lower concentrations in the East can therefore be attributed to a pronounced eastward drift importing high CHL-*a* waters from the adjacent Southern Bight into the western German Bight. To further substantiate the influence of hydrodynamics on the mesoscale bloom structure, the simulation for 2005 is also conducted with the 2004 currents (Fig. 2.8). All other forcings and boundary conditions remain unchanged in this set-up. The results of this model set-up clearly fail to generate the steep CHL-*a* gradients observed in the data. Hydrodynamics in 2004 lack the pronounced inflow that causes the eastward advection of particles with high initial CHL-*a* values far into the central areas of the study area.

## 2.6 Discussion

Despite the model's simplicity regarding spatial resolution and ecosystem structure, it is capable of reproducing the general spatio-temporal distribution of CHL-*a* off the Frisian Wadden Sea as measured by the FerryBox on the Cuxhaven - Harwich ferry in 2004 and 2005. More important, our results suggest that different mechanisms - turbidity dynamics and variability of alongshore currents - have led to the observed mesoscale differences in blooming patterns of phytoplankton in the two years of interest.

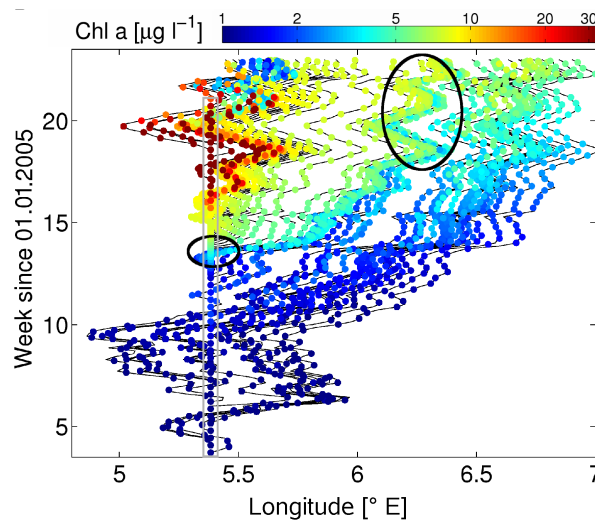


Figure 2.7: Model trajectories coloured according to their simulated CHL-*a* values; all particles are released at  $5.4^{\circ} E$ . The small ellipse marks the eastward inflow of a water mass with elevated phytoplankton concentrations; the big grey circle indicates the fate of the first particles released within the small circle that later in the spring bloom form the border between a high and a low CHL-*a* region.

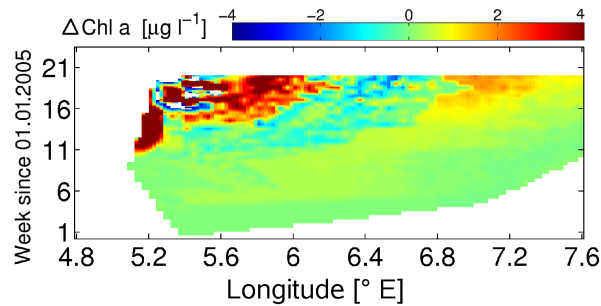


Figure 2.8: Differences in CHL-*a* between the reference run in 2005 and the same run with 2004 hydrodynamics. Deviations are only attributable to differences in the current system.

### 2.6.1 Light climate

Typical for phytoplankton in temperate coastal seas, the 2004 spring bloom was triggered by a change in the light climate [Weston et al. 2008, Iriarte and Purdie 2004, Cloern 1996]. Besides increasing solar irradiances, especially a drop in turbidity greatly improved growth conditions for autotrophs in this year. Turbidity close to estuaries can, in general, be related to winds, tides, and SPM input from rivers [Iriarte and Purdie 2004, May et al. 2003, Cloern 1996], but it may also be raised by planktonic organisms in the water column [Tilzer 1983]. It is beyond the scope of this study to explicitly assess the role of different factors in leading to the rapid decrease of turbidity. Weak winds from easterly directions in weeks 15 to 19, however, likely favoured the clearance of the water column (data from Wadden Sea measurement pile, not shown). Consequences of ceasing light limitation are accurately predicted by the model, in particular with respect to the spring bloom timing throughout the entire study area. The rapid response of phytoplankton to changes in the available light resource, both in the data as well as in the model, thus, corroborates the pivotal role of SPM in controlling the spring bloom, at least in some years [Tian et al. 2009].

In 2005, the spring bloom developed despite unfavourable light conditions. Instead of a clear water phase, measurements reveal highest turbidity values along with maximum CHL-*a*. Weak temporal and spatial variability in the LPT in 2005 cannot account for the observed variability in CHL-*a*. Even strong incident irradiance does not significantly improve the light availability for phytoplankton in highly turbid waters. Phytoplankton blooming is, hence, not always a direct consequence of the local light conditions.

### 2.6.2 Hydrodynamics

The phytoplankton distribution in 2005 is clearly controlled by advection underlining the importance of the circulation for modelling ecosystems in highly dynamic coastal seas [Skogen and Moll 2005]. In this case, bloom formation is determined by the simulated eastward inflow of a distinct water mass

with elevated CHL-*a* concentration. This is supported by the interpretation of the particle trajectories as well as by the occurrence of high saline water off the West Frisian coast (FerryBox data, not shown). In contrast, water masses that form the CHL-*a* minimum zone east of  $6.3^{\circ} E$  have resided in coastal waters off the Frisian coast for months experiencing unfavourably light conditions due to high turbidity. The light history of particles is hence distinctively affected by hydrodynamics which in 2005 prevented higher CHL-*a* further east.

The influence of the current pattern is also shown by the artificial alteration of the hydrodynamics in the model. In the 2005 simulation with 2004 hydrodynamics the spatial CHL-*a* gradient is significantly reduced compared to the reference run.

There is further evidence for the inflow hypothesis from observations of the MERIS satellite described by Petersen et al. [2008]: In week 15 a high CHL-*a* area extended from the Rhine estuary to western German Bight waters. Five weeks later, the westward detachment of a large patch of the coastal bloom from the Dutch West Coast indicates the end of eastward inflow. Another two weeks later in week 22, the bloom already decayed in the western German Bight while a huge area of elevated CHL-*a* still persisted offshore in the English Channel.

Hence, hydrodynamic events can bring together water masses with very different history and biogeochemical signature and, as a consequence, lead to the development of steep gradients. This mechanism is strong in 2005, leading to an apparent division of the coastal German Bight into a western and an eastern part. Moreover, our results as well as the FerryBox data demonstrate that steep alongshore gradients may persist in the coastal German Bight despite high current variability.

### 2.6.3 Nutrients

Despite the reduction of riverine phosphorus inputs into the southern North Sea in the last decades, high winter values of phosphate and other nutrients still provide favourable conditions for primary producers in the German Bight [Cadée and Hegeman 2002]. The results from 2004 underline the crucial role of initial, i.e. winter, nutrient concentrations for the spring bloom since the simulated phytoplankton biomass is built up using solely the initial amount of phosphate in the Lagrangian particles. Remineralisation of nutrients through the microbial loop and benthic-pelagic coupling as well as additional nutrient inputs from one of the large rivers discharging into the German Bight are all neglected. We hence suggest that these processes only have a minor importance for algal growth during spring and/or can be compensated by setting a reference CHL:P ratio which is potentially overestimating values during spring. While nutrients are not affecting the timing or the spatial distribution of the spring bloom, phosphate limitation determines its duration in the coastal German Bight in most of the years [Loebl et al. 2009, Kuipers and van Noort 2008, van der Zee and Chou 2005, Skogen et al. 2004]. Also the amplitude of the bloom is generally determined by the incipient phosphate concentration. In 2004, the model does, however, not reproduce the observed eastward increase of CHL-*a* concentration, pos-

sibly due to the omission of additional nutrient inputs from major rivers (Ems, Weser and Elbe). The crucial role of phosphate motivates the usage of phosphorus as the currency of the ecosystem model. Silicate availability may, however, also become a driving factor as diatoms typically prevail before mass occurrence of *Phaeocystis* (see below and Loebel et al. [2007], Peperzak et al. [1998]).

In 2005, and unlike in 2004, nutrient supply remains sufficient during the entire simulation period since the model clearly underestimates phytoplankton growth and, as a consequence, also biomass in the western part of the study area. This also explains the failure of the model to reproduce the termination of the bloom correctly. We suggest that the disagreement is due to an underestimation of phytoplankton light requirements in 2005, possibly pointing at differences in the dominant algal groups in the two years of interest (see below).

#### 2.6.4 Grazing

Significant grazing on phytoplankton only occurs in the simulation towards the end of the spring bloom. This finding is also supported by Loebel et al. [2007] who observed a strong seasonality of microzooplankton in the coastal German Bight with low grazing pressure in early spring. High zooplankton levels are only hindcasted in the western part of the study area in both years. Here, the bloom starts earlier giving the zooplankton more time to respond to the higher prey availability. Together with decreasing growth rates because of the starting nutrient depletion, zooplankton grazing provokes a steep collapse of CHL-*a* in 2004 within 1 – 2 weeks. Farther East, both nutrient limitation and zooplankton grazing are still less strong by the end of the simulation in week 20.

In 2005, the inflow of CHL-*a* rich water masses, spatially uniform growth conditions, and weak grazing can only partly explain the marked alongshore differences in the observed CHL-*a* distribution. The model clearly overestimates CHL-*a* levels in the eastern part of the study area resulting in a less pronounced CHL-*a* gradient. The species distribution of zooplankton in the German Bight is strongly linked to water masses. Martens and Brockmann [1993] and Greve and Reiners [1988] suggest a wave-like spread of zooplankton originating in coastal or estuarine waters. During a winter survey Krause et al. [1995] found a significant eastward increase, i.e. towards less saline or more coastal waters, of zooplankton biomass. Stelfox-Widdicombe et al. [2004] compared microzooplankton at two locations in the Southern Bight of the North Sea during the spring bloom reporting distinctively higher grazing rates at the nearshore station. In the German Bight, a grazing gradient from oceanic to coastal waters may therefore also occur on an alongshore axis towards the estuaries of Elbe, Weser and, the Jade bay, along with the rising influence of estuarine water.

On the base of these findings, we suppose that the abrupt change of CHL-*a* in 2005, which is caused by the convergence of different water masses, may also be reflected in spatial heterogeneity of the zooplankton community, which is not resembled by the model. An important, yet often overlooked, factor that temporarily enhances grazing in nearshore waters is the mass occurrence of meroplanktonic lar-

vae of benthic invertebrates, which mostly originate in the adjacent intertidal Wadden Sea and can be therefore associated with low saline water masses [Brandt et al. 2008, Martens and Brockmann 1993]. Unlike other zooplankton groups, meroplanktonic larvae can appear in high abundances without a preceding phytoplankton bloom since their occurrence is solely depending on spawning. Smetacek and Cloern [2008] support this argument by recently stating that meroplankton has the potential to significantly influence lower trophic levels in coastal ecosystems like the German Bight.

### 2.6.5 Algal community structure and stoichiometry

Despite the general agreement with observations, the model results lack few features inherent to the data. The simulated phytoplankton growth, for example, is slower during the first weeks of the spring bloom than the measurements suggest in 2004. This mismatch is partly due to specific model formulations. The multiplication of terms in the formulation of the primary production (Eq. (2.1)) clearly leads to a conservative estimate compared to other approaches (e.g. the Liebig law of the minimum or temperature independence of the initial slope of the P/I-curve [Geider et al. 1998]).

Another origin of model errors can be linked to simplifications in the ecosystem model that completely neglects the intrinsic variability of all considered compartments (i.e. nutrients, algae and herbivores). Wirtz and Eckhardt [1996] have shown the critical relevance of variable traits in modelling multi-species phytoplankton communities. Intracellular element ratios are key variables of algal physiology, which also critically affect all model–data comparisons. Keeping CHL:C and C:P constant is, thus, not consistent with known variations in phytoplankton stoichiometry and introduces significant uncertainty. Deviations in the observed range between simulated and measured data are even much smaller than the reported range of variability of the two stoichiometric ratios [Llewellyn et al. 2005, Hecky and Kilham 1988, Geider 1987, Tett et al. 1985]. Much of the unexplained deviations between model and data could be, thus, mainly attributed to errors linked to fixed intracellular element ratios. That is, the consideration of variable intracellular element ratios appears essential to simulate the steepness of the observed gradients. In fact, measurements in the English Channel [Llewellyn et al. 2005] and Helgoland Roads (Wiltshire, unpublished) indicate the strong variability in CHL:C and it is an ongoing effort to represent the underlying mechanisms causing these fluctuations [Pahlow 2005].

Another important and variable trait for this study is the optimal irradiance  $I_{opt}$  [Macedo et al. 2001]. Changing photosynthetic characteristics do not only matter when simulating the course of a bloom, but may also be relevant for understanding interannual differences. In 2005, the underestimation of CHL-*a* in the western part can be attributed to an overrated light limitation that is caused by the selection of a too large  $I_{opt}$ . It appears therefore likely that diatoms, which have lower light requirements, e.g. a lower  $I_{opt}$ , than *Phaeocystis*, dominated the spring bloom in this year [Wiltshire et al. 2008, cf.]. Observations in the Dutch Wadden Sea in 2004, however, identified *Phaeocystis* to be the dominating species during April [Kuipers and van Noort 2008]. Higher numbers of diatoms were only observed

thereafter in May. It is likely that *Phaeocystis* was able to outcompete diatoms already early in 2004 because of the exceptionally high light availability after week 12.

### 2.6.6 1D Lagrangian modelling

The simplified approach of using moving particles along a one-dimensional projection entails several advantages: First, the transect matches the two adjacent ferry routes, so that the availability and reliability of physical forcing data and fluorescence measurements. This is particularly important as results indicate that mesoscale variability may originate from high-frequency fluctuations of ambient conditions. Of course, an extrapolation of simulated values to a larger area beyond the transect would require a different approach.

Advantages of the Lagrangian over the more common Eulerian approach for this study comprise the ability to preserve strong gradients and the possibility to easily assess the particle history. Furthermore, the one-dimensional approach entails a greatly reduced computational effort compared to higher-dimensional set-ups, facilitating parameter calibration and sensitivity studies [Soetaert and Middelburg 2008].

## 2.7 Conclusion

The study identified two different mechanisms explaining the observed spring dynamics of phytoplankton in a coastal marine ecosystem. In 2004 the buildup of CHL-*a* is determined by short term variability in turbidity. In contrast, detailed knowledge of the history of individual water masses is essential to understand the phytoplankton dynamics in 2005. Under severe light limitation due to high turbidity, the bloom has to be triggered by the import of water masses containing higher phytoplankton concentrations. In addition, spatial variability of zooplankton grazing with higher impact in coastal waters is probably enhancing the horizontal gradients in spring. Reducing the uncertainties regarding the variability of intracellular element ratios presents a major challenge to further improve the understanding of observed CHL-*a* gradients in the future.

The successful simulation of fundamentally different spring bloom dynamics in two consecutive years with constant parameters demonstrates the appropriateness of this simple coupled model for analysing the origin of mesoscale CHL-*a* patterns in spring blooms. Against the common trend of building ever more complex models, the reduction of hydrodynamic information to a lowpass filtered horizontal transect facilitates the understanding of mesoscale structures along the shore. The availability of high-frequency FerryBox data has thereby proven to be paramount. In this context, the attempt to reproduce time-series data of dynamic coastal systems without taking into account horizontal transport appears to be at least difficult. A satisfying correlation between ecosystem dynamics and local conditions in one period does not guarantee its validity in other time intervals. It remains surprising, however, that

the reproduction of alongshore variability is relatively successful despite the ignorance of cross-shore processes and turbulent diffusion in this tidally-dominated coastal sea.

Though our coupled Lagrangian ecosystem model is able to simulate the basic dynamics of the plankton community, it is obviously limited to the winter and spring period. Many assumptions, e.g. the ignorance of remineralisation processes or adaptation in algal stoichiometry and/or community structure, have to be re-considered prior to a potential application to the entire season. Our study also points to the relevance of time-continuous as well as spatially explicit data of herbivores including microzooplankton. A combination of operational FerryBox and CPR measurements would be, thus, an important step towards an effective characterisation of ecosystem dynamics in a regional shelf sea like the North Sea.

## 2.8 Appendix

### 2.8.1 Data integration

The considered FerryBox variables were measured by the following devices (analyser, manufacturer, country): Temperature  $T$  [ $^{\circ}C$ ] (PT100, FSI, USA), turbidity  $Tb$  [ $FTU$ ] (CUS31W2A, Endress & Hauser, Germany), salinity  $S$  [ $PSU$ ] (EXCELL, FSI, USA), and chlorophyll a (CHL- $a$ ) [ $\mu g l^{-1}$ ] (SCUFA-II, Turner Design, USA). All measured data are binned in time and space with a bin size of 7  $d$  and  $0.2^{\circ}$  to eliminate high frequency fluctuations and to fill smaller data gaps. By interpolating these coarse distributions to a higher resolution grid with a bin size of 1  $d$  and  $0.02^{\circ}$  smooth and consistent distributions are generated (Fig 2.5). Data gaps are filled with the nearest available value in time dimension, since a failure of a measurement device normally leads to missing data along the entire spatial domain.

Irradiance data are composed from pile data recorded at  $7.47^{\circ} E$ ,  $53.71^{\circ} N$  in the Wadden Sea during spring and summer (source: [www.coastlab.org](http://www.coastlab.org)) and synthetic values derived with the astronomic method described by Ebenhöf et al. [1997] for data gaps, which occur mainly in winter when the pile is not operating. Phosphate was measured in filtered surface water 4 and 10  $km$  off the Dutch coast ( $5.10^{\circ} E$ ,  $53.46^{\circ} N$  and  $5.15^{\circ} E$ ,  $53.41^{\circ} E$ ) approximately once a month (source: database DONAR operated by the Dutch Ministry of Transport, Public Works and Water Management, [www.waterbase.nl](http://www.waterbase.nl)).

### 2.8.2 Model architecture

The linear regression of vertically integrated, mean daily currents produced by a 3  $nm$  set-up of the General Estuarine Transport Model (GETM) reveals a significant correlation between their zonal and the meridional components ( $u$  and  $v$ ) in the vicinity of the ferry route (2004: Pearson  $r = 0.86$ ,  $p < 0.01$ , 2005:  $r = 0.81$ ,  $p < 0.01$ , vertically integrated daily mean currents during the 140 first days of the respective year, Fig. 2.1). Hence, daily mean currents are directed either to the Northeast or to the Southwest. The reliability of this projection, however, declines outside the range between  $5.2^{\circ} E$  and  $7.5^{\circ} E$  where the correlation is calculated. The particle tracking algorithm uses the mean daily zonal velocity component  $u$  generated by GETM to compute the meridional velocity component  $v$

$$v = a \cdot u + b \quad (2.5)$$

with the parameter values  $a = 0.349$  and  $b = 0.003 m \cdot s^{-1}$  derived by linear regression (first 140  $d$  of both years). In the following,  $b$  is neglected for its smallness. The current velocity  $w$  along the model domain at position  $x$  and time  $t$  is hence solely a function of  $u$  and given by

$$w(t, x) = \sqrt{u^2(t, x) + v^2(t, x)} = \sqrt{1 + a^2} \cdot u(t, x) \quad (2.6)$$

resulting in the change of position of particle  $i$

$$dx(t, x_i) = w(t, x_i) \cdot dt. \quad (2.7)$$

An explicit fifth-order Runge-Kutta algorithm is applied to integrate Eq. (2.7).

### 2.8.3 Ecosystem model

$P_P$  denotes the primary production of phytoplankton

$$P_P = \mu_P \cdot \overbrace{\epsilon_P}^{\text{Temperature}} \cdot \overbrace{\frac{N}{N + k_N}}^{\text{Nutrients}} \cdot \overbrace{\frac{1}{k_z \cdot \zeta} \cdot \int_{x_D}^{x_0} \frac{4}{1 + 4 \cdot x} dx}_{\text{Light}} \cdot P \quad (2.8)$$

with the maximum growth rate  $\mu_p$ , the half saturation constant for nutrient uptake  $k_N$ , the light attenuation coefficient  $k_z$ , and the water depth  $\zeta$ . The labelled terms in Eq. (2.8) are the dimensionless terms for the nutrient production (NPT) and the light production (LPT) and the temperature production (TPT). Following Ebenhöf et al. [1997], the depth integral of the  $p/I$ -curve is dimensionless with

$$x_0 = \frac{I_0}{I_{opt} \cdot \epsilon_P} \quad (2.9)$$

$$x_D = \frac{I_D}{I_{opt} \cdot \epsilon_P} \quad (2.10)$$

where  $I_0$  and  $I_D$  are the photosynthetically active radiation (PAR) at the surface and the bottom, respectively. PAR is assumed to be a constant fraction  $r_{PAR} = 0.5$  of the incident irradiance [Ebenhöf et al. 1997]. The corresponding  $p/I$ -curve is a Monod function with the scaling parameter  $I_{opt}$ .

All biological processes dependent exponentially on the water temperature  $T$

$$\epsilon_X = Q_{10,X}^{(T-T_0)/10}, \quad (2.11)$$

with  $Q_{10,X}$  determining the sensitivity to changes in  $T$  and the temperature  $T_0$  at which  $\epsilon_X = 1$ . The subscript  $X$  stands for either  $P$  (phytoplankton) or  $Z$  (zooplankton).

Observational evidence supports the use of a Holling-type III functional response to simulate the zooplankton grazing  $P_Z$  on phytoplankton [Gentleman et al. 2003, Verity 1991].

$$P_Z = \epsilon_Z \cdot \mu_Z \cdot \frac{P^2}{P^2 + k_P^2} \cdot Z, \quad (2.12)$$

with  $\mu_Z$  and  $k_P$  indicating the specific growth rate and the half saturation constant for grazing, respectively.

### 2.8.4 Initial conditions and forcing

The surface PAR  $I_0$  is regarded spatially uniform. Turbidity is a relative quantity that can be related to the diffuse light attenuation coefficient  $k_Z$ . This relationship is, however, variable and should be ideally established empirically [Davies-Colley and Smith 2001]. Here, it is estimated as

$$k_Z = a \cdot Tb + b \quad (2.13)$$

with the parameters  $a = 0.15 \text{ m}^{-1} \cdot \text{FTU}^{-1}$  and  $b = 0.05 \text{ m}^{-1}$ .

We assume that the initial value for the zooplankton concentration is a fraction  $r_Z$  of phytoplankton biomass  $P$  at the time  $t_0 - \tau_Z$

$$Z(t_0, x_0) = \max(Z_{\min}, P(t_0 - \tau_Z, x_0) \cdot r_Z), \quad (2.14)$$

where  $Z_{\min}$  and  $\tau_Z$  are the minimum zooplankton biomass and time lag for zooplankton, respectively.

## Acknowledgements

We thank F. Schroeder and W. Petersen for providing FerryBox data, J. Staneva for the hydrodynamic data from GETM and G. Flöser for the irradiance data from the GKSS measurement pile.

## Bibliography

- C. Ainsworth. Oceanography: FerryBoxes Begin to Make Waves. *Science*, 322(5908):1627, 2008.
- S. Beddig, U. Brockmann, W. Dannecker, D. Körner, T. Pohlmann, W. Puls, G. Radach, A. Rebers, H. J. Rick, M. Schatzmann, et al. Nitrogen fluxes in the German Bight. *Mar Pollut Bull*, 34(6): 382–394, 1997.
- G. Brandt, A. Wehrmann, and K. W. Wirtz. Rapid invasion of *Crassostrea gigas* into the German Wadden Sea dominated by larval supply. *J Sea Res*, 59(4):279–296, 2008.
- G. C. Cadée and J. Hegeman. Phytoplankton in the Marsdiep at the end of the 20th century; 30 years monitoring biomass, primary production, and Phaeocystis blooms. *J Sea Res*, 48(2):97–110, 2002.
- J. E. Cloern. An empirical model of the phytoplankton chlorophyll: Carbon ratio– the conversion factor between productivity and growth rate. *Limnol Oceanogr*, 40(7):1313–1321, 1995.
- J. E. Cloern. Phytoplankton bloom dynamics in coastal ecosystems: a review with some general lessons from sustained investigation of San Francisco Bay, California. *Rev Geophys*, 34(2):127–168, 1996.
- R. J. Davies-Colley and D. G. Smith. Turbidity, suspended sediment, and water clarity: A review . *J Am Water Resour As*, 37(5):1085–1101, 2001.
- M. J. Devlin, J. Barry, D. K. Mills, R. J. Gowen, J. Foden, D. Sivyver, and P. Tett. Relationships between suspended particulate material, light attenuation and Secchi depth in UK marine waters. *Estuar, Coast and Shelf Sci*, 79:429–439, 2008.
- W. Ebenhöh, J. G. Baretta-Bekker, and J. W. Baretta. The primary production model in the ecosystem model ERSEM II. *J Sea Res*, 38:173–192, 1997.
- J. J. Elser, R. W. Sterner, A. E. Galford, T. H. Chrzanowski, D. L. Findlay, K. H. Mills, M. J. Paterson, M. P. Stainton, and D. W. Schindler. Pelagic C: N: P stoichiometry in a eutrophied lake: responses to a whole-lake food-web manipulation. *Ecosystems*, 3(3):293–307, 2000.
- V. Faure, C. Pinazo, J. P. Torréton, and P. Douillet. Relevance of various formulations of phytoplankton chlorophyll a: carbon ratio in a 3D marine ecosystem model. *C. R. Biologies*, 329(10):813–822, 2006.
- M. J. Furnas. In situ growth rates of marine phytoplankton: approaches to measurement, community and species growth rates. *J Plankton Res*, 12(6):1117–1151, 1990.

- R. J. Geider. Light and temperature dependence of the carbon to chlorophyll *a* ratio in microalgae and cyanobacteria: implications for physiology and growth of phytoplankton. *New Phytol*, 106(1): 1–34, 1987.
- R. J. Geider, H. L. MacIntyre, and T. M. Kana. A dynamic regulatory model of phytoplankton acclimation to light, nutrients, and temperature. *Limnol Oceanogr*, pages 679–694, 1998.
- W. Gentleman, A. Leising, B. Frost, S. Strom, and J. Murray. Functional responses for zooplankton feeding on multiple resources: a review of assumptions and biological dynamics. *Deep-Sea Res II*, 50:2847–2875, 2003.
- W. Greve and F. Reiners. Plankton time-space dynamics in German Bight—a systems approach. *Oecologia*, 77(4):487–496, 1988.
- W. Greve, F. Reiners, J. Nast, and S. Hoffmann. Helgoland Roads meso- and macrozooplankton time-series 1974 to 2004: lessons from 30 years of single spot, high frequency sampling at the only off-shore island of the North Sea. *Helgol Mar Res*, 58:274–288, 2004.
- P. J. Hansen, P. K. Bjornsen, and B. W. Hansen. Zooplankton grazing and growth: Scaling within the 2–2000  $\mu\text{m}$  body size range. *Limnol Oceanogr*, 42(4):687–704, 1997.
- R. E. Hecky and P. Kilham. Nutrient limitation of phytoplankton in freshwater and marine environments: a review of recent evidence on the effects of enrichment. *Limnol Oceanogr*, 33(4):796–822, 1988.
- A. Iriarte and D. A. Purdie. Factors controlling the timing of major spring bloom events in an UK south coast estuary. *Estuar, Coast and Shelf Sci*, 61(4):679–690, 2004.
- I. Joint and A. Pomroy. Phytoplankton biomass and production in the southern North Sea. *Mar Ecol Prog Ser*, 99:169–169, 1993.
- C. A. Klausmeier, E. Litchman, and S. A. Levin. Phytoplankton growth and stoichiometry under multiple nutrient limitation. *Limnol Oceanogr*, 49(4):1463–1470, 2004.
- M. Krause, J. W. Dippner, and J. Beil. A review of hydrographic controls on the distribution of zooplankton biomass and species in the North Sea with particular reference to a survey conducted in January–March 1987. *Prog Oceanogr*, 35(2):81–152, 1995.
- B. R. Kuipers and G. J. van Noort. Towards a natural Wadden Sea? *J Sea Res*, 60(1-2):44–53, 2008.
- G. Lacroix, K. Ruddick, Y. Park, N. Gypens, and C. Lancelot. Validation of the 3D biogeochemical model MIRO&CO with field nutrient and phytoplankton data and MERIS-derived surface chlorophyll *a* images. *J Mar Syst*, 64(1-4):66–88, 2007.

- S.A. Levin. The problem of pattern and scale in ecology: the Robert H. MacArthur award lecture. *Ecology*, 73(6):1943–1967, 1992.
- C. A. Llewellyn, J. R. Fishwick, and J. C. Blackford. Phytoplankton community assemblage in the English Channel: a comparison using chlorophyll a derived from HPLC-CHEMTAX and carbon derived from microscopy cell counts. *J Plankton Res*, 27(1):103–119, 2005.
- M. Loebl, T. Dolch, and J. E. E. van Beusekom. Annual dynamics of pelagic primary production and respiration in a shallow coastal basin. *J Sea Res*, 58(4):269–282, 2007.
- M. Loebl, F. Colijn, J. E. E. van Beusekom, J. G. Baretta-Bekker, C. Lancelot, C. J. M. Philippart, V. Rousseau, and K. H. Wiltshire. Recent patterns in potential phytoplankton limitation along the northwest european continental coast. *J Sea Res*, 61(1–2):34–43, 2009. submitted.
- L. V. Lucas, J. R. Koseff, S. G. Monismith, J. E. Cloern, and J. K. Thompson. Processes governing phytoplankton blooms in estuaries 2: the role of horizontal transport. *Mar Ecol Prog Ser*, 187: 17–30, 1999.
- L. V. Lucas, J. R. Koseff, S. G. Monismith, and J. K. Thompson. Shallow water processes govern system-wide phytoplankton bloom dynamics: a modeling study. *J Mar Syst*, 75(1-2):70–86, 2009.
- M. F. Macedo, P. Duarte, P. Mendes, and J. G. Ferreira. Annual variation of environmental variables, phytoplankton species composition and photosynthetic parameters in a coastal lagoon. *J Plankton Res*, 23(7):719–732, 2001.
- P. Martens and U. Brockmann. Different zooplankton structures in the German Bight. *Helgol Mar Res*, 47(2):193–212, 1993.
- A. P. Martin. Phytoplankton patchiness: the role of lateral stirring and mixing. *Prog Oceanogr*, 57 (2):125–174, 2003.
- C. L. May, J. R. Koseff, L. V. Lucas, J. E. Cloern, and D. H. Schoellhamer. Effects of spatial and temporal variability of turbidity on phytoplankton blooms. *Mar Ecol Prog Ser*, 254:111–128, 2003.
- K. Muylaert, R. Gonzales, M. Franck, M. Lionard, C. van der Zee, A. Cattrijse, K. Sabbe, L. Chou, and W. Vyverman. Spatial variation in phytoplankton dynamics in the Belgian coastal zone of the North Sea studied by microscopy, HPLC-CHEMTAX and underway fluorescence recordings. *J Sea Res*, 55(4):253–265, 2006.
- M. Pahlow. Linking chlorophyll-nutrient dynamics to the Redfield N:C ratio with a model of optimal phytoplankton growth. *Mar Ecol Prog Ser*, 287:33–43, 2005.

- L. Peperzak, F. Colijn, W. W. C. Gieskes, and J. C. H. Peeters. Development of the diatom-*Phaeocystis* spring bloom in the Dutch coastal zone of the North Sea: the silicon depletion versus the daily irradiance threshold hypothesis. *J Plankton Res*, 20(3):517–537, 1998.
- W. Petersen, M. Petschatnikov, F. Schroeder, and F. Colijn. FerryBox systems for monitoring coastal waters. In H. Dahlien, N. C. Flemming, K. Knittis, and S. E. Petersson, editors, *Building the European Capacity in Operational Oceanography: Proc. Third International Conference on Euro-GOOS, Elsevier Oceanography Series Publication series*, volume 19, pages 325–333, 2003.
- W. Petersen, H. Wehde, H. Krasemann, F. Colijn, and F. Schroeder. FerryBox and MERIS – Assessment of coastal and shelf sea ecosystems by combining in situ and remotely sensed data. *Estuar, Coast and Shelf Sci*, 77(2):296–307, 2008.
- T. C. Prins, A. C. Smaal, A. J. Pouwer, and N. Dankers. Filtration and resuspension of particulate matter and phytoplankton on an intertidal mussel bed in the Oosterschelde estuary (SW Netherlands). *Mar Ecol Prog Ser*, 142(1):121–134, 1996.
- G. Radach. Ecosystem functioning in the German Bight under continental nutrient inputs by rivers. *Estuaries Coasts*, 15(4):477–496, 1992.
- J. A. Raven and R. J Geider. Temperature and algal growth. *New. Phytol.*, 110(4):441–461, 1988.
- F. Siegismund and C. Schrum. Decadal changes in the wind forcing over the North Sea. *Climate Res.*, 18(1/2):39–45, 2001.
- M. D. Skogen and A. Moll. Importance of ocean circulation in ecological modeling: An example from the North Sea. *J Mar Syst*, 57(3-4):289–300, 2005.
- M. D. Skogen, H. Söiland, and E. Svendsen. Effects of changing nutrient loads to the North Sea. *J Mar Syst*, 46(1-4):23–38, 2004.
- V. Smetacek and J. E. Cloern. Oceans: On Phytoplankton Trends. *Science*, 319(5868):1346, 2008.
- A. F. Hofmann K. Soetaert and J. J. Middelburg. Present nitrogen and carbon dynamics in the Scheldt estuary using a novel 1-D model. *Biogeosciences*, 5(4):981–1006, 2008.
- U. Sommer. *Biologische Meereskunde*. Springer, 1998.
- J. Staneva, E. V. Stanev, J. O. Wolff, T. Badewien, R. Reuter, B. Flemming, A. Bartholomä, and K. Bolding. Hydrodynamics and sediment dynamics in the German Bight. a focus on observations and numerical modelling in the East Frisian Sea. *Cont Shelf Res*, 29(1):302–319, 2009.

- C. E. Stelfox-Widdicombe, S. D. Archer, P. H. Burkill, and J. Stefels. Microzooplankton grazing in Phaeocystis and diatom-dominated waters in the southern North Sea in spring. *J Sea Res*, 51(1): 37–51, 2004.
- A. Stips, K. Bolding, T. Pohlmann, and H. Burchard. Simulating the temporal and spatial dynamics of the north sea using the new model getm (General Estuarine Transport Model). *Ocean Dyn*, 54 (2):266–283, 2004.
- A. H. Taylor, R. J. Geider, and F. J. H. Gilbert. Seasonal and latitudinal dependencies of phytoplankton carbon-to-chlorophyll *a* ratios: results of a modelling study. *Mar Ecol Prog Ser*, 152:51–66, 1997.
- P. Tett, S. I. Heaney, and M. R. Droop. The redfield ratio and phytoplankton growth rate. *J Mar Biol Ass U.K.*, 65(2):487–504, 1985.
- A. C. Thomas, D. W. Townsend, and R. Weatherbee. Satellite-measured phytoplankton variability in the Gulf of Maine. *Cont Shelf Res*, 23(10):971–989, 2003.
- T. Tian, A. Merico, J. Su, J. Staneva, K. Wiltshire, and K. W. Wirtz. Importance of resuspended sediment dynamics for the phytoplankton spring bloom in a coastal marine ecosystem. *J Sea Res*, 2009. doi: 10.1016/j.seares.2009.04.001.
- M. M. Tilzer. The importance of fractional light absorption by photosynthetic pigments for phytoplankton productivity in Lake Constance. *Limnol Oceanogr*, 28(5):833–846, 1983.
- D. W. Townsend, L. M. Cammen, P. M. Holligan, D. E. Campbell, and N. R. Pettigrew. Causes and consequences of variability in the timing of spring phytoplankton blooms. *Deep-Sea Res*, 41(5): 747–765, 1994.
- P. G. Verity. Measurement and simulation of prey uptake by marine planktonic ciliates fed plastidic and aplastidic nanoplankton. *Limnol Oceanogr*, 36(4):729–750, 1991.
- K. Weston, N. Greenwood, L. Fernand, D. J. Pearce, and D. B. Sivyer. Environmental controls on phytoplankton community composition in the Thames plume, UK. *J Sea Res*, 60:262–270, 2008.
- K. H. Wiltshire and B. F. J. Manly. The warming trend at Helgoland Roads, North Sea: phytoplankton response. *Helgol Mar Res*, 58(4):269–273, 2004.
- K. H. Wiltshire, A. M. Malzahn, K. W. Wirtz, W. Greve, S. Janisch, P. Mangelsdorf, B. F. J. Manly, and M. Boersma. Resilience of North Sea phytoplankton spring bloom dynamics: An analysis of long-term data at Helgoland Roads. *Limnol Oceanogr*, 53(4):1294–1302, 2008.
- K. W. Wirtz and B. Eckhardt. Effective variables in ecosystem models with an application to phytoplankton succession. *Ecol Modell*, 92(1):33–53, 1996.

- 
- J. D. Woods, A. Perilli, and W. Barkmann. Stability and predictability of a virtual plankton ecosystem created with an individual-based model. *Prog Oceanogr*, 67(1-2):43–83, 2005.
- C. van der Zee and L. Chou. Seasonal cycling of phosphorus in the southern bight of the North Sea. *Biogeosciences*, 2(1):27–42, 2005.



## Chapter 3

---

# Rapid invasion of *Crassostrea gigas* into the German Wadden Sea dominated by larval supply

### 3.1 Introduction

Invasions of non-indigenous species into the North Sea have occurred numerous times in the past [Reise et al. 1999]. Besides shipping, the escape from aquaculture sites is a dominant vector promoting the introduction of alien species into the ecosystem. A recent example for the latter is the filter-feeding Pacific oyster (*Crassostrea gigas*), one of the most successful marine invaders, which is present at most Northeast Atlantic coasts today [Gollasch 2006, Ruesink et al. 2005]. Starting from two aquaculture sites in Oosterschelde, the Netherlands and Sylt, Germany (Fig. 3.1) the species spread along the coast of the Wadden Sea, which constitutes a large part of the continental coast of the North Sea and comprises extensive tidal flats. Although aquaculture activities with *C. gigas* started already in 1964, its distribution was restricted to the vicinity of the aquaculture sites for many years. Only in the last two decades, rising temperatures facilitated the successful reproduction in the field and promoted the colonisation of the entire Wadden Sea [Diederich et al. 2005]. Juvenile oysters in the Wadden Sea typically settle on valves of the blue mussel *Mytilus edulis*, which is one of the most abundant species in this ecosystem [Dankers and Zuidema 1995] and an important habitat engineer through the formation of extensive beds. These beds often present the only available hard-substrate in the intertidal zone. Besides the ecological relevance of *M. edulis*, the supply of juveniles from natural mussel beds is economically important for the traditional mussel fishery, which operates extensive subtidal culture plots [Smaal 2002]. Both species occupy the same niche in the ecosystem and especially the strong population growth in the recent years made *C. gigas* an important competitor for space and food. Still, it is unclear whether an equilibrium will establish between both species and what consequences will emerge from it [Diederich 2005, Smaal et al. 2005].

Oysters reproduce via free-swimming larvae, which become competent within two to four weeks depending on nutrition and temperature [Collet et al. 1999, His et al. 1989]. Larvae may be transported several tens of kilometres by currents and rely on the encounter of a suitable habitat to settle [Pechenik 1999]. The spawning period in the North Sea is short since favourable temperatures for spawning in this region only appear in summer and good spatfall could be directly related to exceptionally warm years [Diederich et al. 2005]. From the several millions of eggs produced by an adult individual [Kang

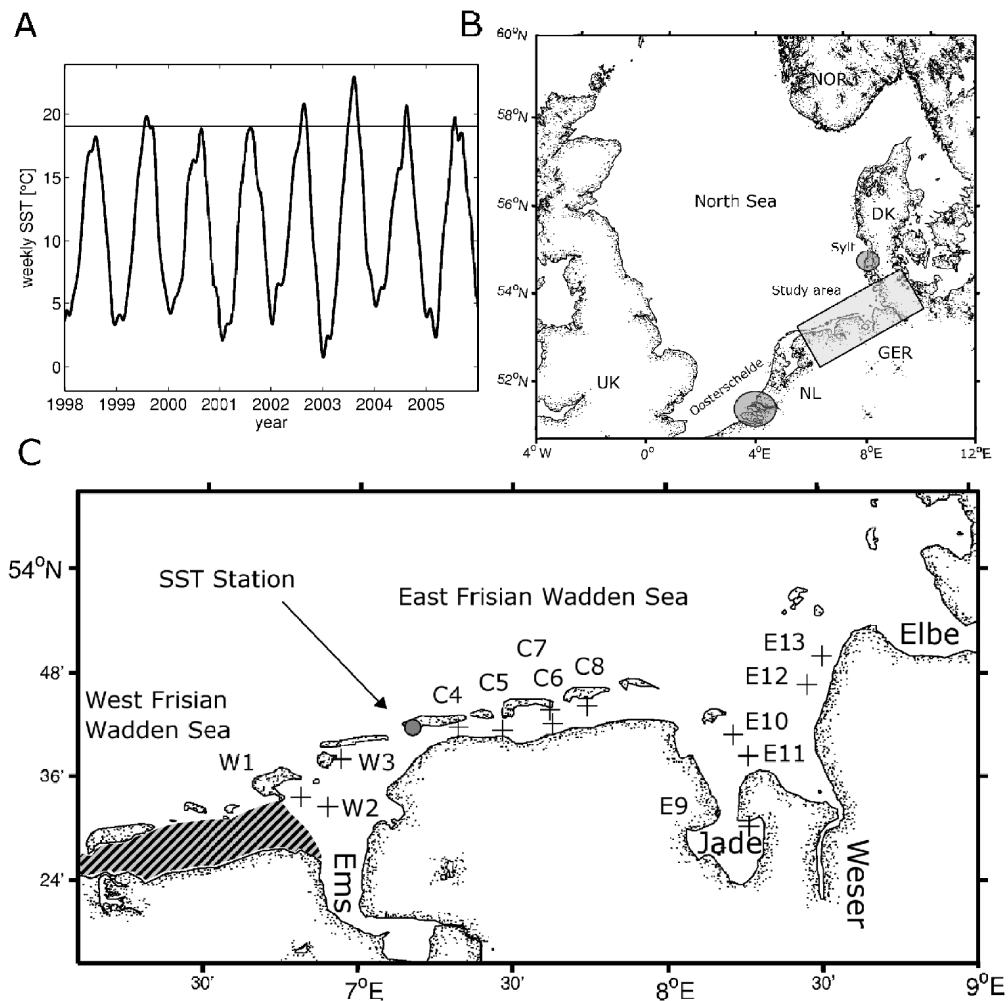


Figure 3.1: A - Reconstructed sea surface temperature (SST) by singular spectrum analysis from weekly measurements in the harbour of Norderney (Data source: Niedersächsischer Landesbetrieb für Wasserwirtschaft, Küsten- und Naturschutz (Regional authority for water management, coastal protection and conservation)). B - Location of the study area and the two regions of aquaculture activities with *Crassostrea gigas* the Oosterschelde, the Netherlands and the island of Sylt, Germany. C - Positions of the monitoring sites within the study area (crosses). The numbering is ascending with the abbreviations W=West, C=Central and E=East. The hatched area marks the area of the initial source population outside the study area in the West Frisian Wadden Sea (WFWS) and the grey dot denotes the position of the SST station at Norderney harbour.

et al. 2003] only very few larvae develop and survive the hazardous planktonic phase to settle [Rumrill 1990]. After successful metamorphosis and settlement, recruitment processes may significantly alter the larval supply pattern and cause mortalities exceeding 90% during the first year [Gosselin and Qian 1997, Hunt and Scheibling 1997]. Juveniles surviving the first life stages, however, grow very fast

and may become sexually mature within one year. Contrary to larvae and juveniles, adults experience only low mortalities [Diederich 2006].

Apparently, recruitment especially affects the success of an invasion, but whether the recruitment is representing the pattern of larval supply or being regulated by processes at the location of settlement, such as predation, competition or the suitability of local environmental conditions, is highly uncertain [Strasser and Günther 2001, Todd 1998, Caley et al. 1996, Underwood and Fairweather 1989, Roughgarden et al. 1988, Lewin 1986, Keough and Downes 1982]. Due to the difficulties in adequately

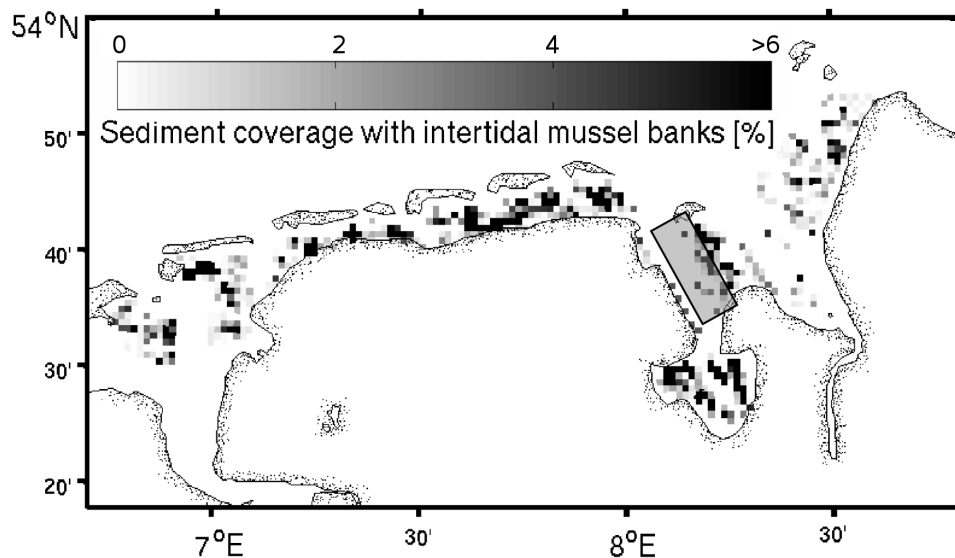


Figure 3.2: *Mytilus edulis*. Coverage of the intertidal zone with mussel beds that serve as substrate for competent larvae of *Crassostrea gigas* as reported by aerial surveys in 1999 (data source: Nationalparkverwaltung Niedersächsisches Wattenmeer (Administration of the Wadden Sea National Park of Lower Saxony)). The box indicates an area of extended mussel culture plots. In the model set-ups aS and SR juvenile *Crassostrea gigas* are artificially added to this box in 2001.

describing the transition between the mobile and the sessile phase, models of marine benthic invertebrates usually simulate only a part of the life cycle focusing either on larval transport [Viard et al. 2006, Barnay et al. 2003, Gilg and Hilbish 2003, Young et al. 1998] or adult physiology [Stillman et al. 2000, Scholten and Smaal 1998, Kobayashi et al. 1997]. Simulated supply patterns of larval transport models are then often directly compared to the observed recruitment assuming a purely supply-driven recruitment and ignoring all factors capable of modifying the supply pattern [van der Meer et al. 2001, Hunt and Scheibling 1997, Keough and Downes 1982].

In contrast, we simulate the invasion of *C. gigas* into a coastal habitat considering both, the adult and the larval phase of the species, and especially assess the impact of different recruitment formulations

on the population dynamics. The model yields predictions of the population dynamics for several years on the basis of an initial abundance estimation and constant parameter values. The simulated results are compared to data from a monitoring programme, which revealed abundance data of adult *C. gigas* in the East Frisian Wadden Sea (EFWS) in the years 2003 to 2005. The main questions of the model study can be divided into three categories: (1) Is the observed distribution of *C. gigas* explainable with an initial population only in the west of the EFWS [e.g. Wehrmann et al. 2000]? (2) Are the population dynamics controlled by larval supply or is there evidence for a significant modification of the supply pattern due to density-dependent or site-specific recruitment processes? (3) What are the potentials and limits of a model that is only constrained by few measurements and relies on many uncertain assumptions?

## 3.2 Methods

### Study Area

The study area reached from the Ems estuary (6.7° E, 53.5° N) to the Elbe estuary (8.6° E, 54.0° N) enclosing the entire East Frisian Wadden Sea (EFWS) (Fig. 3.1). Within this section, the 13 monitoring sites followed the coastline, extending over a distance of approximately 125 km. The shallow EFWS is characterised by extensive intertidal flats and channels, which reach maximum depths up to 30 m in the tidal inlets between the barrier islands. Semi-diurnal tides with amplitudes between 2.1 and 4.1 m [BSH 2006] induce strong currents exceeding  $2 \text{ m s}^{-1}$  in the estuaries of the rivers and the narrow tidal inlets. The freshwater inflow from the three major rivers Elbe, Weser and Ems and diffuse terrestrial drainage generate strong seaward salinity gradients with lowest values below 25 psu in the estuaries of the study area. Measured sea surface temperatures (Fig. 3.1) reveal a high seasonal variability ranging from  $0^\circ\text{C}$  in February to values above  $20^\circ\text{C}$  in July or August. The residual current off the coast of the EFWS is directed eastward due to the counterclockwise rotation of the tidal wave in the North Sea and prevailing westerly winds. Despite the harsh environmental conditions in the intertidal zone, the study area offers good growth conditions for filter feeding organisms due to its high nutrient and phytoplankton concentrations.

### 3.2.1 Monitoring data

The monitoring data were taken in the course of an extensive monitoring programme in the EFWS between 2003 and 2005 [Wehrmann et al. 2006]. 13 mussel beds of *Mytilus edulis* were selected as sampling sites, because settlement of oyster larvae in the Wadden Sea is limited to hard substrates [Diederich 2005]. All sites were located in the backbarrier area, which is defined as the area sheltered by islands. Here mussel beds are persistent over several years. At minimum one mussel bed per

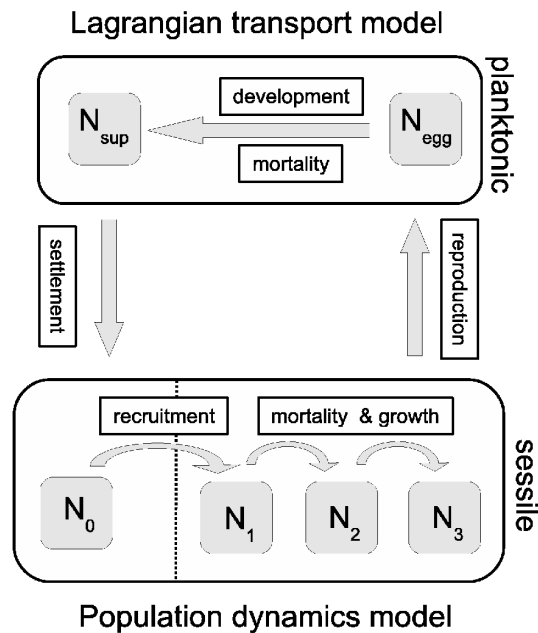


Figure 3.3: Model scheme. The upper box shows the planktonic phase of the life cycle, which is implemented within a Lagrangian particle tracking model. The lower box illustrates the sessile phase, which is represented by a static age-class based population model.

tidal basin was selected. In a first step, the spatial extension and areal coverage of each mussel bed was calculated with the GIS software ArcView 8.3. Within each mussel bed 100 sampling areas were selected by random choice. Sampling areas were  $1 m^2$  in 2003. In 2004 and 2005 sampling areas were reduced to 0.25 to  $0.5 m^2$  where *Crassostrea gigas* occurred in abundances higher than  $10^3 m^{-2}$ . All abundances were calculated for  $1 m^2$  and all measured individuals have been replaced. For the length-frequency distribution, anterior to posterior size of oysters were measured at each site with a calliper rule to the nearest millimetre. In the following, the 13 mussel beds are referred to as the monitoring sites and the values for the population density are given as mean abundance  $D_{obs}$ , hence as the mean calculated from all 100 sampling areas at a mussel bed.

### 3.2.2 Population dynamics model

A simple population model was combined with a Lagrangian drift model to adequately represent the two phases in the life-cycle of *C. gigas* (Fig. 3.3).

In the model, the EFWS is divided into grid squares with an edge length of  $1000 m$ . Each grid square is characterised by the percentage of coverage with intertidal mussel beds as identified by aerial surveys in 1999 (Fig. 3.2). Settlement of *C. gigas* larvae is only allowed in grid cells containing

mussel banks and related to the available area covered with mussel beds. Each subpopulation in a grid square is described by the number of adult individuals  $N_j$  with age  $j$ . The adult mortality rate  $m_a$  acts on all individuals older than one year and reduces the number of individuals upon transition to the next age-class. The mean shell length  $SL(j)$  of all individuals in the age-class  $j$  and the associated standard deviation  $\sigma_{SL}(j)$  (Tab. 3.1) were estimated according to data from Cardoso et al. [2007] and agreed well with data obtained during this study (not shown).  $SL(j)$  and  $\sigma_{SL}(j)$  determine the distribution of shell length of all individuals within one age-class and are used to calculate the biomass and the number of eggs  $EN$  by means of an allometric [Kobayashi et al. 1997] and a linear relation [Kang et al. 2003], respectively (Tab. 3.2).  $EN$  describes the maximal number of eggs that could be produced by a female in one spawning season under optimal conditions. Since spawning of *C. gigas* is temperature-dependent [Steele and Mulcahy 1999, Mann 1979] and not all spawned eggs develop into larvae, the effective reproductive output  $RO$  is defined as a function of  $EN$ , the fertilisation success  $\gamma$  [Marshall 2002, Metaxas et al. 2002] and the spawning intensity  $SI$ , which is related to the period  $\tau_{sp}$  during which the sea surface temperature (SST) stayed above the threshold temperature  $T_{min} = 19^\circ C$ .

$$RO(x, t) = \gamma \cdot EN(x, t) \cdot SI(t), \quad (3.1)$$

with

$$SI(t) = \frac{\tau_{sp}(t)}{\tau_{max}}. \quad (3.2)$$

with the minor indices  $x$  and  $t$  indicating the grid square and the year, respectively.  $\tau_{max}$  is the highest  $\tau_{sp}$  of the simulation period between 1998 and 2004 and was observed in 2003. This exceptionally warm summer gave rise to an excellent spatfall of *C. gigas* in the nearby North Frisian Wadden Sea [Diederich et al. 2005] and was therefore assumed to provide optimal reproductive conditions. In cold summers, in which the weekly mean temperature did not exceed  $T_{min}$ , the length of the spawning period  $\tau_{sp}$  was determined to last a minimum of three days. The spawning intensity, thus, measures the length of the warmest period of each year relative to the year 2003 and is restricted to values between 0 and 1. The weekly SST data to determine  $\tau_{sp}$  was taken from a monitoring station located within the study area at Norderney harbour (Fig. 3.1).

The pelagic phase is represented by a two-dimensional Lagrangian particle tracking model, which simulates the dispersal of a particle considering advection and diffusion. The current data, which determine the advective component, is generated by the General Estuarine Transport Model, which is set-up on a 1 km grid and particularly considers the emergence and submergence of the intertidal area [Staneva et al. 2009]. The horizontal current field is updated every 15 min. Diffusion is treated as a stochastic process and implemented by a random walk algorithm with constant diffusivity [Gardiner 1983]. Particles are considered passive and neutrally buoyant. Each particle in the Lagrangian model

Table 3.1: *Crassostrea gigas*. Mean shell length  $SL(j)$  and the associated standard deviation  $\sigma_{SL}(j)$  as a function of the age. Values were estimated following Cardoso et al. [2007] and supported by observations made during this study.

Age $j$ [y]	$SL(j)$ [mm]	$\sigma_{SL}(j)$ [mm]
1	38	9
2	79	18
3	115	25
4	144	30
5	169	34
6	189	36
7	207	38

is a super-individual representing a cohort of larvae to minimise the computational effort [Scheffer et al. 1995].

The minimum period between spawning and settlement is denoted as the planktonic development time  $\tau_d$ , which is required by the larva to complete their development and become ready to settle. In this model the planktonic development time is a constant parameter and the development of an individual larva is not simulated dynamically. It is assumed that only the small fraction  $s_l$  of all larvae survives the planktonic phase and potentially settles on mussel beds upon encounter during the subsequent settlement phase, whose duration is referred to as  $\tau_{cmp}$ . The number of settlers  $N_0$  in a grid box is defined by its coverage with intertidal mussel beds  $R_{myt}$  and the specific settlement rate  $\lambda$

$$N_0 = \lambda \cdot N_{sup} \cdot R_{myt}, \quad (3.3)$$

with the larval supply time  $N_{sup}$  of the grid box, which is determined by the product of the number of larvae and their residence time in the grid box. Alike the larval survival  $s_l$ , the early survival  $s_e$  describes the fraction of individuals surviving the recruitment phase, which follows the settlement and is here defined as the first year after settlement. The number of one year old individuals  $N_1$  is then related to the number of settlers  $N_0$

$$N_1 = s_e \cdot N_0. \quad (3.4)$$

Assuming an inverse Monod-type mechanism, the early survival is defined as

$$s_e = (1 - m_e) \cdot \frac{k_d}{D + k_d}, \quad (3.5)$$

where  $k_d$  denotes the recruitment saturation,  $D$  is the population density in the subpopulation and  $m_e$  is the minimum early mortality. High population densities, thus, have a negative impact on the survival of recruits. Low values of  $k_d$  indicate a strong influence of density-related processes and reduced survival, whereas values of  $k_d$  distinctively higher than the population density  $D$  lead to

only marginal changes of  $s_e$ . This mechanism, which simulates the finiteness of the resources space and food in the model, has the potential to limit the population growth and to introduce a maximum capacity for the population. Potential positive feedbacks of adults on the recruitment [e.g. Ruesink 2007, Diederich 2005] are neglected for the sake of this required limiting term. The value of  $k_d$  in equation 3.5, thus, indicates the state of competition for food and space of the simulated population. In the model, larvae are supplied from a source population, which is located outside the study area in the adjacent West Frisian Wadden Sea (WFWS) (Fig. 3.1). Since detailed information on the population of *C. gigas* in the WFWS are not available (pers. comm. N. Dankers), a spatially uniform distribution and exponential growth is assumed. Thus, the number of recruits in the WFWS  $N_1^x$  is calculated according to

$$N_1^x = N_{init} e^{(\mu_f \cdot t)} \quad (3.6)$$

with the initial number of recruits in the first simulation year  $N_{init}$  and the external growth rate  $\mu_f$ .

Table 3.2: Variables and reference parameters, the calibration range is given in parenthesis.

Symbol	Definition	Value	Unit	Ref.
<b>Parameters included in the model calibration</b>				
$k_d$	Recruitment saturation	800 (50 – 1200)	$[m^{-2}]$	
$m_a$	Adult mortality rate	0.2 (0.1 – 1.0)	$[y^{-1}]$	
$\mu_f$	External growth rate	1.0 (0.75 – 1.35)	$[y^{-1}]$	
$s_l$	Larval survival	$1.5 \cdot 10^{-4}$ (0.1 – $6.0 \cdot 10^{-4}$ )	$[\ ]$	
$\tau_d$	Planktonic development time	15 (12 – 30)	$[d]$	
<b>Constant parameters</b>				
$a$	Coefficient relating $LW$ and $SL$	$4.34 \cdot 10^{-3}$	$[g\ mm^{-1}]$	+
$\beta$	Ratio between $DW$ and $LW$	0.03	$[\ ]$	
$b$	Allometric index relating $LW$ and $SL$	2.08	$[\ ]$	+
$c$	Coefficient relating $DW$ and $EN$	$38.4 \cdot 10^6$	$[g^{-1}]$	*
$d$	Coefficient relating $DW$ and $EN$	$18.2 \cdot 10^6$	$[\ ]$	*
$\gamma$	Fertilisation success	0.5	$[\ ]$	o
$\lambda$	Settlement rate	0.32	$[h^{-1}]$	
$m_e$	Early mortality	0.9	$[\ ]$	
$NOS$	Number of monitoring sites	13	$[\ ]$	
$NOY$	Number of monitoring years	3	$[\ ]$	
$NY$	Number of years in a simulation	7	$[\ ]$	
$\tau_{cmp}$	Length of settlement phase	10	$[d]$	
$\tau_{max}$	Maximal length of spawning period	53	$[d]$	
$T_{min}$	Minimum temperature for spawning	19	$[^{\circ}C]$	†

+ Kobayashi et al. [1997, and ref. therein], \* Kang et al. [2003], † Mann [1979, modified]

o Marshall [2002], Metaxas et al. [2002, modified]

Table 3.2: (continued)

Symbol	Definition	Value	Unit	Ref.
<b>Variables</b>				
$C$	Cost function	-	[ ]	Eq. 3.7
$C_{av}(t)$	Deviation of mean abundance from measurements in year $t$	-	$[m^{-2}]$	Eq. 3.8
$D_{obs}(t, x)$	Measured mean abundance	-	$[m^{-2}]$	
$D_{sim}(t, x)$	Simulated abundance	-	$[m^{-2}]$	
$DW$	Dry Weight; $DW = \beta \cdot LW$	-	$[g]$	
$EN$	Maximal number of eggs $EN(DW) = cDW(SL) - d$	-	[ ]	
$j$	Age of individuals	-	$[y]$	
$LW$	Live Weight; $LW(SL) = aSL^b$	-	$[g]$	
$N_j(x, t)$	Number of individuals in age-class $j$ $N_j(x, t) = (1 - m_a) \cdot N_{j-1}(x, t - 1)$	-	[ ]	
$N_{sup}(x)$	Larval supply time	-	$[h]$	
$N_1^x$	Number of recruits in the WFWS	-	[ ]	Eq. 3.6
$R_{myt}(x)$	Coverage w. intertidal mussel beds	-	[ ]	◇
$RO$	Effective reproductive output	-	[ ]	Eq. 3.1
$s_e$	Early survival	-	[ ]	Eq. 3.5, 3.9
$SI$	Spawning intensity	-	[ ]	Eq. 3.2
$SL(j)$	Mean shell length in age-class $j$	see Tab.3.1	$[mm]$	‡
$\sigma_{SL}(j)$	Standard deviation of $SL(t)$	see Tab. 3.1	$[mm]$	‡
$\tau_{sp}(t)$	Length of the spawning period	-	$[d]$	
$t$	Simulation year	-	$[y]$	
$x$	Site index	-	[ ]	

◇ Aerial survey in 1999, data source: Nationalparkverwaltung Niedersächsisches Wattenmeer

‡ Cardoso et al. [2007, modified]

### 3.2.3 Simulations and Model set-ups

All simulations started in 1998 and were run over seven consecutive spawning seasons. Though field data were only available for the last three years of the simulations, 1998 was selected as the starting point to minimise initialisation errors by assuming no colonisation in the study area. This assumption is in good accordance with the very rare sightings of *C. gigas* in that region till the end of the 1990s [Wehrmann et al. 2000]. An initial population was only introduced into the adjacent WFWS as described in equation 3.6. During the spawning season, which was defined as the period of  $SST > T_{min}$ , the daily output of larvae  $RO(x, t) \cdot \tau_{sp}^{-1}(t)$  was released at high tide.

Results from four different model set-ups, which vary in the assumptions regarding the recruitment and in the existence of an additional larval source in the Jade estuary, are compared to the field data. The reference run (RR), in which recruitment is assumed to be density-dependent as described in equation 3.5, is based on the best performing parameter set obtained in the calibration process of the model. Parameter values were chosen to minimise the deviations between the field data and the

model results. The five parameters  $m_a$ ,  $s_l$ ,  $k_d$ ,  $\tau_d$  and  $\mu_f$ , which were identified to have the highest impact on the simulation results in a manual sensitivity study (not presented in this study), were variable in the calibration of the model. A cost function  $C$  was introduced to evaluate the misfit between simulated and measured abundances at the monitoring sites.  $C$  is defined as the sum over the logarithmic deviations between simulated and measured values, normalised with the deviations yielded with a very simple model, i.e. the yearly mean of the measured data.

$$C = NOY^{-1} \sum_{t=5}^{NY} C_{av}^{-1}(t) \sum_{x=1}^{NOS} \log(|D_{obs}(t, x) - D_{sim}(t, x)| + 1) \quad (3.7)$$

with

$$C_{av}(t) = \sum_{x=1}^{NOS} \log(|D_{obs}(t, x) - D_{mean}(t)| + 1) \quad (3.8)$$

with the number of monitoring years  $NOY$ , the number of monitoring sites  $NOS$ , the number of simulation years  $NY$  and the measured ( $D_{obs}$ ) and simulated ( $D_{sim}$ ) abundances. Thus, a simulation corresponding to the mean value of the respective year at all sites had a fitness of 1. A two-stage process was applied to allow the simultaneous calibration of all five parameters. First, Monte-Carlo simulations were conducted varying the five parameters to identify the most sensitive parameters and potential correlations between them. At this stage, it was striven for a fixation of at least two parameter values to reduce the number of variable parameters. Most certain information was available on  $m_a$ , which was determined to be around  $0.2 y^{-1}$  in the nearby North Frisian Wadden Sea by Diederich [2006]. Second, a systematic parameter variation with the remaining parameters completed the reference parameter set. In addition to the reference values, this analysis facilitated the identification of potential ranges around the reference values and, thus, contributed to the understanding of sensitivity of the considered parameters.

The second model set-up simulated the effect of an additional source (aS) of larvae in the Jade estuary, where extensive culture plots for *Mytilus edulis* are located. This additional source is related to mussel fishery activities and simulated the transfer of seed mussels from the central EFWS to the culture plots by fishermen and an associated, unintentional transfer of *C. gigas* living on the mussels. In the model a small amount of juvenile *C. gigas* (1180000 individuals of which 2/3 aged one year and 1/3 aged two years) were manually added to an area of  $1.18 km^2$  in the eastern Jade estuary in 2001 (boxed area in Fig. 3.2), which corresponds to an abundance of  $1 m^{-2}$ .

The third model set-up assessed the impact of site-specific recruitment (sR) at the 13 monitoring sites. Therefore, the early mortality was defined to be solely a property of the location. Thus, equation 3.5 was replaced by

$$s_e(x) = 1 - m_e(x) \quad (3.9)$$

where the early mortality  $m_e$  was manually adjusted in a narrow range  $\pm 0.05a^{-1}$  around the reference value of  $0.9a^{-1}$  to better fit the measurements at the monitoring sites. At the vast majority of the grid boxes, where no field data was available to adjust the early mortality, the constant reference value was applied. The recruitment at all but the 13 monitoring sites was, hence, purely supply-driven. The rationale behind this approach was to study the impact of small variations in the local recruitment conditions at the monitoring sites, while the large-scale dynamics of the invasion was simulated as supply-driven with an global estimate for the early mortality. This approach helps to evaluate the general limits of predictability of the population development at individual sites given the uncertainty in the parameters of the recruitment process and its natural variability.

The fourth simulation combined the additional source in the Jade estuary and the site-specific recruitment and is referred to as SR.

### 3.2.4 Drift characteristics

Based on the set-up SR, the distributions of the travelled distance and the drift directions are compiled. The drift distance is the net distance between the origin of a larva and its position at the end of the planktonic development time. This only presents the minimum travel distance of a larva since suitable substrate may not be available and not all larvae settle simultaneously (Eq. 3.3). Drift distances of all larvae and all years are considered to calculate the mean distribution of the travel distance. Deviations of yearly travel distributions, which are derived by data from only a single year, from the mean distribution indicate differences in the prevailing hydrodynamic conditions of the considered spawning period. Directional distributions of single years offer additional information regarding the dominant directions of transport and the variability of the travel direction. Both distributions can be related to the hydrodynamic regime during the spawning season since larvae are regarded as passive particles and their dispersal is exclusively controlled by the currents acting upon them.

## 3.3 Results

### 3.3.1 Rapid invasion of *Crassostrea gigas*

The results from the monitoring programme documented the fast establishment of *Crassostrea gigas* in the East Frisian Wadden Sea (EFWS), leading from low measured abundances in the west and a scarce colonisation in the remaining study area to an ubiquitous occurrence with highest population densities exceeding  $300 m^{-2}$  within only three years [see also Wehrmann et al. 2006]. Yet in 2003, the first year of the monitoring programme, *C. gigas* was present in the entire study area (Fig. 3.4). However, strong spatial gradients were evident in all years with highest measured abundances at the three western sites *W1* - *W3*. In 2003, the highest abundance of  $42 m^{-2}$  was measured at site *W2*,

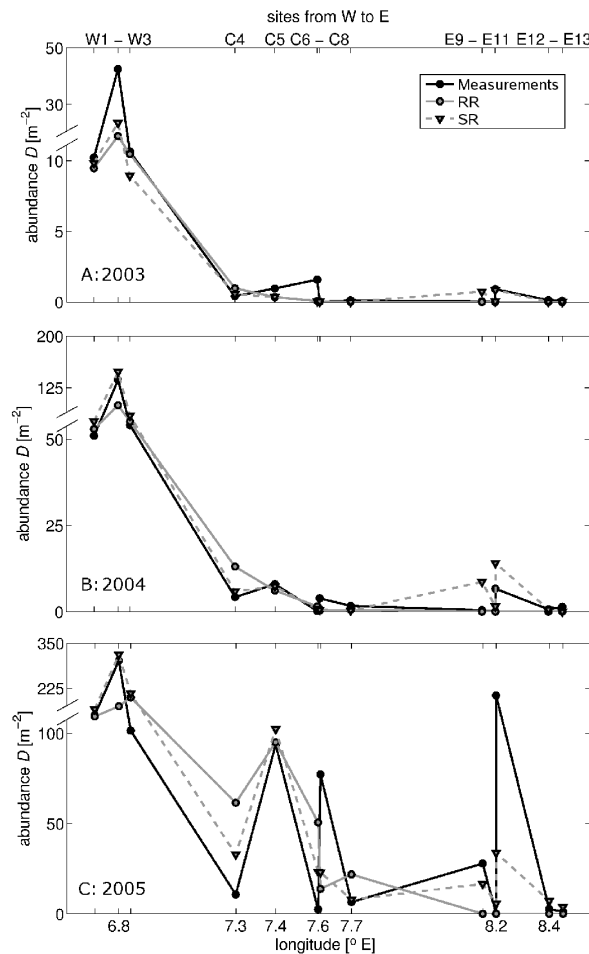


Figure 3.4: *Crassostrea gigas*. Abundance at 13 monitoring sites in the East Frisian Wadden Sea (EFWS) arranged zonally from west to the east for the years 2003 (A), 2004 (B) and 2005 (C). Data from the monitoring programme (solid black) [Wehrmann et al. 2006] are compared to the calibrated reference run of the model (RR, solid grey) and the the SR set-up (dashed grey) including an additional source of larval supply in the Jade estuary and site-specific recruitment at the 13 monitoring sites. Recruitment at all other than the monitoring sites was supply-driven.

while values at all other sites in the central and eastern part of the study area remained close to zero. Though the population grew considerably in 2004, the general spatial trend of the preceding year was conserved (Fig. 3.4). Observed abundances at the three western sites increased severalfold to a maximum of  $136 m^{-2}$ , but stayed well below  $10 m^{-2}$  at most of the remaining sites. Similar to 2003, the measured abundances at site E11 were distinctively higher ( $7 m^{-2}$ ) than at neighbouring sites, where population densities did not exceed  $2 m^{-2}$ . In 2005 the spatial pattern differed considerably compared to the measurements in the preceding years. Especially the eastward decline of the measured abundances was less pronounced and the spatial distribution became more irregular. While population

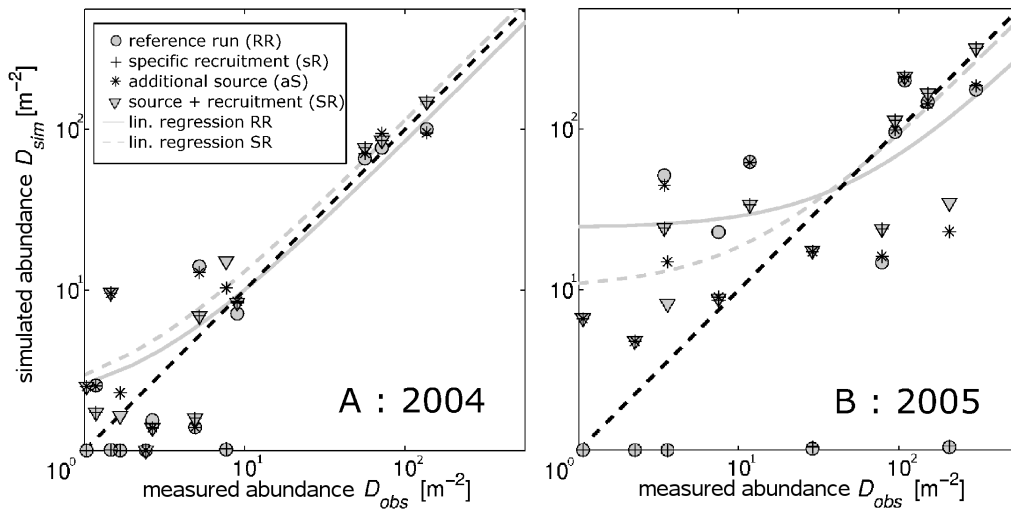


Figure 3.5: *Crassostrea gigas*. Comparing log-transformed measured and simulated abundances in 2004 (A) and 2005 (B). Markers denote 4 different simulations: (1) the reference run (RR), (2) RR with an additional source of larval supply in the Jade estuary (aS), (3) site-specific recruitment at the 13 monitoring sites (sR), (4) an additional larval source and site-specific recruitment at the 13 monitoring sites (SR). Recruitment at all other than the monitoring sites was supply-driven in the set-ups sR and SR. The lines indicate the perfect match between simulation results and field data (dashed black), the linear regression of the RR (solid grey) and the linear regression of the SR (dashed grey), respectively.

growth ceased at the three western sites, abundances at sites *C5* and *C6* had multiplied and almost reached values found in the west. Observed abundances at site *E11* continued to increase much faster than at nearby locations, leading to the second highest values measured during the whole study. The adjacent site *E9* also exhibited strong growth, whereas all other sites in the eastern part remained at very low abundances.

### 3.3.2 Reference run with supply-domination

The RR yielded smooth abundance distributions with eastwardly decreasing values in all years and reproduced the large-scale spatial and temporal patterns inherent to the monitoring data. The parameter set used for the RR represented supply-dominated recruitment with only very weak density-dependent effects since the calibration revealed a reference value of the recruitment saturation  $k_d$  of  $800 \text{ m}^{-2}$  (see Tab. 3.2). In 2003 and 2004, the simulated abundances fitted well the measured values reproducing the distinct differences between high population densities at western sites and several times lower numbers in the remaining area. Large deviations between the measured and simulated abundances only occurred at site *W2*, where the simulated results underestimated the measured data in all years,

Table 3.3: Slope of the linear regression  $p_t$  and correlation coefficients  $r_t^2$  between measurements and simulations where the subscript  $t$  denotes the year (2003 - 2005); results for four different model set-ups are shown: (1) the reference run (RR), (2) RR with an additional source of larval supply in the Jade estuary (aS), (3) site-specific recruitment at the 13 monitoring sites (sR), (4) an additional larval source and site-specific recruitment at the 13 monitoring sites(SR).

model set-up	2003		2004		2005	
	$r^2$	$p$	$r^2$	$p$	$r^2$	$p$
(1) RR	0.94	0.49	0.97	0.83	0.60	0.45
(2) aS	0.93	0.57	0.93	1.15	0.65	0.82
(3) sR	0.99	0.43	0.99	0.83	0.76	0.49
(4) SR	0.99	0.57	0.99	1.12	0.80	0.84

and at site *E11*. At the latter location, the RR failed to explain the field data even qualitatively predicting hardly any colonisation in the eastern region until 2005. As measures of model performance, the slope  $p$  of the linear regression between measured and simulated results and its regression coefficient  $r^2$  were used. While deviations from the optimal value of 1 for  $p$  indicate an under- ( $p < 1$ ) or overestimation ( $p > 1$ ) of population growth (or even a systematic error for huge deviations),  $r^2$  displays the correlation of the measured and simulated data. Therefore, high values of  $r^2$  were interpreted here as an indicator for model validity. The performance of the RR decreased considerably in 2005 (Tab. 3.3 and Fig. 3.5) as it was only partially able to reproduce the rather uneven distribution (Fig. 3.4). While the population dynamics in the western half of the study area (*W1* - *C5*) were reasonably captured, the deviations in the eastern half increased markedly. Especially the soaring abundances at the sites *E9* and *E11* were not predicted at all, which confirmed the inability of the model set-up to explain the development at the two sites located between the two estuaries of the Jade and the Weser.

### 3.3.3 Site-specific recruitment and an additional larval source

Both models, the site-specific recruitment (sR) and the additional source of larvae in the Jade estuary (aS), were able to significantly improve the model performance in terms of the two measures  $p$  and  $r^2$  and their combination (SR) led to a reasonable reconstruction of *C. gigas*' distribution in the EFWS. The additional source in the model aS increased the simulated abundances markedly at most sites that exhibited no colonisation in the RR (Fig. 3.5). This was reflected by distinctively higher values of  $p$  in all years (Tab.3.3). The correlation increased only slightly to 0.65 in 2005 since the additional source resulted in overestimating abundances at three rather sparsely populated sites while still underestimating the abundances at *E9* and *E11*. In contrast, the model set-up sR increased  $r^2$  in all years (Tab. 3.3), but failed to improve the erroneous results at four uncolonised sites in the East (Fig. 3.4 and Fig. 3.5). The slope of the best fit was therefore too flat, especially in 2003 and 2005 (Fig. 3.5). A combination of the additional source in the Jade area and the site-specific recruitment (SR) provided

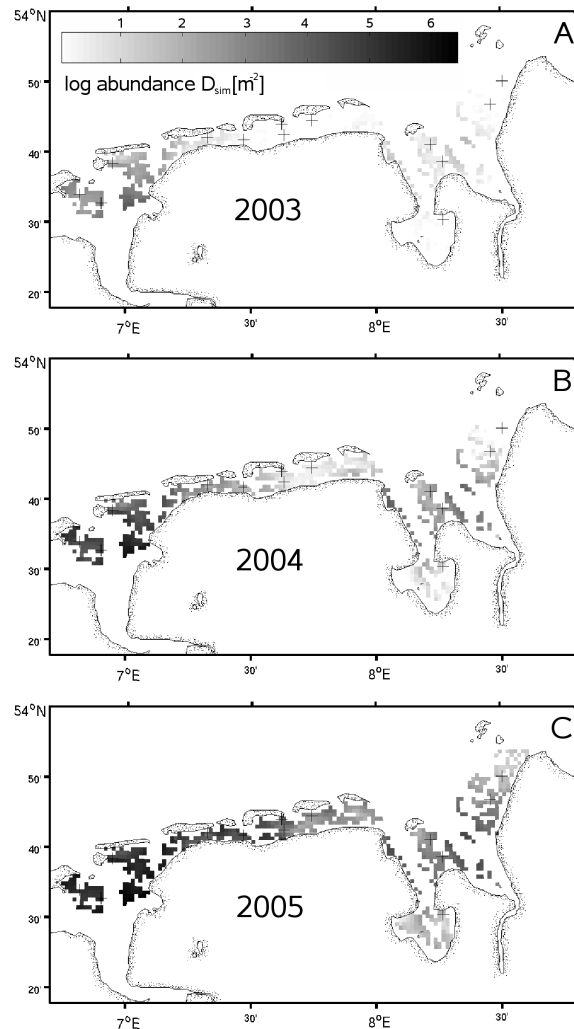


Figure 3.6: *Crassostrea gigas*. Reconstructed abundance distribution in the East Frisian Wadden Sea in 2003, 2004 and 2005 (A-C). Results from the SR set-up including an additional source of larval supply in the Jade estuary and site-specific recruitment at the 13 monitoring sites. Recruitment at all other than the monitoring sites was supply-driven. Crosses indicate monitoring sites.

the best results with respect to both performance measures (Tab. 3.3). The reconstructed spatial distribution of *C. gigas* based on this combined set-up shows the eastward propagation of the population (Fig. 3.6). In the eastern part of the study area the influence of the additional source was noticeable yet in 2003. Besides high simulated abundances in the western part of the study area, a second maximum developed in the Jade estuary, while the Jade inlet and the easternmost parts of the study area were, though close to the additional source, still sparsely colonised in 2005. A complete colonisation of the EFWS was reached in the last year of simulation.

Considering the temporal development of simulated abundances over the entire simulation period in

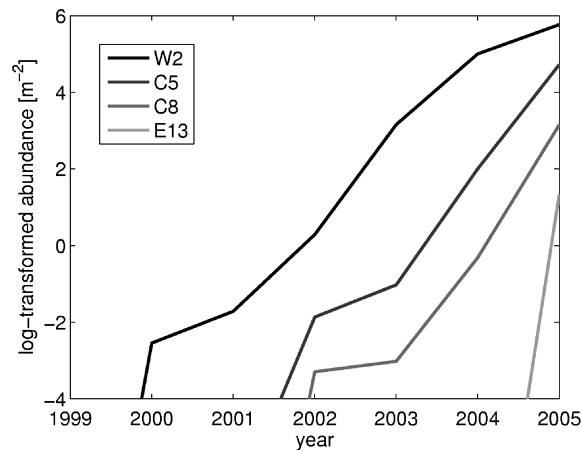


Figure 3.7: *Crassostrea gigas*. Time-series of simulated abundances at four selected sites. Results from the SR set-up including an additional source of larval supply in the Jade estuary and site-specific recruitment at the 13 monitoring sites. Recruitment at all other than the monitoring sites was supply-driven.

the model set-up SR revealed exponential growth of *C. gigas* at all stations. Figure 3.7 clearly shows the simulated wave-like propagation of the invasion from west to east with very similar, but delayed population dynamics at the selected sites.

### 3.3.4 Drift characteristics

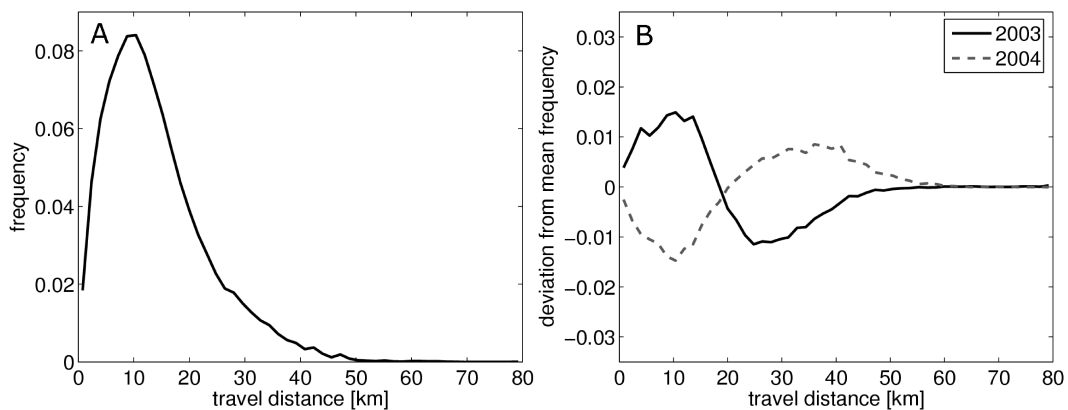


Figure 3.8: *Crassostrea gigas*. (A) Mean frequency of the travel distance for simulated larvae; considered years 1998 – 2004. (B) Deviations from the simulated mean frequency of the travel distance in the years 2003 (solid) and 2004 (dashed). Results from the SR set-up including an additional source of larval supply in the Jade estuary and site-specific recruitment at the 13 monitoring sites. Recruitment at all other than the monitoring sites was supply-driven.

Drift distances of simulated larvae in the best fitting SR set-up ranged, with very few exceptions, from 0 to 50 km in all considered years. Due to the asymmetric mean distribution, which was compiled with data from all years of the simulation, the vast majority of all larvae were transported less than 25 km and the most frequent distance was only 10 km (Fig. 3.8). Interannual variability in the transport was, however, high indicating distinctive differences of the hydrodynamic regimes. In 2003 and 2004, the deviations from the mean distribution were almost perfectly oppositional (Fig. 3.8). In the first year, the fraction of larvae travelling less than 20 km was pronounced, whereas long range dispersal was favoured in the following year. Despite the characteristic differences, the tails of the

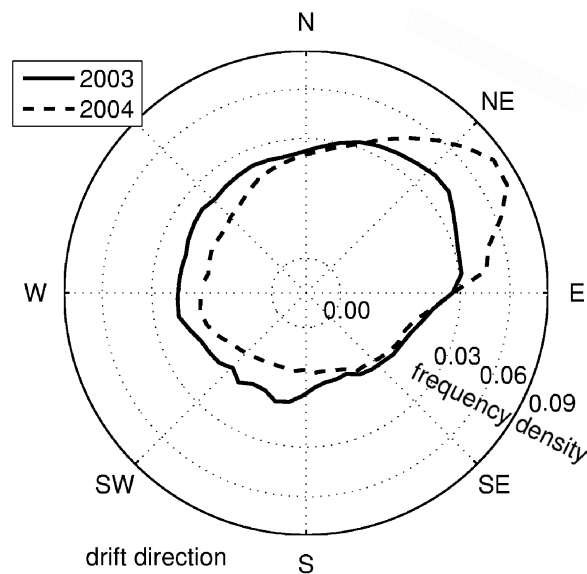


Figure 3.9: *Crassostrea gigas*. Frequency of the drift direction for simulated larvae in 2003 (solid) and 2004 (dashed). Results from the SR set-up including an additional source of larval supply in the Jade estuary and site-specific recruitment at the 13 monitoring sites. Recruitment at all other than the monitoring sites was supply-driven.

distributions, e.g. the fraction of larvae travelling farther than 50 km, were similarly small and, thus, negligible for the observed differences in the population dynamics of *C. gigas*.

Most simulated larvae travelled to directions between north and east with respect to their origin with a preference to the northeast (NE) in both years (Fig. 3.9). The distribution of directions also varied, indicating a stronger directional transport in 2004 and a more diffusive pattern in 2003.

### 3.3.5 Constraining ecological parameters

Besides the reference values, the model calibration revealed insights regarding the sensitivity of the model performance to variations of the considered parameters. The adult mortality  $m_a$  and the larval

survival  $s_l$  had the strongest impact on the model result. The two-dimensional projection of the cost function  $C$  onto the plane of  $m_a$  and  $s_l$  showed a strong positive correlation of the two parameters allowing a division of the parameter plane into three distinct zones (Fig. 3.10). Minimum values of  $C$  were located in a zone diagonally dividing the plane. In the zone above the diagonal, higher  $m_a$  or lower  $s_l$  led to an underestimation of abundances or even an extinction of the population. In contrast, low adult mortalities in combination with high larval survival resulted in a systematic overestimation of population densities. Narrowing  $m_a$  to a reasonable range between 0.15 and 0.25  $y^{-1}$ , the poten-

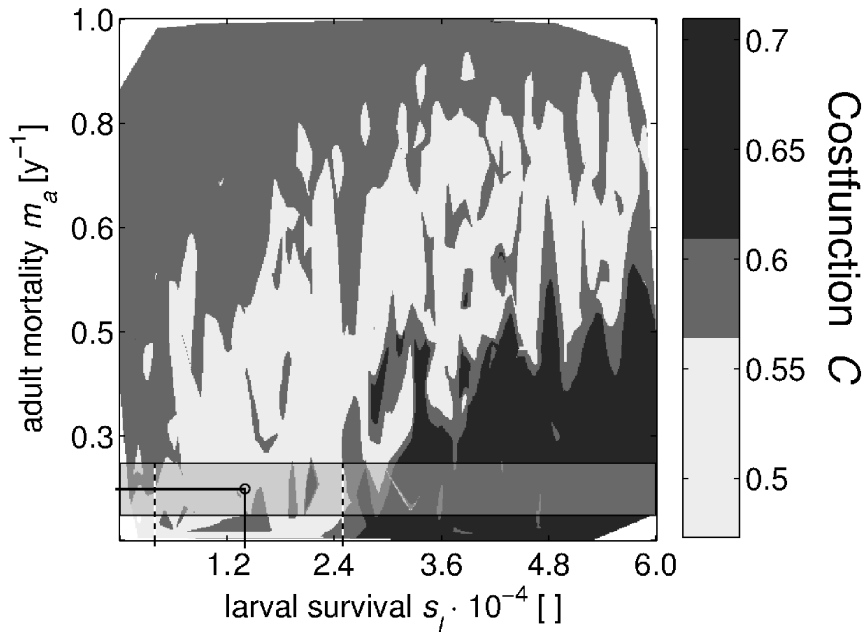


Figure 3.10: Fitness, expressed as the cost function  $C$ , of 695 parameter combinations of the Monte-Carlo simulation. Results were projected onto the parameter plane of the two most sensitive (adult mortality  $m_a$  and larval survival  $s_l$ ) of the considered five parameters. Lower values of  $C$  indicate better fitness; while a fitness value of 0 perfectly matches the measurements, a value of 1 corresponds to the fitness of the yearly mean of the measurements. The shaded area indicates the range of  $m_a$  between 0.15 and 0.25  $y^{-1}$  [Diederich 2006] in which the pair of reference values is denoted by the circle. From this, a range for the larval survival  $s_l$  can be estimated (dashed lines).

tial range of  $s_l$  could be constrained between 0.5 and  $2.5 \cdot 10^{-5}$ . The reference values for  $m_a$  and  $s_l$  were then determined centrally within this limits at  $0.2 y^{-1}$  and  $1.5 \cdot 10^{-5}$ , respectively (as indicated in Fig. 3.10).

In the continuous variation of the remaining parameters best simulations were obtained for the planktonic development time  $\tau_d$  equal to 15  $d$ , though results were not very sensible to changes in this parameter. Most noticeably, shorter planktonic development times extended the range of external larval supply  $\mu_f$  still yielding good model results to lower values ( $< 1.0 y^{-1}$ , Fig. 3.11). The slightly

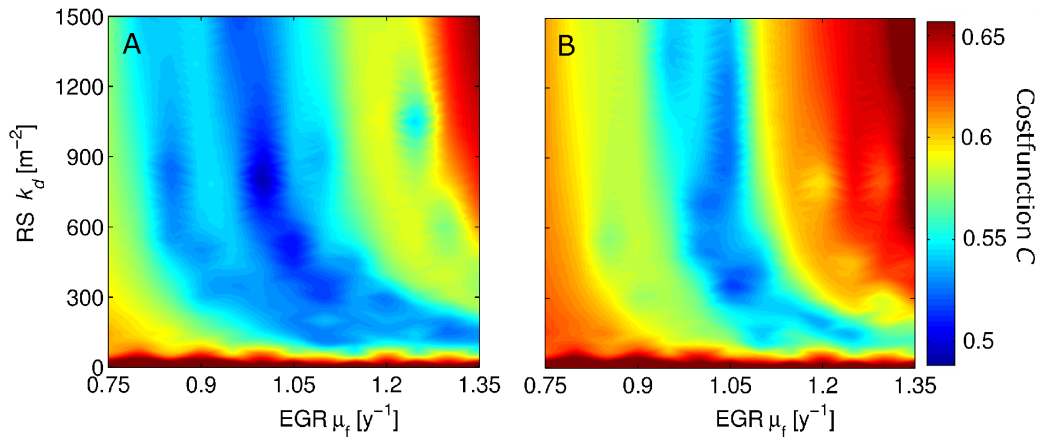


Figure 3.11: Misfit between simulations and measurements, expressed by the cost function  $C$ , as a function of the model parameters external growth rate (EGR)  $\mu_f$  and the recruitment saturation (RS)  $k_d$  for two different planktonic development times  $\tau_d$  (15 d (A) and 30 d (B)). The adult mortality  $m_a$  and the larval survival  $s_l$  are fixed at  $0.2 y^{-1}$  and  $1.5 \cdot 10^{-5}$  respectively. Lower values of  $C$  indicate better fitness.

curved minimum of the cost function  $C$  in the parameter plane of  $\mu_f$  and the recruitment saturation  $k_d$  reflects the transition from supply-dominated (high values of  $k_d$ ) to strong density-dependent (small values of  $k_d$ ) recruitment. Good agreements with the field data were obtained with values of  $k_d$  well above  $300 m^{-2}$  and the best fitting reference values were found at  $k_d = 800 m^{-2}$ ,  $\mu_f = 1.0 y^{-1}$  and  $\tau_d = 15 d$ . While for small values of  $k_d$  a negative non-linear correlation with the external growth rate was apparent, best results for  $k_d > 800 m^{-2}$  were all obtained with  $\mu_f$  close to  $1.0 y^{-1}$ . Increasing the density-dependence of the recruitment process required higher larval supply to account for the additional mortality, which explains the trade-off visible in  $C$  towards greater values of  $\mu_f$ . For  $k_d < 300 m^{-2}$ , however, the performance of the model worsened, regardless of the strength of larval supply. Most well-fitting simulations, thus, represented an invasion process rather controlled by the larval supply than density-dependent recruitment.

## 3.4 Discussion

### 3.4.1 Monitoring data

The monitoring results presented here show a rapid invasion of *Crassostrea gigas* into the East Frisian Wadden Sea (EFWS) leading to an ubiquitous presence within only few years after first sightings [Wehrmann et al. 2000]. Already the observed spatial and temporal distribution during the monitoring programme supports the hypothesis of an invasion from adjacent western regions [Wehrmann et al. 2000] driven by the prevailing residual current in this part of the German Bight. There is no clear

evidence for a slowdown of the population growth in the data and, thus, a continuation of the trend seems to be most likely. Remarkably strong population growth at the two sites *E9* and *E11* in the Jade estuary, however, challenges the assumption of only one source region, but the field data offers no obvious explanation for this observed feature. Further larval sources outside the study area appear very unlikely since all eastern locations exhibited low abundances still in 2005.

### 3.4.2 Simulations

The RR of the model was able to reproduce the large-scale dynamics as supply-dominated and originating in the WFWS, but the failure to even qualitatively match the measurements at the eastern sites strongly suggests a crucial gap in the model assumptions. Density-dependent effects attributed to competition did not play a major role in the simulated early phase of the invasion.

Artificially adding juvenile individuals to the Jade estuary in the model set-up aS improved the model performance in all years, suggesting that mussel fisheries activity noticeably influenced the course of the invasion of *C. gigas* into the EFWS. The unintentional transfer of *C. gigas* together with seed mussels was also reported from the South Island of New Zealand yet in 1977 [Jenkins and Meredyth-Young 1979] and seems not to be an unusual mechanism of dispersal for *C. gigas*. Though this mechanism has not led to the invasion of *C. gigas* into the Wadden Sea it should be considered as a possible vector in other ecosystems. Despite the additional source, the deviations between simulated and measured population densities remained very high at site *E11* and neither the model nor the field data provided an explanation for this discrepancy. Obviously, the site offered favourable conditions for the recruitment of *C. gigas*, which were not accounted for by the model. This could include low predation pressure due to the absence of predators or small-scale hydrodynamic features below the resolution of the hydrodynamic model, which could increase the larval supply to the mussel bed.

Assuming site-specific early mortality at the monitoring sites in the set-up sR increased the fit of the model considerably compared to the RR. The clear improvement of the simulation is remarkable considering the small variational range of the early mortality and underlines the need for detailed knowledge of the recruitment conditions to predict the population density at a specific site. The large-scale invasion pattern in the sR set-up, however, could be sufficiently reproduced assuming supply-driven recruitment with a constant early mortality at all other sites. While the growth of a population at an individual site may be controlled by site-specific recruitment conditions, it appears to be sufficient to know the average early mortality in the area of interest to understand the evolution of the invasion.

Only the set-up SR, which combined the site-specific early mortality and the additional source, captured all characteristics of the measured population dynamics and therefore allowed a reasonable reconstruction of the spatial and temporal distribution of *C. gigas*.

The lag-phase of several years between first sightings [Wehrmann et al. 2000] and exponential growth

(this study) is a known feature of almost all invasions [Crooks and Soulé 1999]. This delay also developed in all model results and is therefore explainable without a phase of species adaptation or reproductive inactivity. Once started, the invasion exhibited remarkable similarities to a travelling wave resembling the general analytical solution to more theoretical models combining advection, diffusion and growth [e.g. Shigesada and Kawasaki 1997]).

### 3.4.3 Drift distances

The distributions of the simulated travel distances demonstrate that self-recruitment, which can be defined as recruitment within a few kilometres from the source, is rather the rule than an exception for *C. gigas* in the EFWS supporting the dispersal estimates based on residual currents by Wehrmann et al. [2000]. Dispersal distances for a planktonic life time of 15 *d* proposed by other authors, however, are remarkably higher in the range of 50 *km* [Shanks et al. 2003, Siegel et al. 2003] and rather correspond to the maximum distances simulated in this study. Hence, our results confirm the maximum dispersal range found by experimental methods, but also indicate that the bulk of the larvae, which is transported considerably less far, primarily determines the speed of an invasion. These findings are compliant with the growing evidence for limited dispersal and local recruitment in several marine species with planktonic larvae [Cowen et al. 2006, Levin 2006, Todd 1998].

The high variability of the distribution of simulated travel distances directly translated into the spatial structure of the population. Despite strong population growth between 2003 and 2004, the shape of the spatial distribution of *C. gigas* only changed marginally due to enhanced short-distance dispersal. In contrast, articulate changes in the spatial pattern and an increasing patchiness were observed and simulated in 2005, which could be attributed to the above-average drift distances. The interannual variation in the drift distances are caused by the different hydrodynamic conditions that prevailed during the two considered spawning seasons. Especially the increasing patchiness in 2005 under uniform recruitment conditions at all sites in the RR suggest that a patchy spatial distribution is not necessarily a result of variable recruitment. The role of hydrodynamics in determining the distribution of adult benthic invertebrates was emphasised by Gaylord and Gaines [2000] and is likely the cause for the interannual differences of the colonisation patterns in this study as well.

### 3.4.4 Constraining ecological parameters

Due to the high number of simulations during the calibration, the modelling approach did not only yield the reference set of parameters but added also to the understanding of the model sensitivity with regard to the considered parameters. Most importantly, there was no unique parameter set that produced the best fit to the measured data, but a large number of parameter combinations yielding comparable results. Especially the correlation between the adult mortality  $m_a$  and the larval survival

$s_l$ , which are the most sensitive parameters, underline the need for additional knowledge from field data to narrow the possible range of parameter combinations. Since direct measurements of the larval survival *in situ* are scarce and afflicted with high uncertainties, the more frequently measured adult mortality rate was used for the required fixation of one parameter value. Though published values for  $m_a$  vary considerably, they generally agree on low mortalities rates of adult oysters around  $0.2 y^{-1}$ , rarely exceeding  $0.4 y^{-1}$  [Diederich 2006, Costil et al. 2005, Bartol et al. 1999]. By fixing  $m_a$  at  $0.2 y^{-1}$ , a range for the larval survival  $s_l$  was obtained implicitly. The only available data from Johnson and Shanks [2003] (bivalve veliger) and Jørgensen [1981] (*Mytilus edulis*) suggest higher larval survival than our inverse estimate, but the applied methods and considered periods make a comparison very difficult. The same holds for estimates based solely on theoretical assumptions [Rumrill 1990]. Our findings, thus, indicate that the combination of low adult mortalities and high fecundity [Reise 1998] allows *C. gigas* to sustain population growth at rather low larval survival. This may explain the success of *C. gigas* to establish itself quickly in new habitats and the competitive advantage over other marine benthic invertebrates, which are mostly less fecund [Bos et al. 2006, and references therein], have at least equal adult mortalities, and likely suffer from comparable larval mortalities [Rumrill 1990].

Model results at the western monitoring sites, where the influence of the source population is highest, are consistent with the measurements and, thus, confirm the assumption of undamped and supply-driven population growth of the source population in the WFWS. It is, however, obvious that population growth will not be sustained at exponential rates over longer periods, but at least in the simulated early phase of the invasion there are no indications for a ceasing growth rate. A plausibility check for the abundance of recruits in the West Frisian Wadden Sea (WFWS) in 2005 reveals a value of  $69 m^{-2}$  based on the reference value  $\mu_f = 1.0 y^{-1}$  and assuming values of  $400 km^2$  for the considered area and 2% for the coverage of that area with mussel beds [de Vlas et al. 2005]. This rough estimate appears to yield a reasonable result given that measured abundances of all age-classes exceeded  $300 m^{-2}$  at the nearby monitoring sites *W1* to *W3* in 2005. Analogue to the development in the WFWS, the population dynamics in the RR were simulated best with high values of the recruitment saturation  $k_d$  corresponding to supply-dominated recruitment and weak density-dependent recruitment effects. The slightly impairing performance of simulations with values of  $k_d$  above the reference value ( $800 m^{-2}$ ) indicates that density-dependent processes may nevertheless become important at higher abundances than measured in this study. Negative feedbacks caused by high population densities, such as competition for space and food, did not seem to play a major role in the measured and simulated early phase of the invasion yet. It should be noted, however, that parametrisation representing strong density-dependent early survival also yielded reasonable model results. Hence, further observational evidence is needed to unambiguously determine the role of larval supply and early mortality though our model calibration study suggests a strong influence of the larval supply in the determination of the population

distribution at an early stage of an invasion.

The reference value for the planktonic development time  $\tau_d$  could be determined at 15 *d*, though reasonable results with  $\tau_d = 30$  *d* indicate that model results are rather insensitive to variations of the planktonic development time. This insensitivity originates likely in the coarse spacing of the monitoring sites that prevents small variations of  $\tau_d$  to be detected since the distance between monitoring sites roughly corresponds to the distance a larva is transported within two weeks (10 to 20 *km*). Development times at rather suboptimal temperatures around 20°C range from 25 to 35 *d* [Thompson and Harrison 1992, His et al. 1989] and are well above the reference value of 15 *d* in this study. It should be noted, however, that the planktonic development time in the model is only defined as the minimum time spent in the plankton whereas other authors often refer to average residence times. Though our estimate for  $\tau_d$  is afflicted with high uncertainties, we propose that larval behaviour that is not explicitly simulated by the model may have influenced the dispersal of larvae in the field. Vertical swimming in strongly sheared flows is often supposed to be a mechanism for weak-swimming larvae to manipulate their dispersal and observations, though not always unambiguous, have supported this hypothesis for several marine benthic invertebrates [Knights et al. 2006, Metaxas 2001, Dobretsov and Miron 2001]. As the model treats larvae as passive particles and does not account for larval behaviour enhancing the retention, this may have been mimicked by shorter planktonic development times in the model.

### 3.4.5 Potential and limitations of the model

This study shows the considerable potential of combined larval drift and population models to understand the general spatial and temporal dynamics of an invasion. Our findings could as well support management decisions regarding the spread of an invasive species or the introduction of aquaculture species, since the large-scale prediction of the population dynamics only required an assumption of the initial distribution of the species and an appropriate parameter set. The determination of this parameter set itself significantly enhanced the understanding of the invasion beyond the measured adult abundances and provided estimates of ecological parameters, which are difficult to obtain experimentally.

The interannual variability of the dispersal underlines the need for detailed hydrodynamic data to reasonably reproduce or predict the spread of larvae. Though this aspect was not treated explicitly in this study, the spawning time and duration are probably sensitive parameters due to the high temporal variability of the hydrodynamics in the coastal North Sea. Increasing spatial variability of adult abundances and considerable discrepancies between model results and field data in 2005 may be attributed to uncertainties regarding the spawning time and period, which have a greater impact on the model results in this year with above-average dispersal distances.

While the model is capable of reasonably predicting the general temporal and spatial population dy-

namics with a supply-driven approach it appears to be inadequate to reproduce the development at a specific site without further information on the local conditions. This finding supports the importance of recruitment processes acting on the early mortality to understand the observed spatial variability in adult abundance between adjacent sites. We suggest, that the goodness of the simulated results could be improved by replacing uniform model parameters by spatially resolved assumptions of e.g. the early mortality.

Nevertheless, we could demonstrate that an appropriate model is a powerful tool to understand the spread of marine species. However, only the combination of the model with field data allowed to obtain reasonable results, since the quality of the model results strongly depends on observational or experimental information. We suppose that reducing the uncertainties in the assumptions and parameters of the model could distinctively improve the predictive capabilities of the model.

### **3.5 Conclusion**

The monitoring data presented in this study revealed the potential of *Crassostrea gigas* to not only invade into a new habitat within a few years, but also to become a prevalent species in this short period. Combining field data and a population dynamics model we were able to produce a reasonable reconstruction of the population dynamics of *C. gigas* in the East Frisian Wadden Sea since 1998. Furthermore, we were able to address the initial questions of this study: (1) Both, the field data as well as the results from the model, support the hypothesis of an eastward invasion of *C. gigas* into the East Frisian Wadden Sea. However, the model strongly suggests an additional source within the study area in the Jade estuary attributed to fishery activities. Typical drift distances of the larvae in the model range between 5 and 15 km with considerable interannual variability emphasizing the importance of the hydrodynamics to the invasion pattern.

(2) In all model set-ups the large-scale invasion pattern could be explained assuming supply-dominated recruitment and despite abundances above  $300 m^{-2}$  at some sites, there was no evidence for a slow-down of population growth due to density-related effects. Nevertheless, site-specific variations of the early mortality could significantly improve the model results indicating the importance of local conditions on the population dynamics at individual sites. (3) Though the model showed the ability to reasonably reproduce the large-scale invasion dynamics the development at single sites could not be described satisfactory only considering the larval supply. We suggest that only a combination of a detailed larval supply pattern with the knowledge of local conditions allows a prediction of small-scale population dynamics. Since the calibration of the model revealed that several parametrisations lead to a reasonable reproduction of the field data, additional observational or experimental evidence can help to narrow these uncertainties and improve the capabilities of the model. With an appropriate parametrisation, however, the model presents a powerful tool to understand and predict the invasion

of species reproducing via planktonic larvae over a period of several years.

## **Acknowledgements**

We thank J. Staneva for providing hydrodynamic data and the NLWKN for the distributional data of *Mytilus edulis* and the SST data for the Norderney harbour. We are grateful to three anonymous reviewers who helped to significantly improve the manuscript. G. Brandt was supported by the Junior Research Group IMPULSE and the GKSS Research Centre. The Research Institute Senckenberg and the Niedersächsische Wattenmeer-Stiftung are gratefully acknowledged for financial support of the monitoring programme.

## Bibliography

- A. S. Barnay, C. Ellien, F. Gentil, and E. Thiébaud. A model study on variations in larval supply: are populations of the polychaete *Owenia fusiformis* in the English Channel open or closed? *Helgol Mar Res*, 56(4):229–237, 2003.
- I. K. Bartol, R. Mann, and M. Luckenbach. Growth and mortality of oysters (*Crassostrea virginica*) on constructed intertidal reefs: effects of tidal height and substrate level. *J Exp Mar Biol Ecol*, 237: 157–184, 1999.
- O. G. Bos, I. E. Hendriks, M. Strasser, P. Dolmer, and P. Kamermans. Estimation of food limitation of bivalve larvae in coastal waters of north-western Europe. *J Sea Res*, 55:191–206, 2006.
- BSH. *Bundesamt für Seeschifffahrt und Hydrographie, Gezeitenkalender 2007, Hoch- und Niedrigwasserzeiten für die Deutsche Bucht und deren Flussgebiete*. Hansonautic, 2006.
- M. J. Caley, M. H. Carr, M. A. Hixon, T. P. Hughes, G. P. Jones, and B. A. Menge. Recruitment and the local dynamics of open marine populations. *Annu Rev Ecol Syst*, 27:477–500, 1996.
- J. F. M. F. Cardoso, D. Langlet, J. F. Loff, A. R. Martins, J. I. J. Witte, P. T. Santos, and H. W. van der Veer. Spatial variability in growth and reproduction of the Pacific oyster *Crassostrea gigas* (Thunberg, 1793) along the west European coast. *J Sea Res*, 57:303–315, 2007.
- B. Collet, P. Boudry, A. Thebault, S. Heurtebise, B. Morand, and A. Gérard. Relationship between pre- and post-metamorphic growth in the pacific oyster *Crassostrea gigas* (Thunberg). *Aquaculture*, 175(3–4):215–226, 1999.
- K. Costil, J. Royer, M. Ropert, P. Soletchnik, and M. Mathieu. Spatio-temporal variations in biological performances and summer mortality of the Pacific oyster *Crassostrea gigas* in Normandy (France). *Helgol Mar Res*, 59:286–300, 2005.
- R. K. Cowen, C. B. Paris, and A. Srinivasan. Scaling of connectivity in marine populations. *Science*, 311(5760):522–527, 2006.
- J. A. Crooks and M. E. Soulé. Lag times in population explosions of invasive species: causes and implications. In O. T. Sandlund, P. J. Schei, and A. Viken, editors, *Invasive Species and Biodiversity Management*, pages 103–125. Kluwer Academic Publishers, Dordrecht, The Netherlands, 1999.
- N. Dankers and D. R. Zuidema. The role of the mussel (*Mytilus edulis* L.) and mussel culture in the Dutch Wadden Sea. *Estuaries*, 18(1A):71–80, 1995.
- S. Diederich. Differential recruitment of introduced Pacific oysters and native mussels at the North Sea coast: coexistence possible? *J Sea Res*, 53:269–281, 2005.

- S. Diederich. High survival and growth rates of introduced Pacific oysters may cause restrictions on habitat use by native mussels in the Wadden Sea. *J Exp Mar Biol Ecol*, 328(2):211–227, 2006.
- S. Diederich, G. Nehls, J. E. E. van Beusekom, and K. Reise. Introduced Pacific oysters *Crassostrea gigas* in the northern Wadden Sea invasion accelerated by warm summers? *Helgol Mar Res*, 59(2): 97–106, 2005.
- S. V. Dobretsov and G. Miron. Larval and post-larval vertical distribution of the mussel *Mytilus edulis* in the White Sea. *Mar Ecol Prog Ser*, 218:179–187, 2001.
- C. W. Gardiner. *Handbook of Stochastic Methods for Physics, Chemistry and the Natural Sciences*. Springer, 1983.
- B. Gaylord and S. D. Gaines. Temperature or transport? Range limits in marine species mediated solely by flow. *Amer Nat*, 155(6):769–789, 2000.
- M. R. Gilg and T. J. Hilbish. Patterns of larval dispersal and their effect on the maintenance of a blue mussel hybrid zone in Southwestern England. *Evolution*, 57(5):1061–1077, 2003.
- S. Gollasch. Overview on introduced aquatic species in European navigational and adjacent waters. *Helgol Mar Res*, 60(2):84–89, 2006.
- L. A. Gosselin and P. Y. Qian. Juvenile mortality in benthic marine invertebrates. *Mar Ecol Prog Ser*, 146:265–282, 1997.
- E. His, R. Robert, and A. Dinet. Combined effects of temperature and salinity on fed and starved larvae of the Mediterranean mussel *Mytilus galloprovincialis* and the Japanese oyster *Crassostrea gigas*. *Mar Biol*, 100:455–463, 1989.
- H. L. Hunt and R. E. Scheibling. Role of early post-settlement mortality in recruitment of benthic marine invertebrates. *Mar Ecol Prog Ser*, 155:269–301, 1997.
- R. J. Jenkins and J. L. Meredyth-Young. Occurrence of the Pacific oyster, *Crassostrea gigas*, off the South Island of New Zealand. *N Z J Mar Freshw Res*, 13(1):173–174, 1979.
- K. B. Johnson and A. L. Shanks. Low rates of predation on planktonic marine invertebrate larvae. *Mar Ecol Prog Ser*, 248:125–139, 2003.
- C. B. Jørgensen. Mortality, growth and grazing impact of a cohort of bivalve larvae, *Mytilus edulis* L. *Ophelia*, 20(2):185–192, 1981.

- S.-G. Kang, K.-S. Choi, A. A. Bulgakov, Y. Kim, and S.-Y. Kim. Enzyme-linked immunosorbent assay (ELISA) used in quantification of reproductive output in the Pacific oyster, *Crassostrea gigas*, in Korea. *J Exp Mar Biol Ecol*, 282:1–21, 2003.
- M. J. Keough and B. J. Downes. Recruitment of marine invertebrates: the role of active larval choices and mortality. *Oecologia*, 54:348–352, 1982.
- A. M. Knights, T. P. Crowe, and G. Burnell. Mechanisms of larval transport: vertical distribution of bivalve larvae varies with tidal conditions. *Mar Ecol Prog Ser*, 326:167–174, 2006.
- M. Kobayashi, E. E. Hofmann, E. N. Powell, J. M. Klinck, and K. Kusaka. A population dynamics model for the Japanese oyster, *Crassostrea gigas*. *Aquaculture*, 149:285–321, 1997.
- L. A. Levin. Recent progress in understanding larval dispersal: new directions and digressions. *Integr Comp Biol*, 46(3):282–297, 2006.
- R. Lewin. Supply-side ecology. *Science*, 234:25–27, 1986.
- R. Mann. Some biochemical and physiological aspects of growth and gametogenesis in *Crassostrea gigas* and *Ostrea edulis* grown at sustained elevated temperatures. *J Mar Biol Ass U.K.*, 59(1): 95–110, 1979.
- D. J. Marshall. In situ measures of spawning synchrony and fertilization success in an intertidal, free-spawning invertebrate. *Mar Ecol Prog Ser*, 236:113–119, 2002.
- J. van der Meer, J. J. Beukema, and R. Dekker. Long-term variability in secondary production is primarily a matter of recruitment variability. *J Anim Ecol*, 70:159–169, 2001.
- A. Metaxas. Behaviour in flow: perspectives on the distribution and dispersion of meroplanktonic larvae in the water column. *Can J Fish Aquat Sci*, 58(1):86–98, 2001.
- A. Metaxas, R. E. Scheibling, and C. M. Young. Estimating fertilization success in marine benthic invertebrates: a case study with the tropical sea star *Oreaster reticulatus*. *Mar Ecol Prog Ser*, 226: 87–101, 2002.
- J. E. Pechenik. On the advantages and disadvantages of larval stages in benthic marine invertebrate life cycles. *Mar Ecol Prog Ser*, 177:269–297, 1999.
- K. Reise. Pacific oysters invade mussel beds in the European Wadden Sea. *Senck marit*, 28:167–175, 1998.
- K. Reise, S. Gollasch, and W. J. Wolff. Introduced marine species of the North Sea coasts. *Helgol Mar Res*, 52:219–234, 1999.

- J. Roughgarden, S. Gaines, and H. Possingham. Recruitment dynamics in complex life cycles. *Science*, 241:1460–1466, 1988.
- J. L. Ruesink. Biotic resistance and facilitation of a non-native oyster on rocky shores. *Mar Ecol Prog Ser*, 331:1–9, 2007.
- J. L. Ruesink, H. S. Lenihan, A. C. Trimble, K. W. Heiman, F. Micheli, J. E. Byers, and M. C. Kay. Introduction of non-native oysters: ecosystem effects and restoration implications. *Annu Rev Ecol Syst*, 36:643–689, 2005.
- S. S. Rumrill. Natural mortality of marine invertebrate larvae. *Ophelia*, 32(1-2):163–198, 1990.
- M. Scheffer, J. M. Baveco, D. L. DeAngelis, K. A. Rose, and E. H. van Nes. Super-individuals a simple solution for modelling large populations on an individual basis. *Ecol Modell*, 80(2-3): 161–170, 1995.
- H. Scholten and A. C. Smaal. Responses of *Mytilus edulis* L. to varying food concentrations: testing EMMY, an ecophysiological model. *J Exp Mar Biol Ecol*, 219:217–239, 1998.
- A. L. Shanks, B. A. Grantham, and M. H. Carr. Propagule dispersal distance and the size and spacing of marine reserves. *Ecol Appl*, 13(1):159–169, 2003.
- N. Shigesada and K. Kawasaki. *Biological Invasions: Theory and practice*. Oxford University Press, 1997.
- D. A. Siegel, B. P. Kinlan, B. Gaylord, and S. D. Gaines. Lagrangian descriptions of marine larval dispersion. *Mar Ecol Prog Ser*, 260:83–96, 2003.
- A. C. Smaal. European mussel cultivation along the Atlantic coast: production status, problems and perspectives. *Hydrobiologia*, 484(1-3):89–98, 2002.
- A. C. Smaal, M. van Stralen, and J. Craeymeersch. Does the introduction of the Pacific oyster *Crassostrea gigas* lead to species shifts in the Wadden Sea? In R.F. Dame and S. Olenin, editors, *The Comparative Roles of Suspension-feeders in Ecosystems*, volume 47 of *Nato Science Series: 4. Earth and Environmental Sciences*, pages 277–289. Springer Netherlands, 2005.
- J. Staneva, E. V. Stanev, J. O. Wolff, T. Badewien, R. Reuter, B. Flemming, A. Bartholomä, and K. Bolding. Hydrodynamics and sediment dynamics in the German Bight. a focus on observations and numerical modelling in the East Frisian Sea. *Cont Shelf Res*, 29(1):302–319, 2009.
- S. Steele and M. F. Mulcahy. Gametogenesis of the oyster *Crassostrea gigas* in Southern Ireland. *J Mar Biol Ass U.K.*, 79(04):673–686, 1999.

- R. A. Stillman, S. McGroarty, J. D. Goss-Custard, and A. D. West. Predicting mussel population density and age structure: the relationship between model complexity and predictive power. *Mar Ecol Prog Ser*, 208:131–145, 2000.
- M. Strasser and C.-P. Günther. Larval supply of predator and prey: temporal mismatch between crabs and bivalves after a severe winter in the Wadden Sea. *J Sea Res*, 46:57–67, 2001.
- P. A. Thompson and T. J. Harrison. Effects of monospecific algal diets of varying biochemical composition on the growth and survival of Pacific oyster (*Crassostrea gigas*) larvae. *Mar Biol*, 113: 645–654, 1992.
- C. D. Todd. Larval supply and recruitment of benthic invertebrates: do larvae always disperse as much as we believe? *Hydrobiologia*, 375/376:1–21, 1998.
- A. J. Underwood and P. G. Fairweather. Supply-side ecology and benthic marine assemblages. *Trends Ecol Evol*, 4(1):16–20, 1989.
- F. Viard, C. Ellien, and L. Dupont. Dispersal ability and invasion success of *Crepidula fornicata* in a single gulf: insights from genetic markers and larval-dispersal model. *Helgol Mar Res*, 60: 144–152, 2006.
- J. de Vlas, B. Brinkman, N. Dankers, M. Herlyn, P. S. Kristensen, G. Millat, G. Nehls, M. Ruth, J. Steenbergen, and A. Wehrmann. Intertidal blue mussel beds. In K. Essink, C. Dettmann, H. Farke, K. Laursen, G. Lüerßen, H. Marencic, and W. Wiersinga, editors, *Wadden Sea Quality Status Report 2004*, pages 190–200. Common Wadden Sea Secretariat, 2005.
- A. Wehrmann, M. Herlyn, F. Bungenstock, G. Hertweck, and G. Millat. The distribution gap is closed - first record of naturally settled Pacific oysters *Crassostrea gigas* in the East Frisian Wadden Sea, North Sea. *Senckenb Marit*, 30(3-6):153–160, 2000.
- A. Wehrmann, A. Markert, P. May, P. Schieck, and A. Schmidt. Gefährdungspotenzial der eulitoralischen Miesmuschelbänke im Niedersächsischen Wattenmeer durch die Bioinvasion der Pazifischen Auster *Crassostrea gigas*. Unpubl. Report, Forschungsinstitut Senckenberg, Wilhelmshaven, 2006.
- E. F. Young, G. R. Bigg, A. Grant, P. Walker, and J. Brown. A modelling study of environmental influences on bivalve settlement in The Wash, England. *Mar Ecol Prog Ser*, 172:197–214, 1998.

## Chapter 4

---

# Tidal vertical migration enhances nearshore retention in weak-swimming meroplanktonic larvae

### 4.1 Introduction

Planktonic larvae are common in the life cycle of many marine benthic invertebrates. The most obvious consequence of larval stages is a great dispersal potential for species with otherwise limited mobility. While this strategy entails several benefits, including a large geographic range, reduced competition, and facilitated recolonisation of lost habitats, it also involves the risk of being transported to unfavourable habitats [Pechenik 1999]. Unlike fish larvae, invertebrate larvae are mostly weak swimmers compared to the strength of oceanic currents and can, thus, not directly influence their horizontal motion. Swimming speeds, however, are often in the range of vertical current speeds [Chia et al. 1984, Mileikovsky 1973] and there is substantial evidence that planktonic larvae of many species do not act as passive particles, but actively influence their vertical position in the water column [reviewed by Metaxas 2001]. By this means, larvae can significantly alter their horizontal transport and may even minimise the dispersal to unfavourable habitats, especially in environments with strong vertical current shear or high temporal current variability. Larvae may react to a variety of different stimuli [Kingsford et al. 2002], but details regarding the effect of behavioural strategies remain speculative since tracking larvae in the field requires tremendous effort and is only possible for very short periods [Genin et al. 2005]. Only numerical models allow a simple and direct assessment of larval dispersal and the role of behaviour over periods of several days or weeks [e.g. Verdier-Bonnet et al. 1997, Manuel and O'Dor 1997, Hill 1991].

In this study, I evaluate the effect of different vertical migration strategies on the spatial distribution of competent larvae in the tidally-dominated coastal North Sea with a three-dimensional Lagrangian particle tracking model.

In the study area, Strasser [2000] observed that surface concentrations of *Mytilus edulis* larvae are strictly in phase with water level over several tidal cycles (Fig. 4.1), suggesting tidal vertical migration (TVM). This strategy, common in megalopae of crabs [Lee et al. 2005, Welch and Forward 2001, Queiroga 1998], implies that larvae swim upwards during flood and remain close to or on the bottom during ebb. The net effect is a shoreward transport. In addition to TVM, I also simulate the effect of diurnal vertical migration (DVM), common in many holoplankton species [Hays 2003], and passive

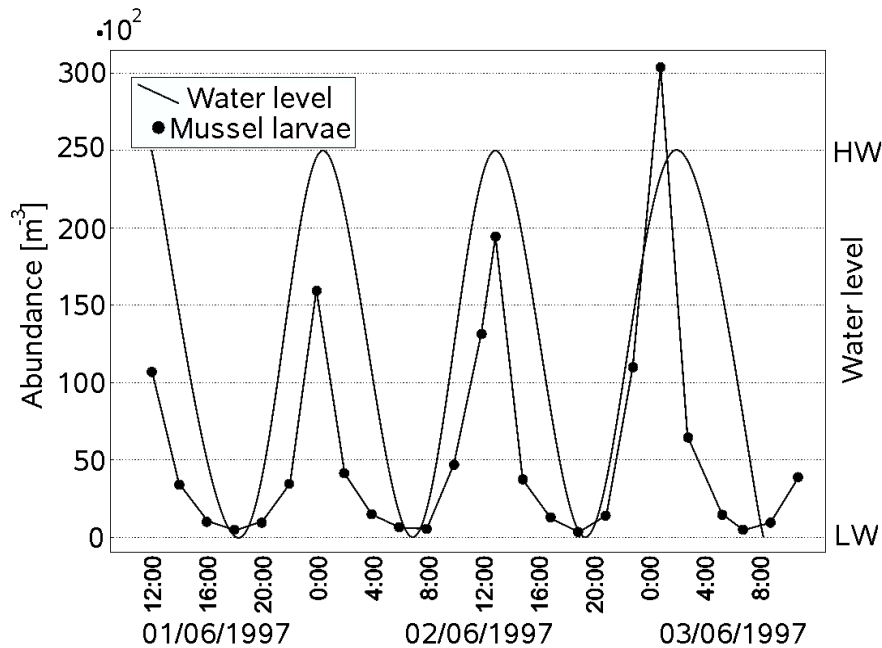


Figure 4.1: Abundance time-series of mussel larvae during several tidal cycles in the Wadden Sea at the ferry pier in List, island of Sylt. Samples were taken bi-hourly in surface waters. LW and HW indicate low and high water, respectively. (Modified from: Strasser [2000])

drifting (PD) on the dispersal of larvae.

## 4.2 Methods

### 4.2.1 Study area and model organism

The German Bight, located in the southeastern part of the North Sea, is a tidally dominated shallow coastal sea. The coastline in the South and the East is protected by several barrier islands or opened to the broad estuaries of the rivers Elbe, Weser and Jade (Fig. 4.2). In the back of the barrier islands, the Wadden Sea presents a highly diverse ecosystem with channels, tidal flats, and marshlands. The residual current in the German Bight is counterclockwise because of the tidal wave and prevailing winds from westerly directions. In the narrow channels of the Wadden Sea, however, ebb and flood result in strong seaward and shoreward currents, respectively. Tides also cause a periodic reversal of the currents and periodic salinity fluctuations since a permanent salinity gradient is sustained by river run-off and diffuse freshwater inflow through the Wadden Sea (Fig. 4.3).

*Mytilus edulis*, a prevalent mussel in the intertidal and shallow subtidal North Sea, is regarded representative for many other benthic invertebrates with planktonic larval stages. The spatial distribution of adult mussel beds in the intertidal Wadden Sea is regularly monitored by regional authorities (Fig.

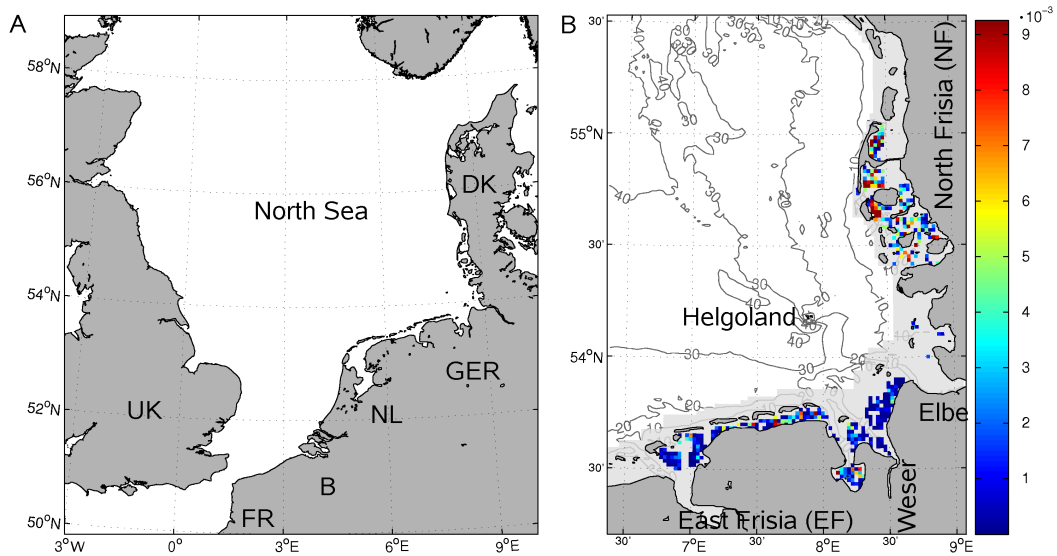


Figure 4.2: **A** The North Sea Region. **B** Study area with bathymetric contours. The shallow coastal area is shaded in light gray and the relative distribution of intertidal blue mussel banks (expressed as a fraction of the total area covered by mussel beds in the study area) is indicated by the colour spectrum. In North Frisia, potential areas for subtidal mussel cultures are also included in the mussel distribution.

4.2). *Mytilus edulis* exhibits multiple spawning events in spring and late summer and its larvae spend several weeks in the plankton. Dispersal to unfavourable offshore areas is a major threat to *Mytilus edulis*, because the required hard-substrate and shallow water depths are scarce in the North Sea. Since the swimming abilities of mussel larvae is comparable to the abilities of many other species, the results of this study may be potentially relevant to other species inhabiting coastal seas.

#### 4.2.2 Model

A three-dimensional Lagrangian drift model is combined with an Individual-Based Model (IBM) that accounts for larval swimming behaviour and growth.

The drift model consists of a particle tracking algorithm that is coupled offline with hydrodynamical data (current velocities  $u$ ,  $v$  and  $w$ , eddy diffusivities  $A_h$  and  $A_v$ ) from the operational model of the German Federal Maritime and Hydrography Agency [BSHcm0d, Dick 2001]. The vertical attenuation of horizontal current speeds with depth is not resolved by the BSHcm0d since it is a  $z$ -coordinate model with a coarse vertical resolution (8 m for the first three levels, 26 and 50 m for the fourth and fifth level). To account for this effect, a logarithmic attenuation of horizontal currents is assumed in the bottommost layer of the model (cf. Appendix).

In addition to passive transport, larvae actively influence their vertical position in the water column according to the different behavioural strategies that are described by the IBM. The direction of active swimming is either determined by the daily light cycle (DVM, upward at night, downward during

daytime) or by the temporal salinity gradient (TVM, upward with increasing salinity, downward with decreasing salinity). PD, which involves no active swimming, presents the reference strategy.

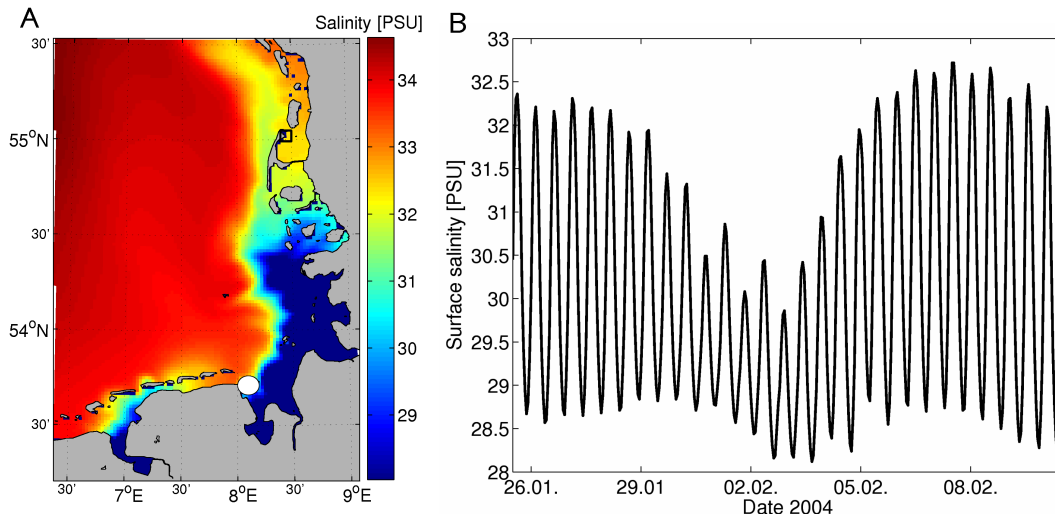


Figure 4.3: **A** Simulated surface salinity by the BSHcmod on 21 March 2004 at 20:00h; the tiny white dot indicates the location where the time-series in Fig. 4.3B is evaluated, the box indicates the sampling site of the mussel larvae in Fig. 4.1. **B** Time-series of simulated surface salinity at a point in the Jade estuary (cf. Fig. 4.3A).

Particles are released simultaneously in each grid box that contains intertidal mussel beds in the study area. The distribution of these mussel beds is derived from aerial surveys in the East and North Frisian Wadden Sea [Herlyn et al. 2008, Herlyn 2005]. The data were collected during surveys in 1999 (East Frisia, source: Nationalparkverwaltung Niedersächsisches Wattenmeer) and 2001 (North Frisia, Landesamt für den Nationalpark Schleswig-Holsteinisches Wattenmeer). In North Frisia sub-tidal culture plots are included in addition to the intertidal mussel beds.

Following Scheffer et al. [1995] each particle is a super-individual representing a number of larvae, which is related to the coverage with mussel beds of the initial grid box. The planktonic development time, the time a larva needs to become competent, is mainly depending on the ambient water temperature and ranges from three to six weeks for *Mytilus edulis* (cf. Appendix).

The influence of a behavioural strategy on the fate of the larvae is assessed by the respective mean spatial distribution of competent larvae. It is compiled from 15 single simulations that differ only in the starting day (Julian day 91, 109 and 127 in each of the years 2000 - 2004) to account for varying hydrodynamic situations. The effect of different maximum swimming speeds (MSSs) on the mean spatial distribution is evaluated for each strategy. While for DVM only three different velocities are considered (2, 4, 6  $mm \cdot s^{-1}$ ), six values (1 - 6  $mm \cdot s^{-1}$ ) are simulated for TVM. Hence, for each migration strategy and each MSS, a mean distribution of competent larvae is calculated. Besides the

spatial distribution, the model results also allow to derive characteristic parameters describing the success of the larval strategy, such as the mean travelled distance, the degree of retention, and return to nearshore waters. Therefore, the study is divided into a shallow coastal zone (Fig. 4.2), which is regarded as the potential natural habitat for settling larvae, and offshore waters, which are considered inadequate for settlement.

## 4.3 Results

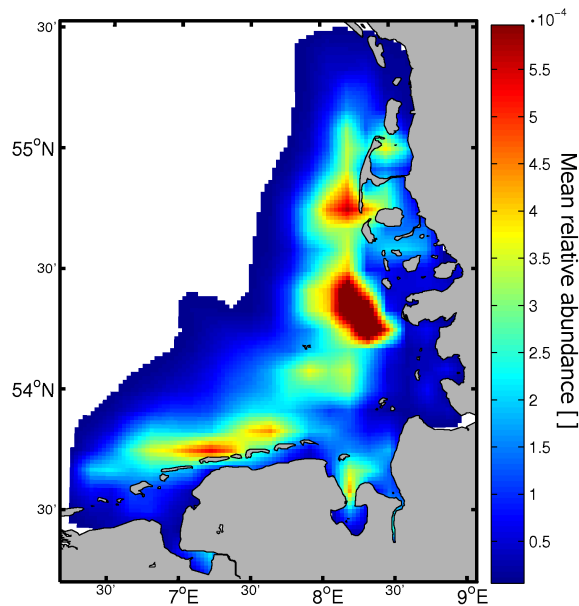


Figure 4.4: Mean relative abundances of passive larvae at the end of their planktonic development phase.

### 4.3.1 Passive larvae

The distribution of competent larvae that act as passive drifters in the German Bight mirrors the spatial pattern of intertidal mussel banks (cf. Figs. 4.2 and 4.4). Most larvae leave the Wadden Sea, but remain close to the coast, so that highest larval abundances are simulated off the coast of North Frisia. Elevated relative abundances also occur in a narrow stretch off the barrier islands in the western part of the study area. In contrast, most tidal inlets and estuaries in the German Bight are free from larvae. This also holds for several sites where adult mussel banks are common, e.g. the area between the Jade and the Weser estuary, the Ems estuary or parts of the North Frisia Wadden Sea (cf. Figs. 4.2 and 4.4). The spatial distribution of competent larvae indicates that alongshore processes clearly dominate the transport outside the Wadden Sea.

Roughly two thirds of all larvae do not reach a suitable habitat for settling within their development

time (Fig. 4.7) and most of the larvae that become competent within the coastal zone have returned from offshore waters. Only a minority is retained within the coastal zone during the entire period of their planktonic life.

Mean travelled distances for passive larvae are in the range of several tens of kilometers (Fig. 4.6) for a mean development time of  $34.5 \pm 4.1 d$ , thus, making local recruitment rather unlikely for planktonic residence times in the order of one month.

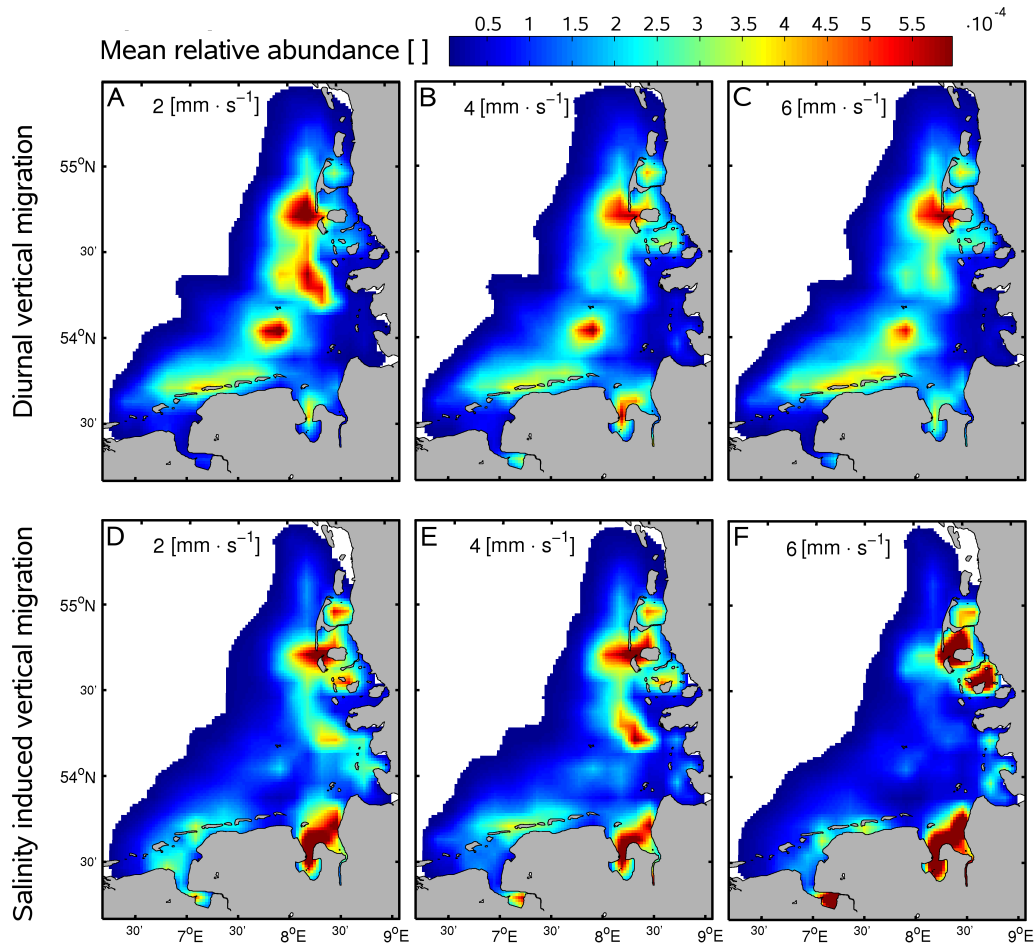


Figure 4.5: **A-C** Mean relative abundances for diurnal vertical migration at the end of the planktonic development phase. **D-E** Mean relative abundances for tidal vertical migration at the end of the planktonic development phase. Each distribution is the mean from 15 simulations (three starting days (91,109 and 127) in the years 2000-2004).

### 4.3.2 Diurnal vertical migration

A diurnal vertical migration strategy changes the distribution of competent larvae within the coastal German Bight only marginally. Most notably, the distinct maxima of larvae in the central part of the

study area diminish with increasing MSS (Fig. 4.5). Instead, slightly more larvae are located within the intertidal coastal area at the end of their development period. This effect is notable especially in North Frisia in the vicinity of the island of Sylt, whereas the distribution off the East Frisian coast remains mostly unchanged. The pronounced aggregation of passive larvae north of Helgoland island weakens when larvae conduct a diurnal vertical migration. Instead, a new local maximum of larvae emerges south of Helgoland. Both patches are divided by a small stretch of low larval concentrations. The ratios of retained and returned individuals reveal that the elevated concentrations in the coastal area of North Frisia are mainly due to an increasing fraction of larvae that returned from offshore to coastal regions with rising MSSs. Mean travelled distances are, in contrast, not affected by DVM (Fig. 4.6).

### 4.3.3 Tidal vertical migration

Tidal vertical migration, here induced by temporal salinity gradients, clearly causes a change in the distribution of competent larvae in the German Bight. In the waters off East Frisia and North Frisia, this strategy enhances the fraction of larvae that are located in favourable coastal areas at the end of their planktonic phase.

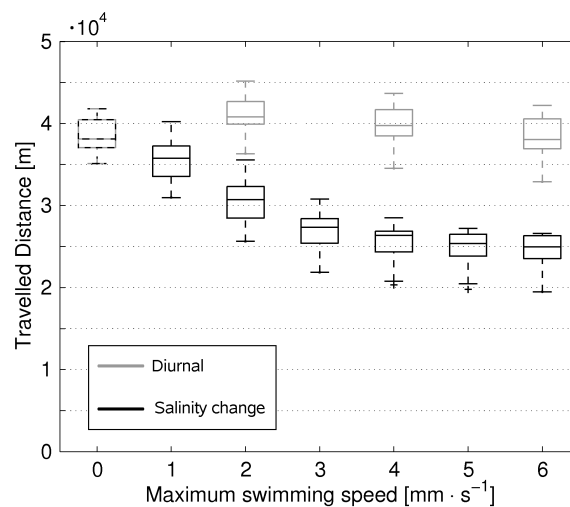


Figure 4.6: Net travelled distance of larvae with different vertical migration strategies (diurnal and tidal vertical migration) as a function of maximum swimming speed.

With increasing MSS, the mean travelled distance of the larvae declines significantly to minimum values around 25 km (Fig. 4.6). In this case, not only the retention, but also the return of larvae is enhanced (Fig. 4.7). There is, however, a difference in the effectiveness of this mechanism between the two regions. While in North Frisian waters the fractions of retained and returned larvae are both monotonically increasing with swimming speed, in East Frisian waters the fraction of returned larvae

has a maximum of 0.35 already at a MSS of  $3 \text{ mm} \cdot \text{s}^{-1}$ . Higher swimming speeds cause a further rise of the retained fraction with the consequence of a smaller fraction of returned individuals in this region.

The spatial distribution of competent larvae changes noticeably already at MSSs as low as  $2 \text{ mm} \cdot \text{s}^{-1}$ . While the prominent offshore maxima disappear, larvae preferentially accumulate in the estuaries of the rivers Ems and Weser and the Wadden Sea south of Sylt island. At the highest MSS of  $6 \text{ mm} \cdot \text{s}^{-1}$ , larvae are able to almost completely avoid the abandonment of the coastal zone. A comparison between the spatial distributions of larvae and salinity (c.f. Fig. 4.3) reveals that pronounced accumulations only occur in areas with low salinities. Moreover, the estuaries are also the regions with the highest spatial and temporal salinity gradients in the German Bight.

TVM distinctively affects the mean travelled distance, which declines to values around  $25 \text{ km}$  for MSSs above  $3 \text{ mm} \cdot \text{s}^{-1}$  (Fig. 4.6). The larval coverage of the German Bight does, however, not change indicating a rather invariable maximum dispersal range of individuals released in the intertidal Wadden Sea.

The larval supply to the Wadden Sea landwards of the barrier islands in East Frisia does not benefit from TVM in these simulations. Though the region is prevalently covered by mussel banks, only few larvae are located here at the end of their planktonic development time.

## 4.4 Discussion

Most passive larvae are dispersed offshore and therefore lost for recruitment since the only favourable offshore habitat for benthic invertebrates requiring shallow waters in the German Bight is the island of Helgoland [Reichert et al. 2008]. Though larvae of benthic invertebrates may delay their metamorphosis for days or even weeks [Pechenik 1990], the failure to find a suitable settling site ultimately leads to mortality, either because of predation or starvation [Pechenik 1999].

The mean spatial distribution of competent passive larvae does not only reflect the heterogeneous distribution of adult biomass in the German Bight, but also the dominance of alongshore transport [O'Connor et al. 2000, Maier-Reimer 1977]. Local concentration maxima off the East Frisian coast are, thus, aligned zonally, whereas larval patterns off the North Frisian coast have a meridional orientation. In contrast, the estuaries of the rivers Weser and Elbe, and wide areas of the North Frisian Wadden Sea only receive a relatively low larval supply challenging the observations of high adult abundances in these areas. Simulated losses of larvae to offshore areas are typically around 70 %, a high portion considering that other important causes of mortality such as predation and starvation are neglected [Pechenik 1999, Bos et al. 2006], thus, making PD an ineffective strategy for maximising larval supply to potential natural habitats in the German Bight.

Diurnal vertical migration (DVM) is a common strategy in marine and freshwater plankton and this

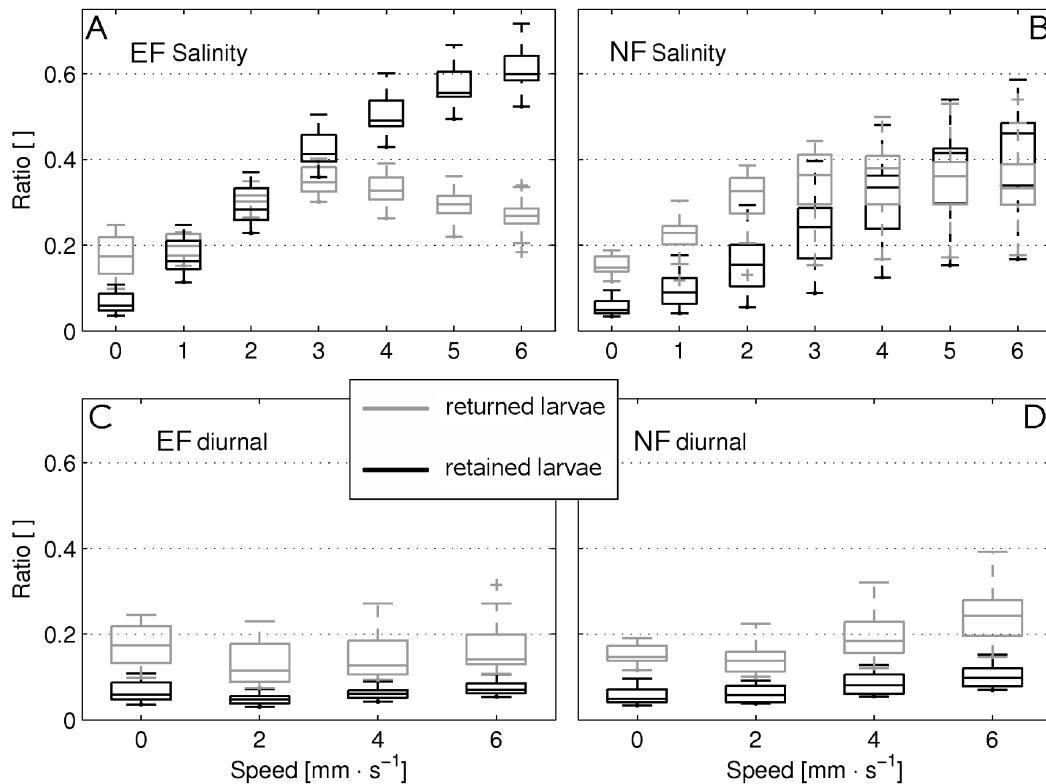


Figure 4.7: Fraction of larvae that are retained within the coastal area or that return to the coastal area as a function of vertical migration strategy and maximum swimming speed. Results are shown separately for the two regions East Frisia (EF) and North Frisia (NF).

costly behaviour can be explained by the need to avoid predation or to avoid the exposure to UV radiation [Hays 2003, Loose and Dawidowicz 1994]. The potential benefit of this strategy seems, however, to be restricted to deeper waters, where predation is weaker at greater depths. In coastal seas with water depths of less than 30 m predation pressure might be very high also close to the bottom where filter-feeding animals can efficiently ingest larvae, including offsprings of their own species [Troost et al. 2008, Lehane and Davenport 2004, André and Rosenberg 1991]. Nevertheless, there is evidence indicating that DVM is also adopted by bivalve larvae [Raby et al. 1994].

When averaged over several simulations (15 spawning dates in five years), DVM has only a minor effect on the spatial distribution of larvae in the study area. The apparent weakening of the maxima with increasing MSSs is due to the interference of the tidal period with the light period. Since the dominant tidal period is approximately 12.25 h in the study area, the timing of ebb and flood shifts slightly from day to day. It is therefore only a matter of coincidence if in a single simulation the time the larvae spends at the surface or at the bottom overlaps mostly with flood or ebb tides. The effect on the mean distribution of several simulations is a decrease of the concentration maxima, because averaging over several simulations with randomly enhanced or reduced dispersal reduces the maxima of

larval concentrations. The clear separation of the concentration maxima north and south of Helgoland is probably caused by a stable front dividing the German Bight into two distinct halves [Becker et al. 1992] probably limiting the transfer of larvae from East Frisian to North Frisian waters. To conclude, the results of this study indicate that DVM does not increase the larval supply to nearshore habitats. This energetically expensive strategy might, however, have other advantages, perhaps connected to metabolic or demographic aspects [Lampert 1989].

TVM cued by salinity changes appears to be very advantageous with regard to the dispersal to favourable habitats in the study area. The fraction of larvae that are retained close to their spawning site or returned to the coastal zone greatly increases with rising MSSs. In the model, the larval supply to estuaries with strong temporal and spatial salinity gradients and strong currents is enhanced by this behaviour since the direction of migration is determined by the temporal salinity gradient. Regions with strong salinity changes during the tidal cycle act as a guide for the larvae, thus explaining the aggregation of offsprings in the estuaries. Hence, TVM cued by salinity changes appears to be an effective strategy to enhance coastal retention in areas where strong temporal salinity gradients and a vertically sheared horizontal flow occur simultaneously.

In the absence of a salinity gradient, the behavioural strategy has no benefit to the larvae. This is especially evident in the East Frisian Wadden Sea, where the hydrodynamic model fails to simulate a realistic spatial salinity gradient. This gradient is sustained by diffuse freshwater inputs that are not considered in the model set-up [Staneva et al. 2009, Burchard et al. 2008].

MSSs that are required to almost completely prevent the loss of larvae to offshore areas in this model are in the same order of magnitude as the values reported for most bivalve larvae [Chia et al. 1984, Mileikovsky 1973], especially considering that the mean swimming speed of competent larvae in the model is only half the MSS. This result implies that larvae of most marine benthic invertebrates should not be regarded as passive particles only because they cannot control their position within the water column in all hydrodynamic conditions [Shanks and Brink 2005, Metaxas 2001]. Knights et al. [2006] have, indeed, observed that the vertical position of *Mytilus spp.* in the Irish Sea varies with the tidal phase and Yaroslavteva and Sergeeva [2003] showed in a laboratory experiment that *Mytilus trossulus* reacts to salinity gradients. Although observations in the Wadden Sea [Verwey 1966] and in the White Sea [Dobretsov and Miron 2001] support the hypothesis that the vertical distribution of *Mytilus* larvae is influenced by the tidal phase, the reason of their behavioural strategy still remains unclear, particularly because observational periods include only few tidal cycles and results are not conclusive. This also holds for almost all marine benthic invertebrate larvae and is mostly due to difficulties in tracking individuals in the field over the required spatial and temporal scale [Levin 2006]. Only in the bigger megalopae larvae of crabs, the existence and benefits of tidally cued vertical migration has been reported by several authors [Lee et al. 2005, Queiroga 1998]. While my study clearly underlines the potential consequences of TVM also for weak swimmers, further research is desirable to clarify

the details of larval behaviour and to quantify its effect.

The invariance of the model results, especially for the tidal migration strategy, depends predominantly on the invariant vertical shear of the horizontal currents. Although measurements and high-resolution simulations generally support the assumption of strong current attenuation with depth in the coastal German Bight, a realistic vertical profile is more complex and variable than the assumed profile in this study. The directions of tidal mean velocities at the bottom and at the surface in the coastal Wadden Sea can, for example, be even oppositional [Burchard et al. 2008]. Moreover, the coarse vertical resolution of the hydrodynamic model limits the representation of the vertical flow and the turbulence profile. A better model resolution can produce more realistic simulations, especially with regard to the ability of weakly swimming larvae to overcome zones of enhanced turbidity, i.e. the ability to control their vertical position in the water column [Metaxas 2001]. Zooplankton species are also known to adapt their swimming behaviour corresponding to the surrounding flow field [Genin et al. 2005], a behaviour that is not considered in this study.

Consequently, my model cannot produce detailed forecasts of larval trajectories. It is, however, capable of explaining the potential effect of different vertical migration strategies on the transport and distribution of larvae in an environment with vertically sheared currents. While more sophisticated models could lead to better results, the bottleneck for real advancements in the understanding of larval dispersal arises from the lack of knowledge regarding *in situ* larval behaviour [Metaxas 2001]. Most progress in assessing the dispersal of individuals has been made with indirect methods, especially tagging larvae and genetics (see Levin [2006] for a review). In contrast, examples of direct approaches to measure the behaviour of zooplankton in natural environments [Genin et al. 2005] are sparse, expensive and may not be applicable to all conditions, which explains the slow progress in this branch of marine ecology.

## 4.5 Conclusion

In this study I evaluated the effects of different vertical migration strategies on the dispersal of marine invertebrate larvae in tidally dominated coastal seas. The majority of passively drifting (PD) larvae originating in the intertidal of the North Sea are transported to unfavourable offshore areas within their planktonic development time. Vertical migration in this environment with strong current shear may significantly influence dispersal, even when swimming speeds are low compared to horizontal currents. While vertical migration in phase with the period of the tides (TVM) greatly enhances the retention close to the coast or the return to coastal areas, diurnal vertical migration (DVM) has only a minor effect on the spatial distribution of larvae. The effectiveness of TVM is correlated with the maximum swimming speed of larvae, suggesting that primarily species with strong swimming abilities may benefit from this strategy. While high hydrodynamic model resolution allows to conduct

---

detailed simulations of larval transport, the limiting factor in understanding larval dispersal is clearly the lack of observations of active larval behaviour in the field.

## 4.6 Appendix

$N_{part} = 500$  particles are released in a discrete pulse at the beginning of a simulation in each grid box that contains adult mussel beds. Each particle is assigned a relative abundance of larvae that corresponds to the spatial coverage of mussel beds  $C$  in the grid box with respect to the total area covered by mussel beds in the study area. Hence, the relative abundance  $B_j$  of a particle released in grid box  $j$  is

$$B_j = \frac{C_j}{N_{part} \cdot \sum_{k=0}^{N_{box}} C_k} \quad (4.1)$$

with the total number of grid boxes  $N_{box}$ .

A Lagrangian algorithm simulates the particle transport after release. Following Visser [1997] and Hunter et al. [1993], the new position of a particle in the  $x$ -th dimension at the time  $t + 1$  is given by

$$x_{t+1} = x_t + u\Delta t + \frac{\partial A_x}{\partial x} \Delta t + Z \sqrt{2A_x \Delta t} \quad , \quad (4.2)$$

where  $x_n$  is the position at time  $n$ ,  $\Delta t$  is the time-step,  $A_x$  is the eddy diffusivity in the dimension  $x$ , and  $Z$  is a  $N(0, 1)$  random number. While in the horizontal  $u$  is equal to the current velocity  $u_c$ , in the

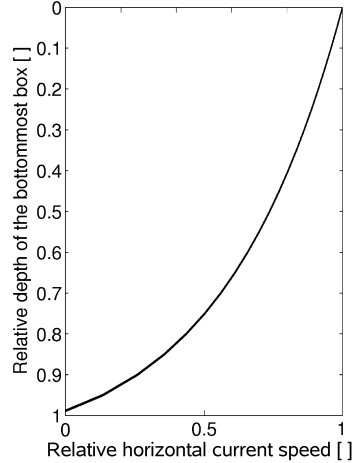


Figure 4.8: Assumed attenuation of horizontal currents with depth in the bottommost grid box of the hydrodynamical model.

vertical a potential active swimming velocity  $w_*$  adds to the current velocity, so that  $u = u_c + w_*$ . The time-step  $\Delta t$  is 900 s, corresponding to the time-step of the current data; eddy diffusivities are updated hourly.

In the bottommost grid box a vertical profile of horizontal currents is assumed, since the coarse vertical resolution of the BSHcmod prevents the realistic simulation of current attenuation with depth (Fig.

4.8). The potential swimming speed of a larva  $w(A)$  is defined as a function of its age  $A$  and the MSS  $w_{max}$ .

$$w(A) = w_{max} \cdot \frac{1}{1 + e^{-\beta \cdot (A - k_A)}} \quad (4.3)$$

with the scaling factor  $\beta = -0.0055 d^{-1}$  and the age  $k_A$  at which larvae reach half of  $w_{max}$ . The parameter  $k_A$  is expressed as a fraction  $r_\tau = 0.15$  of the larval development time  $\tau_d$ . The actual swimming speed  $w_\star$  of a larva is a random function depending on the vertical position  $z$  in the water column.

$$w_\star = \alpha(z) \cdot w_A \cdot Z \cdot D \quad (4.4)$$

where  $\alpha(z)$  is an attenuation function,  $Z$  is a  $N(0.5, 0.0625)$  distributed Gaussian random number, and  $D$  is the swimming direction. Hence, the average swimming speed of all larvae is only half the potential speed  $w(A)$ , and 96% of all individuals have a swimming speed between  $0 \text{ mm} \cdot \text{s}^{-1}$  and  $w(A)$ .

The swimming direction  $D$  is either 1 (downward) or  $-1$  (upward), depending on the vertical migration strategy. While for DVM  $D = -1$  at night and 1 during the day, for TVM

$$D = \begin{cases} -1 & \text{for } \frac{\partial S}{\partial t} \geq 0 \\ 1 & \text{for } \frac{\partial S}{\partial t} < 0. \end{cases} \quad (4.5)$$

Swimming is either directed to the surface or the depth  $\zeta_{aim}$ , which is the minimum of the actual water depth  $\zeta$  and  $\zeta_{max} = 12 \text{ m}$ . Larval swimming speeds are slowed down by the attenuation function  $\alpha$  to achieve a smooth approach of the larvae to the target depth and prevent an overshooting.

$$\alpha(z) = \begin{cases} \frac{z}{\zeta_{aim}} & \text{for } D = -1 \\ 1 - \frac{z}{\zeta_{aim}} & \text{for } D = 1 \end{cases} \quad (4.6)$$

Since larval nutrition is not explicitly treated by the model, the larval development time  $\tau_d$  is defined as a linear function of water temperature  $T$  [Beaumont et al. 2004, Beaumont and Budd 1982, Hrs-Brenko and Calabrese 1969] and evaluated at each model time step

$$\tau_d = a_\tau - b_\tau \cdot T \quad (4.7)$$

with the parameters  $a = 56.0 \text{ d}$  and  $b = -1.75 \text{ d} \cdot ^\circ \text{C}^{-1}$ . The increment of body length  $\Delta L$ , which determines the development time, is inversely related to  $\tau_d(t)$

$$\Delta L = \frac{L_{comp} - L_{init}}{\tau_d(t)} \quad (4.8)$$

with the initial length of a larva  $L_{init} = 70 \mu\text{m}$  and the length  $L_{comp} = 250 \mu\text{m}$  at which larval development is regarded complete. The simulation of a larval trajectory ends when the body length of a larva  $L(t)$  reaches  $L_{comp}$ . The relative abundance of the particle is then recorded and used to process the spatial maps of larval concentrations.

## **Acknowledgements**

I thank the Bundesamt für Seeschifffahrt und Hydrographie for the hydrodynamical model data. I am grateful to the Landesamt für den Nationalpark Schleswig-Holsteinisches Wattenmeer and the Nationalparkverwaltung Niedersächsisches Wattenmeer for providing distribution data of *Mytilus edulis* in the German Wadden Sea. Agostino Merico contributed valuable comments that helped to improve the manuscript.

## Bibliography

- C. André and R. Rosenberg. Adult-larval interactions in the suspension-feeding bivalves *Cerastoderma edule* and *Mya arenaria*. *Mar Ecol Prog Ser*, 71:227–234, 1991.
- A. R. Beaumont and M. D. Budd. Delayed growth of mussel (*Mytilus edulis*) and scallop (*Pecten maximus*) veligers at low temperatures. *Mar Biol*, 71(1):97–100, 1982.
- A. R. Beaumont, G. Turner, A. R. Wood, and D. O. F. Skibinski. Hybridisations between *Mytilus edulis* and *Mytilus galloprovincialis* and performance of pure species and hybrid veliger larvae at different temperatures. *J Exp Mar Biol Ecol*, 302:177–188, 2004.
- G. A. Becker, S. Dick, and J. W. Dippner. Hydrography of the German Bight. *Mar Ecol Prog Ser*, 91 (1-3), 1992.
- O. G. Bos, I. E. Hendriks, M. Strasser, P. Dolmer, and P. Kamermans. Estimation of food limitation of bivalve larvae in coastal waters of north-western Europe. *J Sea Res*, 55:191–206, 2006.
- H. Burchard, G. Flöser, J. V. Staneva, T. H. Badewien, and R. Riethmüller. Impact of density gradients on net sediment transport into the Wadden Sea. *J Phys Oceanogr*, 38(3):566–587, 2008.
- F.-S. Chia, J. Buckland-Nicks, and C. M. Young. Locomotion of marine invertebrate larvae: a review. *Can J Zool*, 62(7):1205–1222, 1984.
- S. Dick. The operational circulation model of BSH (BSHcmod) - model description and validation. *Berichte des BSH*, 29:49pp., 2001.
- S. V. Dobretsov and G. Miron. Larval and post-larval vertical distribution of the mussel *Mytilus edulis* in the White Sea. *Mar Ecol Prog Ser*, 218:179–187, 2001.
- A. Genin, J. S. Jaffe, R. Reef, C. Richter, and P. J. S. Franks. Swimming against the flow: a mechanism of zooplankton aggregation. *Science*, 308(5723):860–862, 2005.
- G. C. Hays. A review of the adaptive significance and ecosystem consequences of zooplankton diel vertical migrations. *Hydrobiologia*, 503(1):163–170, 2003.
- M. Herlyn. Quantitative assessment of intertidal blue mussel (*Mytilus edulis* L.) stocks: combined methods of remote sensing, field investigation and sampling. *J Sea Res*, 53:243–253, 2005.
- M. Herlyn, G. Millat, and B. Petersen. Documentation of sites of intertidal blue mussel (*Mytilus edulis* L.) beds of the Lower Saxonian Wadden Sea, southern North Sea (as of 2003) and the role of their structure for spatfall settlement. *Helgol Mar Res*, 62(2):177–188, 2008.

- A. E. Hill. Vertical migration in tidal currents. *Mar Ecol Prog Ser*, 75:39–54, 1991.
- M. Hrs-Brenko and A. Calabrese. The combined effect of salinity and temperature of the mussel *Mytilus edulis*. *Mar Biol*, 4:224–226, 1969.
- J. R. Hunter, P. D. Craig, and H. E. Phillips. On the use of random walk models with spatially variable diffusivity. *J Comp Phy*, 106:366–376, 1993.
- M. J. Kingsford, J. M. Leis, A. Shanks, K. C. Lindeman, S. G. Morgan, and J. Pineda. Sensory environments, larval abilities and local self-recruitment. *B Mar Sci*, 70(1):309–340, 2002.
- A. M. Knights, T. P. Crowe, and G. Burnell. Mechanisms of larval transport: vertical distribution of bivalve larvae varies with tidal conditions. *Mar Ecol Prog Ser*, 326:167–174, 2006.
- W. Lampert. The adaptive significance of diel vertical migration of zooplankton. *Funct Ecol*, pages 21–27, 1989.
- J. T. Lee, R. A. Coleman, and M. B. Jones. Vertical migration during tidal transport of megalopae of *Necora puber* in coastal shallow waters during daytime. *Estuar, Coast and Shelf Sci*, 65:396–404, 2005.
- C. Lehane and J. Davenport. Ingestion of bivalve larvae by *Mytilus edulis*: experimental and field demonstrations of larviphagy in farmed blue mussels. *Mar Biol*, 145:101–107, 2004.
- L. A. Levin. Recent progress in understanding larval dispersal: new directions and digressions. *Integr Comp Biol*, 46(3):282–297, 2006.
- C. J. Loose and P. Dawidowicz. Trade-offs in diel vertical migration by zooplankton: the costs of predator avoidance. *Ecology*, pages 2255–2263, 1994.
- E. Maier-Reimer. Residual circulation in the North Sea due to the M2-tide and mean annual wind stress. *Ocean Dyn*, 30(3):69–80, 1977.
- J. L. Manuel and R. K. O’Dor. Vertical migration of horizontal transport while avoiding predators: I. a tidal/diel model. *J Plankton Res*, 19(12):1929–1949, 1997.
- A. Metaxas. Behaviour in flow: perspectives on the distribution and dispersion of meroplanktonic larvae in the water column. *Can J Fish Aquat Sci*, 58(1):86–98, 2001.
- S. A. Mileikovsky. Speed of active movement of pelagic larvae of marine bottom invertebrates and their ability of regulate their vertical positions. *Mar Biol*, 23:11–17, 1973.
- W. P. O’Connor, B. F. Chao, D. Zheng, and A.Y. Au. Wind stress forcing of the North Sea ‘pole tide’. *Geophys J Int*, 142(2):620–630, 2000.

- J. E. Pechenik. Delayed metamorphosis by larvae of benthic marine invertebrates: Does it occur? Is there a price to pay? *Ophelia*, 32:63–94, 1990.
- J. E. Pechenik. On the advantages and disadvantages of larval stages in benthic marine invertebrate life cycles. *Mar Ecol Prog Ser*, 177:269–297, 1999.
- H. Queiroga. Vertical migration and selective tidal stream transport in the megalopa of the crab *Carcinus maenas*. *Hydrobiologica*, 375/376:137–149, 1998.
- D. Raby, Y. Lagadeuc, J. J. Dodson, and M. Mingelbier. Relationship between feeding and vertical distribution of bivalve larvae in stratified and mixed waters. *Mar Ecol Prog Ser*, 103:275–284, 1994.
- K. Reichert, F. Buchholz, and L. Giménez. Community composition of the rocky intertidal at Helgoland (German Bight, North Sea). *Helgol Mar Res*, 62(4):357–366, 2008.
- M. Scheffer, J. M. Baveco, D. L. DeAngelis, K. A. Rose, and E. H. van Nes. Super-individuals a simple solution for modelling large populations on an individual basis. *Ecol Modell*, 80(2-3): 161–170, 1995.
- A. L. Shanks and L. Brink. Upwelling, downwelling, and cross-shelf transport of bivalve larvae: test of a hypothesis. *Mar Ecol Prog Ser*, 302:1–12, 2005.
- J. Staneva, E. V. Stanev, J. O. Wolff, T. H. Badewien, R. Reuter, B. Flemming, A. Bartholomä, and K. Bolding. Hydrodynamics and sediment dynamics in the German Bight. A focus on observations and numerical modelling in the East Frisian Wadden Sea. *Cont Shelf Res*, 29(1):302–319, 2009.
- M. Strasser. *Recruitment patterns of selected Wadden Sea fauna after winters of differing severity*. PhD thesis, Univ. Hamburg, 2000. (in german).
- K. Troost, P. Kamermans, and W. J. Wolff. Larviphagy in native bivalves and introduced oyster. *J Sea Res*, 60:157–163, 2008.
- C. Verdier-Bonnet, F. Carlotti, C. Rey, and M. Bhaud. A model of larval dispersion coupling wind-driven currents and vertical larval behaviour: application to the recruitment of the annelid *Owenia fusiformis* in Banyuls Bay, France. *Mar Ecol Prog Ser*, 160:217–231, 1997.
- J. Verwey. The role of some external factors in the vertical migration of marine animals. *Neth J Sea Res*, 3(2):245–266, 1966.
- A.W. Visser. Using random walk models to simulate the vertical distribution of particles in a turbulent water column. *Mar Ecol Prog Ser*, 158:275–281, 1997.

- 
- J. M. Welch and R. B. Forward. Flood tide transport of blue crab, *Callinectes sapidus*, postlarvae: behavior responses to salinity and turbulence. *Mar Biol*, 139:911–918, 2001.
- L. M. Yaroslavteva and E. P. Sergeeva. The reaction of *Mytilus trossulus* larvae (Bivalvia, Mytilidae) to desalination and increase of water column temperature. *Russ J Mar Biol*, 29(3):156–160, 2003.



The distribution of planktonic and even benthic organisms in the coastal ocean is significantly influenced by ocean currents. Interactions between organisms and their physical environment take place on different temporal and spatial scales, from millimeters and seconds as in the example of active larval swimming (cf. Chap. 4) to kilometers and years as in the example of the invasion of oysters into a new habitat (cf. Chap. 3).

Physical factors were also mainly responsible for the timing and the medium-scale spatial distribution of phytoplankton spring blooms in the German Bight in two consecutive years (cf. Chap. 2). In the first year, light availability, which was mainly controlled by turbidity, triggered phytoplankton growth. In the following year, however, the spring bloom was advected into the study area and developed despite an unfavourable light climate. While the light climate can be regarded as a local factor, the advection of water masses with elevated chlorophyll concentrations imported a non-local signal to the area of interest. In the latter case, considering the propagation of information was indispensable for the explanation of the observed chlorophyll dynamics. Only the combination of all relevant information on hydrodynamics, turbidity, and chlorophyll allowed to unravel the different mechanisms leading to the interannual differences. Opposing the trend of developing ever more complex ecosystem models to reproduce observed biological variability, our result suggests that high model complexity might not be required to explain fundamentally different spring bloom dynamics. It is rather the availability of realistic physical and biological data at an adequate resolution for the phenomenon of interest that limits the system understanding.

Hydrodynamics also controlled the invasion of *Crassostrea gigas* into the German Bight between 1998 and 2004 (cf. Chap. 3). Our model results suggest that the recruitment of young oysters primarily depend, at least in the early phase of the invasion, on the supply of competent larvae. The spatio-temporal evolution of the simulated invasion wave corresponded to the direction and the speed of the residual currents. On average, the population wave propagated with a speed of only  $10 \text{ km a}^{-1}$  at a planktonic development time of  $15 \text{ d}$ , hence, much slower than the speed of surface currents may suggest. In fact, maximum dispersal distances of individual larvae were severalfold higher than mean distances explaining episodic observations of far distance transport of planktonic larvae. These exceptional individuals did, however, not significantly contribute to the population dynamics of *Crassostrea gigas*. The comparison with measurements from a monitoring programme revealed that the

density of new recruits was correlated to the simulated larval supply at most sites, but clearly not at all. Additional factors influencing the recruitment apparently suppressed the development of measured population densities at single sites. Already small variations of the simulated site-specific early mortalities significantly decreased the discrepancies between simulated and measured population densities underlining the sensitivity of recruitment to the survival of juveniles. It is, however, desirable for future studies to make these assumptions rather on the base of observational evidence than on model performance.

While passively drifting organisms unbiasedly follow ocean currents, active swimming of organisms in the complex three-dimensional flow field of coastal oceans may result in significant deviations from the trajectories of passive individuals (cf. Chap. 4). Planktonic larvae of the blue mussel *Mytilus edulis* mostly originate nearshore in the intertidal and shallow subtidal in the German Bight. Simulations revealed that passive drifting results in a dispersal to unfavourable offshore areas for the majority of larvae. A diel vertical migration strategy does not change this distributional pattern indicating that this behavioural strategy has no immediate benefits for the recruitment of benthic invertebrates in the intertidal Wadden Sea. In contrast, tidal vertical migration results in a selective shoreward transport. Larvae swim upwards during flood to benefit from strong shoreward currents at the surface and stay close to the bottom during ebb to limit seaward transport. The net result is a greatly enhanced fraction of larvae that is located in the Wadden Sea at the end of their planktonic life-stage. Despite slow swimming speeds, larvae may, hence, significantly influence their own dispersal by interacting with the complex flow field in the coastal ocean. The result of this study clearly shows the potential impact of vertical migration in vertically sheared currents and demonstrated the sensitivity of larval distributions to larval behaviour. Organisms that have the ability to swim should therefore not be regarded as passive drifters without strong evidence. Since the strategies of active larval behaviour in this study are based on several uncertain assumptions, more observational evidence is needed to quantify this effect.

To conclude, the results of all three studies consistently underline the importance of physical conditions, especially hydrodynamics, on the temporal and the spatial distributions of living organisms in the coastal ocean. This finding might appear trivial for processes like the invasion of *Crassostrea gigas* that followed the persistent residual current in the German Bight for several years. Often the outcome of interactions between the physical environment and living organisms are, however, less obvious. This is particularly true if currents are highly variable or if organisms actively swim in complex flow fields.

In all studies, the level of explainable variability in the biological variables was mainly determined by the resolution of the observational data used to constrain boundary conditions and not by the availability of appropriate numerical models or computational power. High resolution boundary conditions are, thus, indispensable to understand the high variability in coastal ecosystems. However, only the

combination of such data with realistic information regarding the transport of organisms leads to reasonable model results that are able to explain observed phenomena. The Lagrangian approach proved to be a valuable tool to simulate effects of advection and diffusion on the distribution of planktonic and, indirectly, even benthic organisms. It intuitively supports the adoption of the natural perspective of dispersing organisms and greatly facilitates the understanding of processes that are performed by individuals and not by average concentrations.

The results of this thesis demonstrate that the population dynamics at a fixed site may not be explainable even when all relevant growth and mortality factors at this location are known. Instead, non-local effects, i.e. effects caused by processes that happened at a remote location, may significantly influence local dynamics, particularly in heterogeneous coastal environments. The most important process linking remote causes to locally observable effects is advection. In larval ecology the links between sources and sinks of larvae that are established by currents are referred to as connectivity. Although less obvious, this concept also appears to be useful for phytoplankton. The phytoplankton concentration at an arbitrary location and time is determined by the integral of growth and mortality factors that were experienced by the individuals of the population along their trajectory. Hence, unless there is no advection or the environment is spatially homogeneous, both rare conditions in coastal seas, the population dynamics at a fixed location may only be weakly influenced by local factors.

In summary, physical factors have a substantial impact on ecological processes in the coastal ocean. It is, however, challenging to derive a unifying concept of these effects. As the examples of this thesis show, the consequences of biological-physical interactions are diverse and each observed phenomenon may require an individual explanation. Lagrangian Individual-based models present a powerful tool to obtain insights into complex coastal systems by disentangling the interactions between planktonic organisms and their physical environment and, by this means, to generate substantial understanding of ecological variability.



---

## Acknowledgments

I am grateful to Kai Wirtz for giving me the opportunity to conduct this endeavour and for the persistent support during all the years. His unconventional ideas and his demanding questions continuously challenged me and often pushed me to my limits, and sometimes even beyond.

Many colleagues contributed to the success of this piece of work one way or another or just became friends over the years. Almut, AnnKa, Dietmar, Jan, Joanna, Knut, Micha, Oliver, Sonja, Susanne, Xin, and many others made working at the ICBM enjoyable, thanks for that! I want to also thank my colleagues in the working group KOE at the GKSS in Geesthacht for advice, help and coffee. Special thanks go to Agostino Merico, who taught me a lot about science and ultimately achieved to keep alive my faith in science. Kudos to Ago!

I am indebted to my family for the encouragement, the comprehension, and for not questioning my way, which has not always been a direct one in the last decade.

I love Steffi for unconditional support during the last years (and for other things!) - she kept me afloat particularly in the most difficult times. And Karla, for just being here with us ...



---

## Curriculum Vitae

### **Gunnar Brandt**

geboren am 21.05.1978 in Minden (Westfl.)

Ledig, deutsch

- 10/2007 - heute Promotionsstudent Carl von Ossietzky Universität Oldenburg, Matrikel-Nr. 9803530
- 02/2006 - heute Freiberuflicher Gutachter, Technische Risikoanalyse für Offshore Windparks
- 02/2005 - heute Wiss. Mitarbeiter, GKSS-Forschungszentrum, Geesthacht
- 07/2004 - 03/2008 Wiss. Mitarbeiter, ICBM-Terramare, Oldenburg
- 03/2004 - 06/2004 Technischer Mitarbeiter, Offshore Wind Technolgy GmbH, Leer
- 10/1998 - 01/2004 Studium Marine Umweltwissenschaften, Universität Oldenburg
- Titel der Diplomarbeit: *Ansiedlungspotentiale meroplanktischer Larven an Offshore Bauwerken in der deutschen Bucht*
- 09/1997 - 07/1998 Wehrdienst, Minden (Westfl.)
- 06/1997 Allgemeine Hochschulreife am Besselgymnasium, Minden (Westfl.)



---

## **Erklärung**

Hiermit erkläre ich, dass ich die vorliegende Dissertation selbstständig verfasst habe und nur die angegebenen Hilfsmittel verwendet habe. Teile der Dissertation wurden bereits veröffentlicht bzw. sind zur Veröffentlichung eingereicht, wie an den entsprechenden Stellen angegeben. Die Dissertation hat weder in Teilen noch in ihrer Gesamtheit einer anderen wissenschaftlichen Hochschule zur Begutachtung in einem Promotionsverfahren vorgelegen.

Oldenburg, den 16. November 2009

---

Gunnar Brandt